Assessing the Impact of Transposon Activity and Megaplasmid Characteristics on the Genetic Stability of the Model Organism *Shewanella oneidensis*

Vom Promotionsausschuss der
Technischen Universität Hamburg

Zur Erlangung des akademischen Grades

Doktor der Naturwissenschaften

(Dr. rer. Nat.)

genehmigte Dissertation (Monografie) von

Benjamin Fritz

Aus

Wurzen

2026

Gutachter:

Prof. Dr. Gescher

Prof. Dr. Heinz

Tag der mündlichen Prüfung:

08.10.2025

Acknowledgements

Natürlich ist eine solche Arbeit nie das Produkt eines Einzelnen – vielmehr das Resultat einer langwährenden Zusammenarbeit vieler begabter Menschen und deren Ideen und Expertise. Damit möchte ich mich hier bei den Personen bedanken, die es mir ermöglichten zu den hier aufgeführten Resultaten zu gelangen und eine wissenschaftliche Arbeit zu formen, die hoffentlich den gewünschten Wert in sich trägt und vermittelt.

Danke Johannes, für das Vertrauen, welches du mir über die Jahre geschenkt hast und den Platz in deiner Gruppe. Ich habe höchsten Respekt vor deiner kompromisslosen Zielstrebigkeit, unerschöpflichen Energie für die Sache und deiner Intelligenz – alles Eigenschaften, die mir in meiner Zeit hier zugutekamen.

Danke an Laura und Lukas und eure Leitung des SIGs. Ihr habt mir viel Input zur Laborarbeit geben können und ich habe stets neue Sachen lernen und mitnehmen können. Außerdem danke ich euch für die Resilienz gegenüber meiner Unfähigkeit in der Bearbeitung der Strain Collection.

Danke an Jonas. Du hast trotz deiner begrenzten Zeit, da täglich viele Leute an deine Expertise interessiert sind, meine amateurhaften Fragen nie unbeantwortet gelassen. Ohne dich hätte ich den Einstieg in die Bioinformatik nie geschafft. Danke für die Auswertungen und Ideen und dein geduldiges Gemüt, das sehr gut mit mir resoniert hat.

Danke Edi. Das war die zweite Phase meines akademischen Lebens, die ich mit dir zusammenarbeiten und auch in Freizeit deine Freundschaft genießen durfte. Ich war begeistert, wie viel Professionalität und Skill du im Vergleich zu mir entwickelt hast, seitdem wir im Studium gleich auf waren in unserer Unfähigkeit. Ohne dich und dein Vertrauen wäre ich nicht an dem Punkt hier eine Doktorarbeit abgeben zu können.

Danke Rene. Es war fantastisch mit dir dasselbe Rennen antreten zu dürfen. Deine wissenschaftliche Neugier und Offenheit hat mir viel Spaß in Konversationen über das Laborleben gegeben. Über die Zeit begann ich eine tief verbindende Freundschaft zu empfinden, was mir die Sache hier in schwierigen Zeiten sehr viel erträglicher machte.

Danke Vivi und Chrissi, ohne unser gemeinsames Blödeln, Unternehmen, Mensen und Schnacken hätte ich den Laboralltag als eher trist empfinden müssen. Danke euch für eine Freundschaft, in der ich mich so bedingungslos verstanden fühlte.

Danke Beri, Mashid, Leonie, dass ihr es mit mir und meiner leichten Verrücktheit ausgehalten habt. Entschuldigt die hin und wieder trocknenden Socken und Sport Sachen auf der Heizung. Ich habe es sehr genossen ein Büro mit euch zu teilen und vermisse die Atmosphäre sehr – in einer öffentlichen Bibliothek sitzend.

Danke auch an Nina, die eine ausgezeichnete Bachelorarbeit hingelegt, sowie Zuarbeit für einen Teil dieser Arbeit vorgelegt hat, welcher sonst nicht so möglich gewesen wäre.

Abstract

The facultative anaerobe *Shewanella oneidensis* is a model organism widely studied for its extracellular electron transfer capabilities, making it a promising candidate for bioelectrochemical systems (BES). However, its presumed genetic instability presents a key challenge, particularly for long-term industrial applications. This study investigates two major factors influencing genetic robustness in *S. oneidensis*: transposon activity and the presence of the megaplasmid (MP).

Transposable elements (TEs) play a crucial role in genome plasticity. Their high activity can lead to disruptive mutations, compromising strain stability. To assess transposase mobility under TE-activating conditions, transcriptomic analysis and stress-induced transposition experiments were combined with whole-genome sequencing. The results indicate that certain insertion sequences (IS), particularly ISSOD1, ISSOD2 and ISSOD9, exhibit high transposition rates, contributing to genetic instability. To mitigate these effects, CRISPR-Cas-deaminase-based genome editing was employed to introduce premature stop codons into active transposase genes. This deactivation successfully reduced transposase-related mutations emanating from the ISSOD2 family, demonstrating a viable strategy for stabilizing the *S. oneidensis* genome. ISSOD9 activity appeared to be strongly linked to the presence of plasmids in transformed strains, suggesting its transposition mechanism is associated with horizontal gene transfer. This finding has significant implications for studies utilizing external plasmids, as it underscores the potential for unintended genomic alterations.

In parallel, the role of the megaplasmid in genetic stability was examined, which harbors numerous TEs and contains mutation-prone regions, increasing TE motility potential. Using an adaptive evolutionary approach, it was attempted to delete the MP while circumventing post-segregational killing caused by toxin-antitoxin pairs that contribute to stabilized vertical plasmid transfer. Although complete megaplasmid loss was not achieved, approximately 35 % of its sequence was deleted, including nine TEs and an identified hotspot for integration. Notably, the unexpected loss of the region containing the *origin of replication* suggests a metastable state for the MP.

By integrating genome-wide analyses with targeted genetic modifications, this study provides valuable insights into the mechanisms governing genetic stability in *S. oneidensis*. These

findings contribute to optimizing *S. oneidensis* as a robust production strain for BES applications, with broader implications for microbial engineering and industrial biotechnology.

Table of Contents

Table of Figures

List of Tables

Abbreviations

ackA	Acetate kinase
alsD	Acetolactate decarboxylase
alsS	Acetolactate synthase
araP	Arabinose promoter
AT	Antitoxin
BAC	Bacterial artificial chromosomes
BES	Bioelectrochemical systems
bp	Base pair
Cas	CRISPR-associated genes
CDS	Coding sequence
CRISPR	Clustered regularly interspaced short palindromic repeats
DAP	Diamino pimelic acid
ddH_2O	Double deionized H_2O
DMSO	Dimethyl sulfoxide
DSB	Double stand breaks
dsDNA	Double strand deoxyribonucleic acid
DUF	Domains of unknown function
EET	Extracellular electron transfer
FAD	Flavin-adenine-dinucleotide
FccA	Flavocytochrome *fumarate reductase A*
HDR	Homology-directed repair
HGT	Horizontal gene transfer
indels	Insertions or deletions
IR	Inverted repeat
IS	Insertion sequence
ISSOD	Insertion sequence *Shewanella oneidensis*
MEC	Microbial electrolysis cell
MFC	Microbial fuel cell
MITE	Miniature inverted-repeat transposable elements
MP	Megaplasmid
NCBI	National center for biotechnology information
NHEJ	Non-homologous end joining
OD	Optical density

ORF	Open reading frames
PHB	Poly-3-hydroxybutyrate
ppm	Parts per million
pta	Phosphotransacetylase
RFP	Red fluorescent protein
rpm	Rounds per minute
sgRNA	Single guide RNA
SNV	Single-nucleotide variants
STC	Small tetraheme cytochrome *c*
TALEN	Transcription activator-like effector nucleases
TMAO	Trimethylamine-N-oxide
TPM	Transcripts per million
UV	Ultraviolet
WGS	Whole-genome sequencing
WT	Wild type
ZFN	Zinc finger nucleases

1 Introduction

1.1 Microbial production and electrode-assisted fermentation

Since the industrial era, fossil fuel consumption has increased relentlessly, releasing vast quantities of carbon dioxide (CO_2) into the atmosphere. This has been conclusively linked to irreversible climate changes and widespread environmental damage. Despite a strong scientific consensus, political inaction, skepticism, and outright denial have often hindered effective responses (Cook *et al*., 2016; Hornsey & Fielding, 2020; Hou *et al*., 2023; Rosado, 2017; Wang & Azam, 2024).

It is therefore imperative to develop alternative industrial production methods that reduce fossil fuel consumption while remaining economically viable. Microbial processes for chemical production and bioremediation offer a promising solution, as they leverage the metabolic pathways of organisms to drive energy-efficient conversions (Philipp *et al*., 2020; Qumsani, 2024).

Fermentation has been a cornerstone of industrial production for centuries. A key characteristic of this process is its typically low net energy yield, which necessitates the consumption of substantial amounts of substrate for microbial growth. This, however, can be exploited to achieve rapid conversion rates for target products (Cowan *et al*., 2023).

One of the limitations in fermentation is that the total redox equivalent must be balanced between formed products and used substrates. Energy gain is often limited to substrate level phosphorylation where phosphate groups are directly transferred to convert energy in a utilizable form like ATP. Without an external electron acceptor, the overall oxidation state of the product (mixture) must match that of the substrate(s), causing the process to stall as product accumulates. While oxygen may serve as an electron acceptor to expand the range of possible oxidative states, it has drawbacks in applications. Oxygen increases energy availability for microbial anabolism, reducing product yield. Additionally, aeration requires energy (Drewnowski *et al*., 2019) and many microorganisms are sensitive to oxygen (Hackmann, 2024; Müller, 2008).

Besides the use of oxygen, some microorganisms overcome the limitations of sole substrate level phosphorylation by utilizing an external electron acceptor, a process known as extracellular electron transport (EET). These organisms, called exoelectrogens, can transfer excess metabolic electrons to soluble or insoluble extracellular electron sinks, such as iron or

manganese compounds, thereby connecting their metabolism with respiration of an external source. This process typically occurs under strict anoxic conditions (Myers & Nealson, 1988; Sturm *et al*., 2015).

The electron transfer is usually facilitated via multiple *c*-type cytochromes localized across the membranes and the periplasm of the bacteria. This electron transfer occurs along an increasing redox potential from an electron donor to the acceptor. The principle of outward directed electron transfer is applied by the organisms in different ways. It happens either directly by cell to substrate contact, via soluble exogenic redox-shuttles or in conductive biofilms residing on the electron- sink forming so-called nanowires (Gralnick & Newman, 2007; Hartshorne *et al*., 2009; Kerisit *et al*., 2007; Lovley & Walker, 2019; Velasquez-Orta *et al*., 2010).

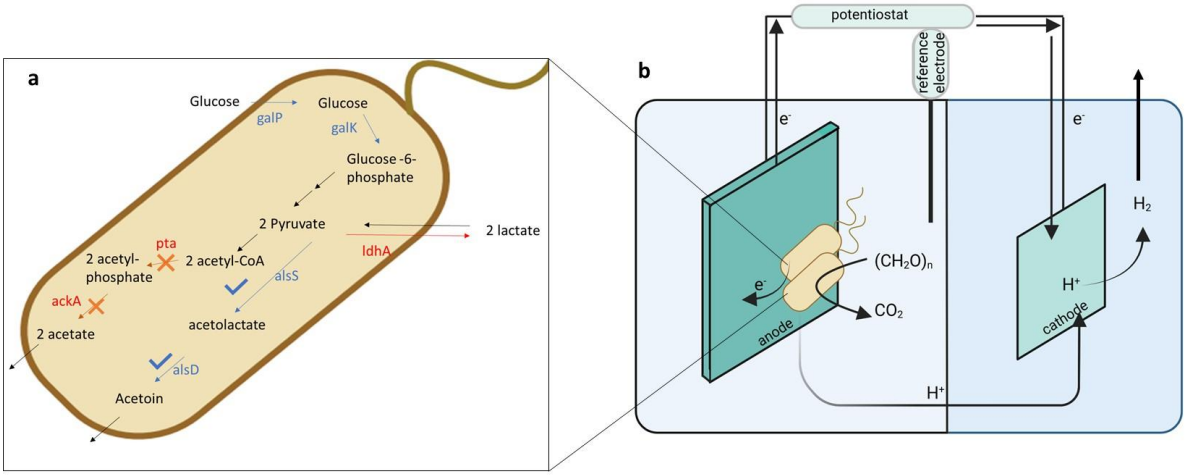

Figure 1: Depiction of a microbial electrolysis cell with a possible *S. oneidensis* production strain. The genetically engineered pathway is depicted in the bacterial cell in panel **a**. Heterologously expressed genes for the conversion of glucose to acetoin are colored blue. Genes that were deleted are indicated in red. Panel **b** shows the schematic of a BES system where excess electrons emerging from the metabolic activity of the microorganisms are transferred to the electrode that is kept at a stable potential via the connection to a potentiostat. Hydrogen is released as an energetically utilizable product at the cathodic site.

Bioelectrochemical systems are a versatile biotechnological platform that leverages extracellular electron transfer for applications such as bioremediation, chemical production, and electricity generation. In these systems, exoelectrogens act as biocatalysts, transferring electrons externally. This capability is harnessed by providing a constant electron sink, such as an anode. By doing so, redox equivalents are continuously replenished, enhancing fermentation efficiency and driving product formation (Chandrasekhar, 2021). This engineered process leads to a non-stochiometric fermentation also called electrode-assisted fermentation and can be

applied in microbial fuel cells (MFCs) and microbial electrolysis cells (MECs) (Flynn *et al*., 2010; Kumar *et al*., 2018).

MECs operate as galvanic cells, converting chemical energy into electrical energy and hydrogen. A potentiostat applies a favorable potential to facilitate electron transport and product formation. Microorganisms metabolize substrates into CO_2 or other carbon compounds, electrons and protons. In this process a redox gradient drives electron flux when a suitable potential is applied to the anode (see Figure 1 b; (Nakagawa *et al*., 2015).

Conversely, in microbial electrosynthesis (MES), the process is reversed: electrons are supplied by a cathode, often as hydrogen, enabling cells to synthesize complex molecules. This includes the production of poly-3-hydroxybutyrate (PHB), a biodegradable base molecule for an alternative to fossil-based plastics (McAdam *et al*., 2020). Additionally, MES offers the added benefit of potential CO_2 capture (Rabaey & Rozendal, 2010).

The scope of BES applications continues to expand through genetic engineering. Researchers are enhancing EET pathways in native organisms or transferring key components of the exoelectrogenic transport to non-native hosts, unlocking new bioprocess possibilities (Philipp *et al*., 2020).

1.2 *Shewanella oneidensis* in the field of EET

S. oneidensis has emerged as a model organism in the study of extracellular electron transfer processes. This facultative anaerobic bacterium can use oxygen as a terminal electron acceptor, allowing it to grow more rapidly under oxic conditions. This trait simplifies experimental setups and makes the organism easier to handle. Additionally, *S. oneidensis* is genetically accessible, enabling detailed examination of its underlying mechanisms. Its product spectrum and bioprocess efficiency can potentially be engineered for broader application and higher performance. The organism shares genetic and functional homologies with *E. coli*, one of the most extensively studied model organisms, making it an excellent candidate for adapting well-established genetic and molecular techniques (Deutschbauer *et al*., 2011; Heidelberg *et al*., 2002; Philipp *et al*., 2020).

The versatility of *S. oneidensis* in utilizing a wide range of electron acceptors and its robust degradation pathways make it highly applicable for bioremediation. Its spectrum of electron acceptors includes insoluble compounds like iron and manganese oxides (Fe[III], Mn[III], Mn[IV]) as well as soluble molecules such as trimethylamine-N-oxide (TMAO), dimethyl sulfoxide (DMSO), nitrate, nitrite and sulfate (Beblawy *et al*., 2018).

The EET mechanism in *S. oneidensis*, as currently understood, is facilitated by a network of *c*-type cytochromes. These cytochromes, with partially redundant functions, span the inner membrane, periplasm, and outer membrane, extending to external electron acceptors. The CymA protein plays a central role by oxidizing the cytoplasmic quinone pool and transferring electrons into the periplasm, creating a hub for electron transfer pathways, where soluble *c*-type cytochromes, such as *FccA* and STC, mediate further transfer. These cytochromes either reduce soluble electron acceptors like fumarate, DMSO and nitrate or pass electrons to the transmembrane MtrCAB complex, which spans the outer membrane (Hartshorne *et al*., 2009; Sturm *et al*., 2015).

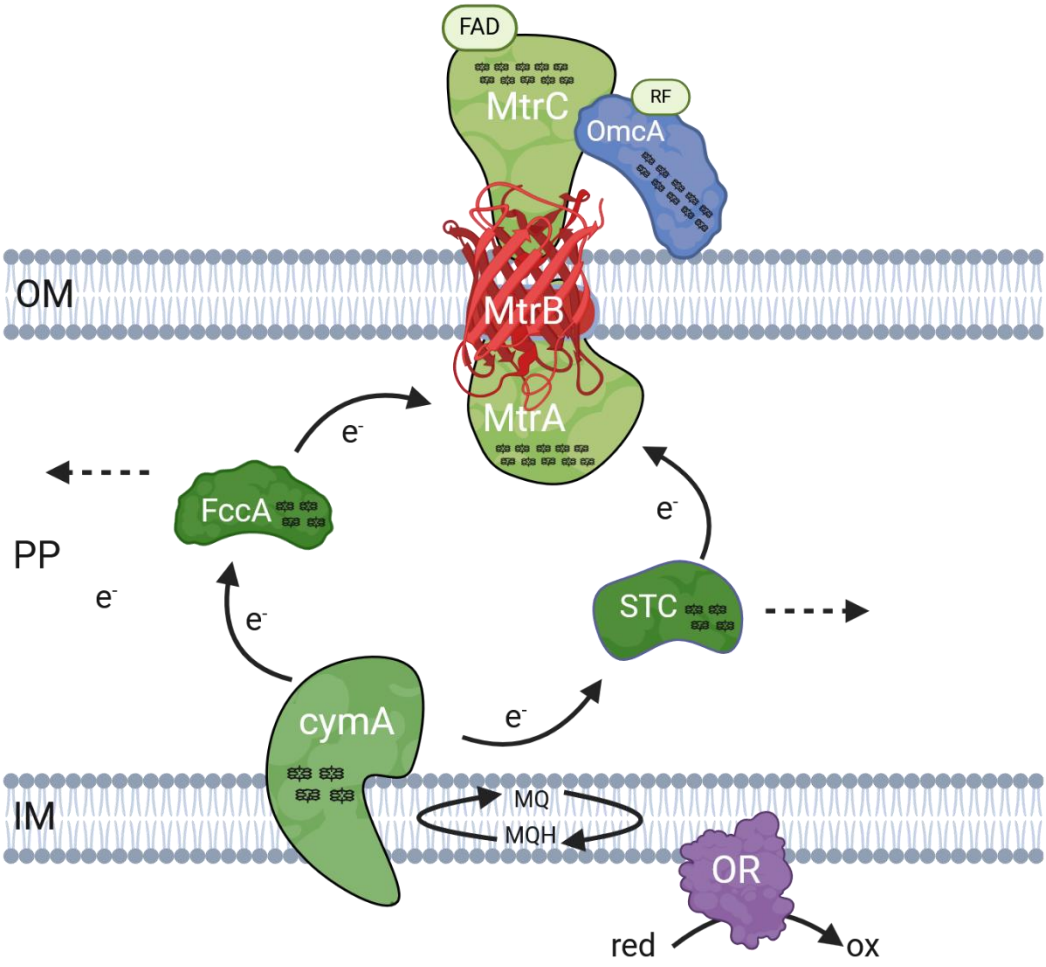

Figure 2: A schematic depiction of the EET transfer of *S. oneidensis*. The electron transfer is facilitated along a redox gradient from the inner membrane (IM) via *cymA* over the periplasm (PP) to the outer membrane (OM) spanning MtrCAB complex. The electrons can divert to different electron acceptors over fumarate reductase (*FccA*) or small tetraheme cytochrome *c* (STC). The menaquinone pool (MQ - MQH) is fed with metabolic electrons over inner membrane bound oxidoreductases (OR).

In the MtrCAB complex, the MtrB β-barrel protein is thought to connect two *c*-type cytochromes, MtrA and MtrC, forming a pore for electron conduction (Edwards *et al*., 2020). At the bacterial surface, MtrC and OmcA transfer electrons to external acceptors, possibly through direct interactions via exposed heme groups or through flavins, which facilitate electron transfer by forming semiquinones (see Figure 2; Von Canstein *et al*., 2008, Marsili *et al*., 2008; Okamoto *et al*., 2013, 2014). It should be noted that although CymA is the predominant quinol oxidase the electron transfer in the periplasm depicted in Figure 2 is simplified and not exhaustive. In fact, the redundancy of the 41 *c*-type cytochromes encoded by *S. oneidensis* with their respective roles in electron transport is still under investigation (Sun *et al*., 2021).

Uncovering the underlying mechanisms of EET in *S. oneidensis* is valuable because these processes could potentially be transferred to other organisms, such as *E. coli*. As mentioned above, by integrating EET mechanisms with the well-established genetic and metabolic tools available for *E. coli*, the potential for applications is substantial (Philipp *et al*., 2020; Teravest *et al*., 2014).

1.3 *S. oneidensis* as a potential production strain

Besides the ability to use diverse external electron acceptors *S. oneidensis* can use electrodes as an inexhaustible electron sink. This is beneficial for applications like BES systems. Here a setup is feasible where the organism is grown as a biofilm residing on the anode, continually feeding its excess electrons to the anode, driving electrode-assisted fermentation (Pinto *et al*., 2018). In the current setups the excess electrons are released as hydrogen on the cathodic side and can be used in downstream applications (see Figure 1 **b**).

Acetoin, a valuable industrial chemical, has been successfully produced in BES setups utilizing *S. oneidensis* (Bursac *et al*., 2017). Traditional acetoin production relies on aerobic sugar processing, which is energy-intensive due to the need for aeration and provides organisms with anabolic energy, reducing overall efficiency (Sun *et al*., 2012; Wang *et al*., 2013). Anaerobic production, potentially offering higher conversion efficiencies, remains desirable.

To enable acetoin production in *S. oneidensis*, heterologous expression of the acetoin biosynthetic genes *alsS* (acetolactate synthase) and *alsD* (acetolactate decarboxylase) from *Bacillus subtilis* were introduced. These genes catalyze the conversion of two pyruvate molecules into acetoin via an acetolactate intermediate (Kipf *et al*., 2014). However, the

observed turnover rates were low, partly due to insufficient electron transfer rates in BES systems.

To redirect metabolic flux away from the native, energetically favorable acetate production pathway, the genes encoding acetate kinase (*ackA*) and phosphotransacetylase (*pta*) were deleted (Bursac *et al*., 2017; see Figure 1 **a**). This modification effectively prevented acetate production, eliminating substrate-level phosphorylation and significantly reducing energy generation. Acetoin has a lower oxidation state than acetate. Although the conversion helps to regenerate NAD^+, there is no net energy yield for the cells in the form of ATP, constraining growth.

The native substrate spectrum of *S. oneidensis* under anoxic conditions is limited to compounds such as lactate, pyruvate, formate, and N-acetylglucosamine (Hunt 2010). To expand this range to include glucose, a widely available and high-energy substrate, the glucose importer gene *galP* and the kinase gene *galK* were introduced. This enabled uptake and phosphorylation of glucose to glucose-6-phosphate, allowing its entry into the Entner-Doudoroff (ED) and pentose phosphate (PP) pathways. These pathways enable glucose degradation to pyruvate, theoretically yielding a net gain of 1 ATP for cellular growth. However, under glucose-fermenting conditions, substantial growth was not observed (Chubiz, 2017; Nakagawa *et al*., 2015; Rodionov *et al*., 2010).

Glucose metabolism can lead to excess electron buildup, often resulting in the conversion of pyruvate to lactate for electron storage. To mitigate this, the *ldhA* gene, encoding a NADH-dependent lactate dehydrogenase, was deleted. This modification effectively reduced lactate accumulation, although other lactate dehydrogenases, such as Dld-II, remain active. Dld-II is found to interact with the menaquinone pool. Based on the FAD-dependency of the enzyme and the connection to the menaquinone pool, lactate formation is dependent on redox potential. By applying a suitable electrode potential, lactate accumulation can be minimized (Kasai *et al*., 2019; Pinchuk *et al*., 2009). However, the role of lactate metabolism requires further investigation.

Despite the demonstrated ability of *S. oneidensis* to produce acetoin in BES setups, substantial yields have not been achieved, particularly during glucose consumption. The underlying mechanisms are still under investigation. One possibility is the disruption of the process via mutation. Important for a production strain as is described here, or for any strain meant for production in that matter, is a robust genetic background. Its robustness should allow the

continuity of the process over long periods of time, without mutating key elements of the process.

1.4 Genetic robustness is important for production strains

The heterologous expression of genes - genes derived from different organisms - has become increasingly significant in microbial biotechnology, finding applications in the production of insulin, vaccines, and other chemicals (Endy, 2005). As biotechnological tools advance, heterologous production systems are expected to become more prevalent. However, these genes are subject to the same evolutionary pressures as native host genes. In fact, they may be especially prone to mutations due to the high metabolic burden they impose on the host. This metabolic strain often results in selective pressures that favor the rapid elimination of key production elements, reducing the stability and efficiency of the system (Czajka *et al*., 2020).

Several factors influence genetic stability and mutation rates, including batch size, the number of engineered components, and the use of plasmids. Mutation rates are inherently difficult to predict, and tracing yield losses back to genetic instability during an ongoing production process can be both time-consuming and costly. These challenges become even more pronounced during scale-up, which introduces additional complexities. As production scales up, the larger cell populations increase the probability of mutations that generate non-producer strains. These non-producers not only reduce overall yield but may also outcompete producer strains. This is due to their lower metabolic burden, which allows them to proliferate more efficiently, potentially supplanting the producer population over time. Larger bioreactors are more challenging to control, with gradients in temperature, pH, oxygen availability, or nutrient concentrations creating localized areas of stress. These stress conditions may trigger higher mutation rates (Foster, 2007; MacLean *et al*., 2013). Additionally, some subpopulations can develop into hypermutator strains (Oliver & Mena, 2010) in response to environmental pressures, further increasing the risk of non-producer emergence. Genetic plasticity, driven by mutations and selective pressures, is an unavoidable phenomenon that impacts all biological processes (Rugbjerg *et al*., 2018; Rugbjerg & Sommer, 2019; Wehrs *et al*., 2019).

Given these challenges, the role of transposase activity in *S. oneidensis* was investigated as a potential factor in genetic instability. This organism possesses a substantial number of transposase-encoding genes, which suggests significant transposable element (TE) activity. If

S. oneidensis indeed exhibits high TE activity, it could have critical implications for its suitability as a production strain in industrial applications.

High transposase activity may exacerbate genetic instability by increasing the frequency of insertions and large-scale genomic rearrangements, which could combine with other mutations, such as single nucleotide variants (SNVs), to disrupt key metabolic pathways. Understanding the extent of TE activity in *S. oneidensis* is essential for evaluating its potential as a stable and reliable host for industrial-scale production.

1.5 Transposases in *S. oneidensis*

Transposases are genetic elements that are likely related to viruses and have developed the ability to mobilize within the genome of the host (Mustafin, 2018). TEs have developed a multitude of mechanisms facilitating genetic motility. They are therefore, at least partially, categorized into distinct groups, where borders get increasingly blurry with the discovery of new TEs and subclasses. Although there are many similarities, like the chemistry of mobilization, there is a distinction between the categorization in eukaryotes and bacteria. In eukaryotes the two major classes are either retro transposons mobilizing through a copy and paste mechanism, where the RNA intermediate is reverse transcribed and integrated elsewhere (class 1), or DNA TEs that transpose via a DNA intermediate using a cut and paste mechanism (class 2). Although most bacterial TEs are DNA TEs they are categorized in a different way. In this domain the simplest and most common forms of TEs are called insertion sequences (IS), primarily encoding enzymes for excision and reinsertion along with necessary flanking repeats. They are usually divided into subclasses based on the catalytical chemistry of the transposase they encode, including DDE, DEDD, HUH and Ser transposases. Although accumulation of statistically robust data uncovers more refined insertion patterns, the target sequence for integration often doesn’t require extensive sequence specificity, making propagation possible for almost the entirety of host genomes (Cain *et al*., 2020; Siguier *et al*., 2015).

The function and role of transposable elements, once dismissed as "selfish DNA" (Doolittle & Sapienza, 1980), are now understood to be more complex. TEs can contribute to adaptive responses under environmental stress, such as facilitating the acquisition of antibiotic resistance (Vandecraen *et al*., 2017; Che *et al*., 2021). While many TE activities can have harmful effects, others can enhance gene function, compensate for gene loss, or even cause emergence of beneficial operons (Fan *et al*., 2019; Hall, 1999; Kanai *et al*., 2022). Over time, TEs and their

host genomes often reach a state of equilibrium where TE activity becomes mostly neutral (Iranzo *et al*., 2014), preventing excessive genomic burden that could otherwise reduce TE numbers or lead to lineage extinction (Mira *et al*., 2001). It is proposed that new TEs undergo a "transposition burst"- a period of rapid activity that diminishes as a stable state is achieved (Siguier *et al*., 2014; Wu *et al*., 2015).

Thus far, 219 transposable elements (TEs) have been identified in *S. oneidensis*. Although the number of transposable elements in *S. oneidensis* has been studied and there are strong indications that the genome is highly dynamic based on TE transposition, factors driving activity in this organism remain mostly unexplored. In *S. oneidensis*, roughly 4.7 % of the genome or 5.6 % of coding sequences (Romine *et al*., 2008) are found to be related to TEs. Bacterial TEs counts vary widely across all species and clades of bacteria which makes it challenging to categorize IS levels as high or low. There seems to be almost no correlating factors with environment, host dependency or even numbers within the same genus, with the only exception perhaps being genome size (Touchon & Rocha, 2007). Notwithstanding, given the notable portion of *S. oneidensis* coding sequences and the reports on genetic plasticity caused by IS leading to substantial phenotype alterations (Bordi *et al*., 2003; Cheng *et al*., 2020; Schicklberger *et al*., 2013), it is postulated that activity of *S. oneidensis* TEs might be significant, with strong indications for strain development in experimental and industrial application.

It is found that the induction of stress can increase mobility of IS. The changes following stress induction in regulatory expression such as SOS - response can activate transposition. Strand breaks cause activation of host repair machinery and leave break points for insertions of transposons (Capy *et al*., 2000). These stress factors include nutrient deprivation, UV-radiation, temperature and chemical stress like antibiotics or metal ions. The genetic plasticity that results from these stress factors can lead to adaptations (Eichenbaum & Livneh, 1998; Lartigue *et al*., 2006; Takahashi *et al*., 2007).

Transposable elements often exist in multiple copies within an organism due to their ability to move and propagate within the genome. These elements can be grouped into families based on sequence homology. In *S. oneidensis*, up to 41 transposase families have been identified, along with three miniature inverted-repeat transposable elements (MITEs). MITEs are small, non-autonomous mobile elements that rely on the activity of other transposases for their propagation (Lu *et al*., 2012).

The following section provides a detailed introduction to three specific transposase families identified in *S. oneidensis*.

1.5.1 The ISSOD9/Tn3 Transposase

Tn3 transposases are a widespread family of transposases found across all bacterial groups. They were initially identified due to their association with passenger genes, such as those conferring antibiotic resistance (Hedges & Jacob, 1974). A defining feature of these transposons is their mechanism of transposition, which involves simultaneous duplication of the TE and integration into the target DNA (Shkumatov *et al*., 2022). The process begins with cleavage at the 3′ ends of the transposon and the target DNA. These ends are then ligated by transposase activity, creating a fused single-stranded DNA intermediate between the donor DNA (e.g. a plasmid carrying the transposase) and the target DNA. This mechanism, known as replicative or "copy-and-paste" transposition, utilizes the host's replication machinery to convert the single-stranded intermediate into double-stranded DNA (dsDNA). Consequently, the entire donor molecule becomes fused to the acceptor molecule, forming an intermediate structure known as a cointegrate (Shapiro, 1979).

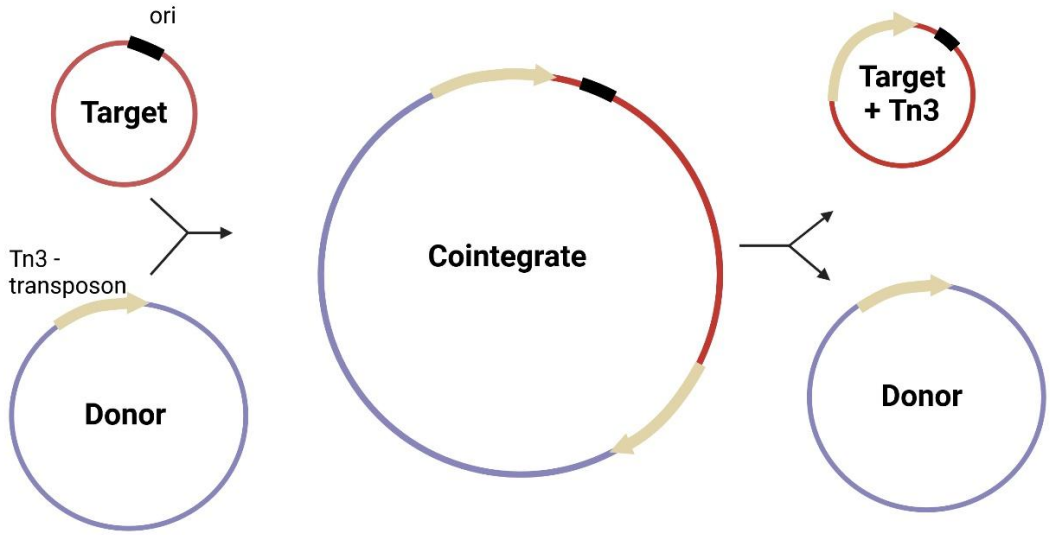

Figure 3: Transposition mechanism of the Tn3 transposase. The donor molecule containing the Tn3-transposon integrates into the target molecule via transposase activity as a whole and forms a cointegrate intermediate by utilizing the host replication machinery. This intermediate is separated into two molecules by a resolvase encoded by the transposon completing the cycle of propagation. The target sequence now contains a copy of Tn3 while the donor replicon retains the original copy.

In the final step of the transposition process, the cointegrate is resolved by Tn3 resolvase through site-specific recombination between the original and newly formed transposon copies.

This resolution separates the cointegrate into two distinct loci: the donor remains intact, while the recipient acquires a new Tn3 copy (see Figure 3; Shkumatov *et al*., 2022). The propagation of Tn3 transposons is less arbitrary compared to other transposons, as it relies on the host's replication machinery. Tn3 transposases have been shown to interact with the β-sliding clamp, a replication-associated protein, which likely enhances their propagation efficiency (Tang *et al*., 2024). This interaction increase the chance of horizontal transfer of Tn3 transposons between individuals and species, in horizontally transferable replicons such as plasmids where the replication machinery is recruited frequently (Kretschmer & Cohen, 1977). A noticeable feature of Tn3 transposons is their ability to establish transposition immunity once a copy has integrated into a DNA fragment. This mechanism prevents further integration of additional Tn3 copies into a replicon that already contains one (Wallace *et al*., 1981). This property may play a role in limiting over-propagation of Tn3 transposons within the host genome, ensuring stability in replicative elements.

1.5.2 The ISSOD1 and ISSOD2 family

The abundance of transposase families can vary significantly both within and across species, as indicated by their copy numbers. Insertion sequence *Shewanella oneidensis* (ISSOD1; 45 copies) and ISSOD2 (4 copies) are IS belonging to the IS3 family, a highly prevalent and widely distributed group of transposases found across numerous bacterial species. With increasing sequencing throughput, it is likely that additional members of this family will be uncovered (Siguier *et al*., 2015).

The IS3 family archetype consists of two partially overlapping open reading frames (ORFs), *orfA* and *orfB*, flanked by inverted repeats (IRs). The 5′ end of *orfB* overlaps with the 3′ end of *orfA*, enabling two translational reading frames that result in the expression of three possible proteins (Sekine *et al*., 1999). The *orfA* product contains a conserved leucine zipper motif and helix-turn-helix (HTH) domain. These features are likely involved in recognizing the inverted repeats and functioning as a transcriptional regulator critical for multimerization and transposition initiation (Haren *et al*., 1998). The exact function of *orfB* remains unidentified, but it may interact with *orfA* to inhibit transposome formation. A fusion product, *orfAB*, is produced through programmed ribosomal frameshifting, resulting in a full-length transposase. This ribosomal slippage regulates the expression levels of both transcripts, adding an additional layer of control (Chandler & Fayet, 1993).

The IS3 mobilization mechanism, termed "copy-out-paste-in," begins with the cleavage of one DNA strand, producing a free 3′-OH group. This group attacks the opposite end, forming a single-stranded DNA (ssDNA) bridge. Replication *in situ* generates a circular double-stranded DNA (dsDNA) IS copy, while the donor DNA is restored, retaining the original IS copy. The circular intermediate is integrated into the target DNA at junctions formed by single-strand cleavage and two 3′-OH groups (see Figure 4; Siguier *et al*., 2015).

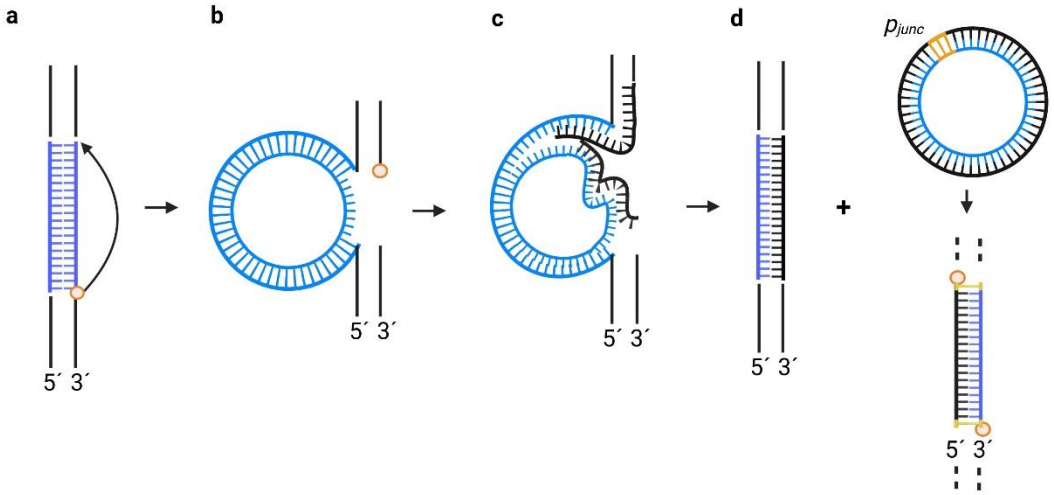

Figure 4: The transposition mechanism of the IS3 transposase family. The transposase activity leads to the cleavage of one strand where the transposon is located. The resulting 3′ - OH group attacks the opposite end forming a bridge (**a**). This in turn leads to the formation of a circular intermediate (**b**) where replication is initiated at both strands (**c**). The completion of replication leads to the restoration of the donor transposon and a circular copy which can integrate at another position in the genome (**d**). A hybrid promoter p_{junc} is formed by combining promoter components of the inverted repeats of the transposon, important for transposase expression and motility.

The left inverted repeat (LIR) contains an inward -10 promoter component paired with a low-activity promoter (p_{IRL}), while the right inverted repeat (RIR) features a -35 outward promoter component. Together, these components form a strong promoter region in the circular intermediate, termed p_{junc}, when paired with the LIR promoter (see Figure 4 **d**). This junction promotes robust transposase expression and is critical for completing the transposition pathway (Lewis *et al*., 2004). These highly condensed elements incorporate multiple layers of regulation, enabling intricate propagation patterns influenced by the host's genetic background.

This overview highlights the complexity of transposition regulation, illustrating why predicting transposase activity is challenging. The mere identification of IS members and their copy number are insufficient to determine activity levels. Several additional factors influence motility. The genomic location of IS elements and their interaction with regulatory components

can significantly affect their activity. The regulatory mechanisms governing IS3 transposase activity are intricate and multifaceted. Understanding these complexities is essential for studying transposase function and predicting their behavior within diverse host genomes.

1.6 The megaplasmid of *S. oneidensis*

Plasmids are extrachromosomal genetic elements known for their diversity in structure, size, and function. They exist in circular or linear forms and typically replicate independently of the host chromosome, although integration and chromosomal replication is possible. Plasmid sizes vary widely, spanning several orders of magnitude. Megaplasmids (MPs) are generally defined by arbitrary size thresholds due to the lack of universally accepted criteria (Hall *et al*., 2022). In *S. oneidensis* the megaplasmid constitutes 3.2 % of the genome with a size of 161 kbp.

Advancements in long-read, high-throughput sequencing technologies and refined assembly tools have increased the identification of large replicons, many of which do not fit the category of “traditional” multicopy plasmids (Schmid *et al*., 2018). However, accurately identifying MPs remains challenging due to the presence of repetitive elements, such as insertion sequences, which are often shared with the chromosome.

Megaplasmids are distinguished from secondary chromosomes and chromids by their lack of essential genes (Harrison *et al*., 2010). However, this distinction is context-dependent, as the definition of "essential" varies with environmental conditions and host strain. Moreover, plasmids can undergo fusion events, resulting in hybrid replicons that complicate their categorization (DiCenzo & Finan, 2017).

Plasmids face opposing selective pressures. On the one hand, they impose a metabolic burden on their hosts, leading to a deletional bias that reduces their size. On the other hand, they may carry accessory genes that provide a selective advantage, stabilizing their presence in the host genome (Hull 2022). These accessory genes can confer valuable traits, such as biodegradation capabilities, antibiotic or metal resistance (Monchy *et al*., 2007), denitrification pathways (Schwartz *et al*., 2003), or carbon fixation (Panich *et al*., 2021) among many others (Dennis, 2005).

Horizontal gene transfer (HGT) frequently introduces transposons into plasmids, which may then serve as propagation platforms for these elements, such as Tn3 (Tang *et al*., 2024). Because plasmids often lack essential genes, here transposon insertions are less detrimental to the host

cell. The resulting redundancy in non-essential loci creates hotspots for insertions and rearrangements (Oliveira *et al*., 2017). In *S. oneidensis*, the megaplasmid is particularly enriched with transposons, comprising approximately 20 % of its coding sequences. Reports suggest 34 to 59 transposons on the megaplasmid, highlighting its role in genomic dynamics (Heidelberg *et al*., 2002).

Over time, megaplasmids accumulate features that enhance their stability within the host genome. A notable mechanism involves addiction modules, consisting of toxin-antitoxin (TA) pairs. These modules are encoded in single expression cassettes, where the toxin inhibits critical cellular functions unless neutralized by its corresponding antitoxin.

If a host cell loses the plasmid carrying a TA module, the more stable toxin persists longer than the antitoxin, resulting in post-segregational killing and elimination of plasmid-free cells. This ensures the retention of the plasmid in the host population (Jurėnas *et al*., 2022; Van Melderen & De Bast, 2009). The *S. oneidensis* megaplasmid contains 11 such TA modules, further stabilizing its genetic background. Interestingly, some TA modules are also associated with transposons, such as Tn3-ISSOD9. The megaplasmid in *S. oneidensis* appears to lack conjugation genes, making it unlikely to participate in horizontal gene transfer. This absence raises questions about its evolutionary origin and current function.

Typically, foreign-origin plasmids can be identified by differences in GC content; however, the *S. oneidensis* megaplasmid shares a GC content comparable to the host chromosome, complicating its classification. While evidence suggests that the megaplasmid is non-essential under laboratory conditions (Deutschbauer *et al*., 2011), its potential role in accessory gene functions and survival benefits remains unclear.

1.7 Genetic molecular tools in *S. oneidensis* – the CRISPR-Cas system

Targeted genetic alteration is highly desirable in genetic engineering. This is because it allows for precise modifications to genetic material, which can be crucial in various applications such as medicine, agriculture, and research. The established methods for this purpose are based on precise recombination, insertion and deletion, rearrangement, or error-prone repair. Over time, methods have evolved to become more precise and effective. Among the most common tools are bacterial artificial chromosomes (BACs), phasmid transfection, phage infection, conjugate transfer, and transposition recombination; zinc finger nucleases (ZFNs), transcription activator-like effector nucleases (TALENs), and the CRISPR-Cas system, which has emerged as one of

the most promising biotechnological tools. It represents a robust genetic engineering tool with high editing efficiency while being easily applicable (Ari *et al*., 2024).

CRISPR stands for clustered regularly interspaced short palindromic repeats, a pattern identified as having non-repeating DNA fragments, called spacers, interspaced by regular repeating sequences. These repeating patterns were identified in a number of bacteria and archaea and found to be in the proximity of CRISPR-associated genes (Cas). Spacers were later identified as being derived from viruses and other mobile elements (Jansen *et al*., 2002). Together, these components were later found to serve as a bacterial adaptive immune system. After exposure to a mobile genetic element like phages, a protospacer derived from foreign DNA is incorporated as a spacer by the Cas machinery (Bolotin *et al*., 2005; Mojica *et al*., 2005). An important step in recognition before incorporation is the presence of a protospacer adjacent motif (PAM) in the target DNA. This is crucial for host immunity against its own CRISPR activity and for recognition by the Cas protein in defense.

Based on this, multiple CRISPR types were identified. Thus far, six types with several subtypes have been identified and divided into two classes. Class 1 contains type I and type III CRISPR systems that are commonly found in archaea. Class 2 contains type II, IV, V, and VI CRISPR systems (Koonin *et al*., 2017). Here, the focus is set on the type II CRISPR-Cas9 system from *Streptococcus pyogenes*, the simplest and most broadly used. In this case, the CRISPR-Cas defense is a simple two-component system where the crRNA (CRISPR-RNA derived from spacer DNA) is expressed and cleaved from a pre-crRNA and guides the respective Cas proteins to the target (Fonfara *et al*., 2016).

In type II CRISPR, the spacer and a trans-activating RNA (tracrRNA) hybridize to guide the Cas protein to its target DNA. This was later designed as a fused RNA called a single guide RNA (sgRNA) and is widely applied today. The sgRNA guides the Cas protein to potentially any position in the genome, with the only requirement being a PAM locus (NGG in the case of SpCas9) present at the target sequence. The Cas protein represents an endonuclease, and once it reaches its target through sequence homology-guided coupling, it forms a complex that leads to a double-strand break (DSB) in the vicinity of the PAM site. In bacterial defense, the Cas protein induces a DSB to inactivate its target (Jinek *et al*., 2012). This capability was repurposed to lead to alterations at the DSB site via homologous recombination or indel formation, aiding genetic engineering.

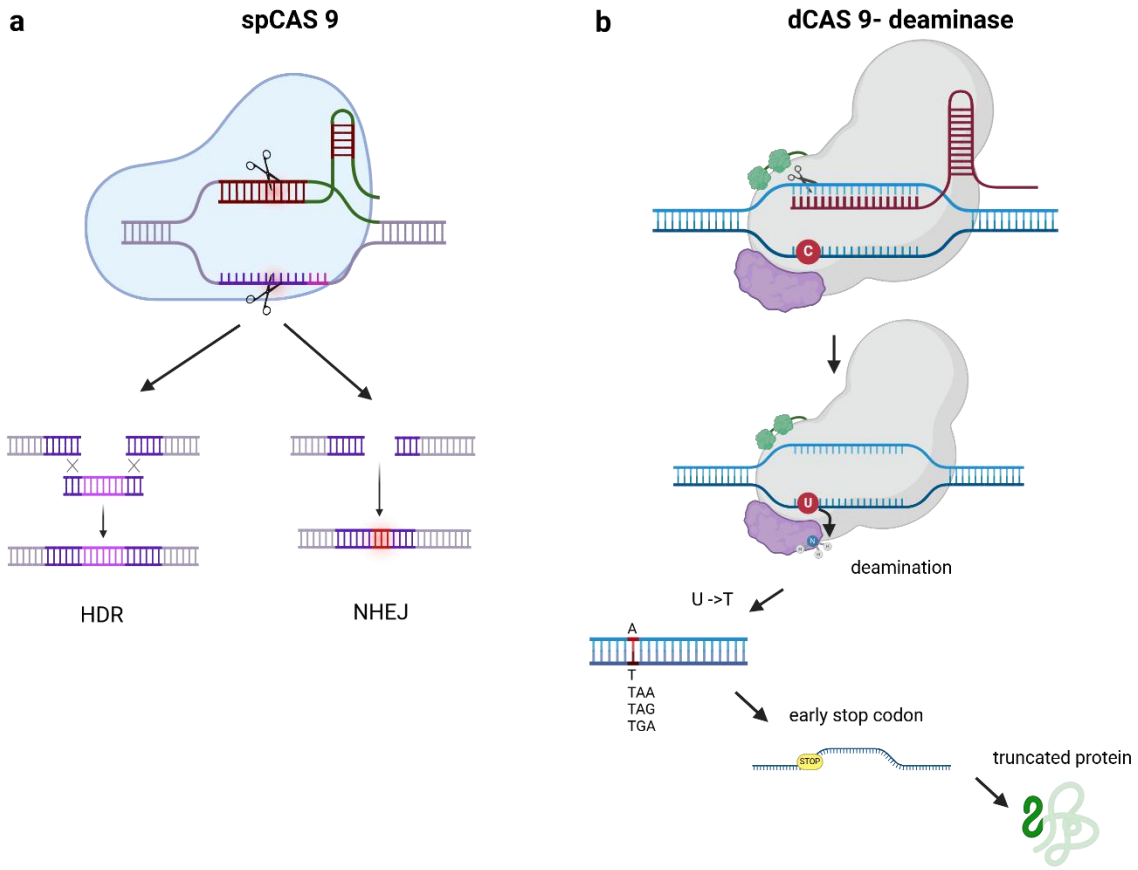

Figure 5: Comparison of two commonly used CRSIPR-Cas techniques. a) Illustration of the commonly used Cas9 variant, which induces a double-strand break (DSB) via nuclease activity. The repair pathway determines the resulting mutation. Homology-directed repair (HDR) uses homologous sequences to introduce precise mutations, while non-homologous end joining (NHEJ), an error-prone mechanism, generates insertions or deletions (indels). **b**) A CRISPR-Cas-base-editing approach, where a catalytically inactive dCas9 is fused to a base-editing enzyme. The guide RNA directs the complex to a target site, facilitating cytosine deamination to introduce an early stop codon, leading to a truncated, inactivated protein.

These Cas-based tools were further modified to enlarge their spectrum of applications. Among these modifications are a catalytically inactivated form of the Cas protein (dCas) or nickase (nCas) that doesn't induce DSBs but instead only targets DNA or nicks a strand. This protein can be fused to a cytidine or adenine deaminase. With appropriate guide design, the Cas-cytidine deaminase is used to introduce uracil in the case of cytosine, which is converted to thymine by the host repair mechanism during subsequent DNA synthesis potentially creating an early stop codon (Komor *et al*., 2016, see Figure 5).

1.8 Aim of this work

This work aimed at identifying key factors of genomic dynamics in *S. oneidensis*. Furthermore, efforts were made to genetically stabilize *S. oneidensis* with consideration for its potential as a production strain, while simultaneously analyzing the causes of the low acetoin yields observed thus far. The stabilization was aimed at decreasing mutations caused by transposon mobility. Therefore, the identification of the entirety of transposases was performed and compared with published data. Furthermore, an exhaustive analysis of the mainly unexplored transposable element activity in *S. oneidensis* was conducted. This analysis was based on transcriptomics and compared with an experiment involving whole-genome sequencing combined with stress-induced evolution. This, in turn, aimed to identify key elements that lead to the highest amount of genetic destabilization by transposition.

Based on the results of the activity experiments, an approach to lower the overall TE activity was undertaken. This approach included the establishment of the CRISPR-Cas system in *S. oneidensis*. More specifically, a Cas deaminase was used to introduce early stop codons, preventing full-length expression of the respective TE.

The second part of this work aimed at deleting the megaplasmid found in the *S. oneidensis* pangenome. A possible deletion was evaluated in terms of genetic stabilization. Here, an adaptive evolutionary approach was chosen, where all antitoxins of type II toxin-antitoxin pairs from the megaplasmid were expressed under the same expression cassette in trans from an additional plasmid.

2 Materials and Methods

2.1 Cell Cultivation

2.1.1 Strains used in this study

In the following table all strains used in this study, together with their respective identification number, genotype, plasmids and origin are listed.

Table 1: Strains used in this study.

Strain	Genotype	Source
JG 0007	*S. oneidensis* wild type strain	Venkateswaran *et al*., 1999
JG 0022	*E. coli* (DH5_Z1) *aci*q *PN25-tetR* Spr *deoR supE44* _(*lacZYAargFV169*)_80d*lacZ*_M15	Lutz & Bujard, 1997
JG 0098	*E. coli* (WM3064) *thrB1004 pro thi rps hsdS lacZ*_M15RP4–1360 _(*araBAD*)*567* _*dapA1341*::[*erm pir*(*wt*)]	Dehio & Meyer, 1997
JG 0574	*E. coli* pBAD_ara_mtrBV5	This study
JG 1892	JG7 MR1.1 adapted to iron citrate respiration	This study
JG 1958	JG98 pMQ150_RFP_in_ISSOD9/Tn3 of mega-plasmid of SO	This study
JG 1959	JG22 pBAD_AT1-10	This study
JG 1960	JG7 araP_RFP_ISSOD9/Tn3_Megaplasmid (pos. 155260-15675)	This study
JG 1981	MR1.1 -pCYR104_sgRNA_ISSOD2_contains stop codons in all ISSOD2 copies	This study
JG1982	JG98 pCYR104_sgRNA_ISSOD2	This study
JG 2034	JG7 -pCYR104_sgRNA_ISSDO1_contains stop_codons in 19 out of 43 copies	This study
JG 2038	JG98 pCYR104_sgRNA_ISSOD1	This study
JG 2045	JG7 pBAD_AT1-10_after 20 transfers	This study

2.1.2 Chemicals and enzymes

All gases used in this study were provided by Westfalen AG (Münster). All chemicals and enzymes used in this study were purchased from New England Biolabs (Frankfurt am Main), AppliChem (Darmstadt), Sarstedt AG & Co. (Nümbrecht), Merck (Darmstadt), Promega (Mannheim), Roche Diagnostics (Mannheim), Bio-Rad (USA), Carl Roth (Karlsruhe), Serva (Heidelberg) Thermo Fisher Scientific (Waltham, USA), Qiagen (Düsseldorf) or Sigma Aldrich (Steinheim).

2.1.3 Media and cultivation process

For all media buffers and solutions, double deionized water (ddH_2O) was used (PURELAB Plus, Veolia Water Technologies Deutschland, Celle). Media was sterilized by autoclavation for 20 min at 121 °C and 1 bar overpressure. All media were adjusted to a pH of 7.4. Anoxic medium was sealed in Schott® flasks with rubber stoppers. Oxygen was purged from the flasks by repeating, 2-minute-long cycles of flushing with nitrogen and applying a vacuum for 40 min before autoclaving. Heat sensitive substances were added to sterilized media through sterile filters (0.2 µm, Sarstedt AG & Co., Nümbrecht) after cooling, to avoid contamination.
For the cultivation of liquid precultures LB (lysogeny broth)-medium was used. The composition of the LB-medium is listed in Table 2.

Table 2: Composition of LB-media.

Component	Amount [g/L]
Tryptone	10
Yeast extract	5
NaCl	5

For the cultivation on solid media 2 % agar-agar (w/v) was added to the solutions. Before agar-plates were poured, medium was brought to a boil and then adjusted to 60 °C. At this point thermo sensitive substances were added if needed and plates were poured.

Table 3: Complementary solutions used in this work.

Component	Final concentration
Diaminopimelic acid (DAP)	0.3 mM
Kanamycin	50 µg/ml
Arabinose	100 µM - 500 µM
Glucose	50 mM
Sucrose	10 % (w/v)
IPTG	0.8 mM

Iron citrate containing minimal M4 medium was used for anoxic cultivation. 100 mM iron citrate was added as electron acceptor in minimal medium. Here, the respective amount of iron citrate was brought to a boil in the microwave while periodically steered. This was done until oxidation was observed (color change to black). Subsequently, M4 media (minimal medium) and 50 mM - 100 mM lactate together with trace elements were added (see Table 4; 5). Anaerobization and sterilization were performed as described above.

Table 4: Composition of the M4 minimal medium (1L).

Component	Amount
K_2HPO_4	0.22 g
KH_2PO_4	0.09 g
HEPES	1.14 g
$NaHCO_3$	0.17 g
NH_4SO_4	1.19 g
NaCl	8.77 g
Caseinhydrolysate	1.00 g
Trace elements (see Table 4)	10.00 mL
$MgSO_4$ (1M)	1.00 mL
$CaCl_2$ (0.1M)	1.00 mL

Table 5: Composition of trace element solution (100x).

Component	Amount [mg/L]
$CoCl_2$ x H_2O	119.0
$CuSO_4$ x H_2O	5.0
H_3BO_3	350.0
Na_2MoO_4 x 2 H_2O	94.4
$ZnSO_4$ x 7 H_2O	30.0
$NiCl_2$ x 6 H_2O	119.0
Na_2SeO_4 x 10 H_2O	55.4
Na_2EDTA x 2 H_2O	2501.5
$Mn(II)SO_4$ x H_2O	22.0
NaCl	58.4
$Fe(II)Cl_2$ x 4 H_2O	107.4

Microorganisms were cultivated at 30 °C (*S. oneidensis*) or 37 °C (*E. coli*), respectively. Liquid LB-medium cultures were continually shaken at 180 rpm (rounds per minute). Agar plates and anaerobic cultures were incubated without shaking. Growth was measured photometrically at 600 nm for LB, and 655 nm for iron citrate media.

2.1.4 Cryopreservation

For long term conservation of the bacterial strains, cryopreservation was applied. 1 mL of a bacterial culture in lag phase was mixed with 300 mL of glycerin in a cryotube and immediately flash-frozen in liquid nitrogen. The tube was then stored at -80 °C as well as in a liquid nitrogen container.

2.2 Molecular Biology Methods

2.2.1 Isolation of plasmid-DNA

Plasmid-DNA was isolated using *Wizard® SV Minipreps DNA Purification Systems* (Promega, Mannheim, Deutschland) according to manufacturer´s instructions. Changes were made for the volume of elution buffer. Instead of 100 µL only 50 µL of ddH_2O was used.

2.2.2 Isolation of genomic DNA

Chromosomal DNA was purified using the *Qiagen DNeasy PowerBiofilm Kit* (Qiagen, Düsseldorf, Germany) according to manufacturer´s instructions. The step for cell disruption was prolonged to 30 min.

2.2.3 Polymerase chain reaction (PCR)

The polymerase chain reaction (PCR) was employed to amplify specific DNA fragments. All reactions were performed in 200 µL PCR tubes and incubated using thermocyclers (C1000, S1000, or MJ Mini, BioRad, Feldkirchen, Germany). Preparative amplifications were carried out using PCRBIO HiFi Polymerase (PCR Biosystems, London, UK) in reaction mixtures of 15 – 50 µL. For verifying cloning steps, MangoMix® (Bioline, Luckenwalde, Germany) was used in 15 µL reaction mixtures. The composition of the reaction mixes is detailed in Table 6, and the incubation protocols for the PCR thermocyclers are outlined in Table 7. A complete list of primers used in this study is provided in Table 8.

For test PCRs targeting specific genetic loci, individual colonies were selected and directly added to the PCR mixture. In these cases, the initial heating step at 95 °C was extended to 10 min to ensure effective cell disruption.

Table 6: Composition of PCR mixtures for 15 µL.

	MangoMix®	*PCRBIO Hifi*
Master mix	7.5 µL	-
Buffer	-	3 µL
$Primer_{fwd}$ [10µM]	0.75 µL	0.6 µL
$Primer_{rev}$ [10µM]	0.75 µL	0.6 µL
Polymerase	-	0.15 µL
Template	50 ng	50 ng
ddH_2O	ad 15 µL	

In Table 7 a scheme of parameters for incubation of PCR reactions is found. Varying incubation times and annealing temperatures arise through differences in product length and primer design respectively.

Table 7: Template for the PCR reactions.

Step	Temperature	Time	Cycles
Initial denaturation	95 °C	300 s	1
Denaturation	95 °C	15-30 s	} 30-32
Hybridization	55-65 °C	15-30 s	
Elongation	72 °C	30 s/kb	
Final polymerization	72 °C	30-300 s	1

Table 8: All primers used in this study.

Primer Nr.	Name	Sequence	Purpose
Test pMQ150			
0041	pMQ150for	CTGGCGAAAGGGGGATGTG	Test-PCR in pMQ150
0042	pMQ150rev	CATTAGGCACCCCAGGCTTTAC	Test-PCR in pMQ150
Test PCR Megaplasmid			
4284	Mp test 1_F	CATAAACTCACGAATTGGAG	Test PCR on megaplasmid pos1
4283	MP test1_R	CATAAACTCACGAATTGGAG	Test PCR on megaplasmid pos1
4269	MP test2_F	GGTTAATGATGTGAGTCATTC	Test PCR on megaplasmid pos2
4270	MP test2_R	CGATACACCTGCAATACA	Test PCR on megaplasmid pos2
4267	MP test3_F	TACTCGCGACTGAAATC	Test PCR on megaplasmid pos3

4268	MP test3_R	ACATATATCCGACGTCATC	Test PCR on megaplasmid pos3
4488	MP test4_F	TCCTTGTATAGAATGTCGATT	Test PCR on megaplasmid pos4
4489	MP test4_R	ATGACATTCCAAGGTTCA	Test PCR on megaplasmid pos4
4432	AT5_F	AACCTGCTACTGACGA	Test PCR on megaplasmid pos5
4365	MP test5_R	ACAAACAGGGAAATACAGG	Test PCR on megaplasmid pos5
RFP-strain construction			
4360	500IS3_pMQ_F	CAGTGCCAAGCTTGCATGCCTGCAGGTCGACTGAACCTATCTTGGCG	Construction 500bp up homology iSSOD9
4365	500d_IS3_R	TACGAATTCGAGCTCGGTACCCGGGGATCAACCTGCTACTGACGA	Construction 500bp down homology iSSOD9
4371	500up_tnpA_ara_RFP_R	TGAATGATGTGTCCACAAAGATGTCATAAGTACACATTGGGACGAGA	Construction 500bp up homology iSSOD9
4372	ara_RFP_MP_F	CCGCAAGATCTCGTCCCAATGTGTACTTATGACATCTTTGTGGAC	Construction of ara_RFP cassette
4373	ara_RFP_MP_R	TGCACCTGTTGGGGTTTCGCTTCGCACCCTAACACCGAAAGAGGC	Construction of ara_RFP cassette
4374	ara_RFP_tnpA_MP_F	AACCGTGCGAAAAGCCTCTTTCGGTGTTAGGGTGCGAAGCGAAAC	Construction of ara_RFP cassette
4422	SO_RFP_TEST_MP_F	AGCCGGTGATAGAGG	Test-PCR im MP *S. oneidensis*
4423	SO_RFP_TEST__MP_R	AGATCACTGAGTTACTGC	Test-PCR im MP *S. oneidensis*
Construction of antitoxin cassette			
0051	pBAD_test_F	GATTAGCGGATCCTACCTG	Test pBAD integration
0052	pBAD_test_R	GGACCACCGCGCTACTGC	Test pBAD integration
4343	AT1_F	TGTTTAACTTTAAGAAGGAGATATACATACCATGAGACAAATTAGAAAACCTT	cloning pBAD_AT 1
4326	AT1_R	ATTTATCAGACAATTGGCAAGACATTATCACTAACCGTAATTAACTTCAGG	cloning pBAD_AT 1
4325	AT2_F	ACGTCACTTCCTGAAGTTAATTACGGTTAGTGATAATGTCTTGCCAATTG	cloning pBAD_AT 2
4327	AT2_R	GCCATTAAGTATTACATTGTAATACTTAATGATTACGCGATCCCTTCC	cloning pBAD_AT 2
4328	AT3_F	GCCAGAGAAAGCCTTGGAAGGGATCGCGTAATCATTAAGTATTACAATGTAATACTTAA	cloning pBAD_AT 3
4329	AT3_R	ATACATCGAAAGTCAACAAAATTGTCTATCTTTACCATTCAGTGCCC	cloning pBAD_AT 3
4330	AT4_F	TTGACGGACGAGTGGGGCACTGAATGGTAAAGATAGACAATTTTGTTGACTT	cloning pBAD_AT 4
4331	AT4_R	TGAACGATTAGTTTTAGTTTGGCCTTTTCTCTATTTCTCCGAAAAAAGAGT	cloning pBAD_AT 4
4332	AT5_F	GTACTAAAGACTCTTTTTTCGGAGAAATAGAGAAAAGGCCAAACTAAAAC	cloning pBAD_AT 5

4333	AT5_R	TTCGACGGTACTTATCAGTCAGCTTGCT ATTTAGTGAGCGGCAAGA	cloning pBAD_AT 5
4334	AT6_F	TAAAATCTACGCAGCTCTTGCCGCTCAC TAAATAGCAAGCTGACTGATAA	cloning pBAD_AT 6
4356	AT6_R	ATAATTAACACTTCAATAATATATGATG TTCTAAAAAAATAATGATACTGGCA	cloning pBAD_AT 6
4357	AT7_F	TTTGGGGTGCCAGTATCATTATTTTTTTA GAACATCATATATTATTGAAGTGTTAAT	cloning pBAD_AT 7
4359	AT7_R	CGATTCGCTCAATTTACACCAGTTGGGC GATTTATACATTGTGCTTTTGTTTC	cloning pBAD_AT 7
4358	AT8_F	GCAATGGTGAAACAAAAGCACAATGTA TAAATCGCCCAACTGGT	cloning pBAD_AT 8
4339	AT8_R	GATTAGTTTTAATTTGGCCTTTTCTTCCG CTTAGTCATACAGCCCTG	cloning pBAD_AT 8
4340	AT10_F	TGATGAGCTGGCTGCAGGGCTGTATGAC TAAGCGGAAGAAAAGGCC	cloning pBAD_AT 9
4341	AT10_R	ACTCGTTGAAATGATATGCAACTGAGA ATATCATAAAATTTTGGCGGTT	cloning pBAD_AT 9
4342	AT11_F	TTGTAAGCGGAAAACCGCCAAAATTTTA TGATATTCTCAGTTGCATATCATTT	cloning pBAD_AT 10
4344	AT11_R_new	CCGCCAAAACAGCCAAGCTGGAGACCG TTTTCATACAGGTCGTGCC	Cloning pBAD_AT 10
RFP integration position test			
4432	Rfp test_ISSOD 9pos 1	ACAAACAGGGAAATACAGG	RFP test_ISSOD 9pos 1
4433	Rfp test_ISSOD 9pos 2	CACAACCGGCACTTATC	RFP test ISSOD 9pos 2
1711	Rfp test_ISSOD9 reverse	GATAAAACGAAAGGCCCAG	RFP test_ISSOD9 reverse for both
Flanking primers for ISSOD1 and ISSOD2			
4418	ISSOD1_flanking_F	TCAACCCAAACTGGACA	For sanger seq – stop codon
4419	ISSOD1_flanking_R	ATGAGTCTGAAAAAATCACATAA	For sanger seq – stop codon
4420	ISSOD2_flanking_F	CATGCAACCATCAATGG	For sanger seq – stop codon
4421	ISSOD2_flanking_R	ATGAAAACATCAAAATTCACC	For sanger seq – stop codon

2.2.4 Quantification of DNA concentrations

The concentration of nucleic acids was determined spectrophotometrically via NanoDrop ND-2000 (Thermo Fisher Scientific, Massachusetts, USA) using 1 µL of sample. If the concentration of actual dsDNA had to be determined, Qubit™ dsDNA Quantification Assay Kit, Thermo Fisher Scientific (Waltham, USA) was used according to manufacturer´s

instructions. Absorption was measured with Tecan Plate reader Infinite 200 PRO at 485/530 nm.

2.2.5 Agarose gel electrophoresis and purification

Agarose gel electrophoresis was used to separate nucleic acids based on size. To prepare the gel, 1 % agarose (w/v) was dissolved in TAE buffer (see Table 9) by heating and repeated stirring. Midori Green Advance DNA Stain (NIPPON Genetics, Düren, Germany) was added at a concentration of 2 ppm to enable DNA visualization under UV or blue light. Once the gel polymerized, it was placed into a gel chamber filled with TAE buffer and connected to a power source (Powerpack Universal, Bio-Rad, California, USA). Samples were separated by applying an electric field at 120 V. For PCR products amplified with PCRBIO HiFi, a loading dye (see table 10) was added before electrophoresis. In contrast, MangoMix® contains a built-in loading dye, allowing samples to be directly loaded without additional preparation. A 1 kb DNA Ladder - *GeneRulerTM 1 kb DNA Ladder* (Thermo Fisher Scientific, Waltham, USA) was used to determine fragment sizes. Gel purification of DNA fragments was performed using *Wizard SV Gel and PCR Clean-up Kits* (Promega, Mannheim, Germany) following the manufacturer's instructions. Bands of nucleic acids were detected via ChemiDocTM XRS+ Systems (Biorad, Feldkirchen, Deutschland).

Table 9: Composition of the TAE- buffer (50x).

Component	*g/L*	*mM*
Tris-HCl (pH 8)	6.30	40
Acetic acid	1.20	20
Na_2EDTA	0.93	1

Table 10: Composition of the loading dye for agarose gel electrophoresis.

Component	Amount
Xylene cyanol	0.05 g
Bromphenolblue	10 mg
Glycerin	12 mL
50x TAE	1.5 mL
ddH_2O	15 mL

2.2.6 Restriction and ligation

The restriction endonucleases were purchased from New England Biolabs (Schwalbach). The digestion was executed according to manufacturer´s instructions and incubation time increased

when digestion turned out to be incomplete. In Table 11 the composition of the reaction mixture is given.

Table 11: Reaction mixture for restriction digest.

Component	Volume/concentration
Plasmid	2-3 µg
Enzyme	1 µL (each)
CutSmart buffer (10x)	2 µL
ddH_2O	ad 20 µL

After nuclease reaction was stopped the reaction mix was purified via agarose gel separation (see Section 2.2.5).

Isothermal *in vitro* ligation of DNA fragments with linearized plasmids was performed following the Gibson assembly method (Gibson *et al*., 2009). Briefly, equimolar concentrations of the DNA fragments, totaling 100 ng in a volume of 5 µL, were mixed with 15 µL of reaction mix. The detailed composition of the reaction mix is provided in Table 12, while the components of the stock solution are listed in Table 13. The reaction mixture was incubated at 50 °C for 90 min. Upon completion, the mixture was dialyzed using a 0.025 µm hydrophilic MF-Millipore membrane (Merck, Darmstadt, Germany) for 30 – 60 min.

Table 12 : Composition of the stock solution for the ligation reaction mix.

Component	Amount
Tris/HCl (pH 7.5 - 1 M)	125 µL
$MgCl_2$ x 6 H_2O (1 M)	12.5 µL
dNTPs (10 mM)	25 µL
DTT (1 M)	12.5 µL
NAD^+ (100 mM)	12.5 µL
Polyethylenglycol-8000	62.5 mg
ddH_2O	62.5 µL

Table 13: Composition of the isothermal *in vitro* ligation reaction mix according to Gibson.

Component	Amount [µL]
Stock solution (5x, see Table 12)	125
PCRBIO Hifi Polymerase (2 U/µL)	5
Taq DNA-Ligase (40 U/µL)	40
T5 Endonuclease (0.1 U/µL)	16
ddH_2O	239

2.2.7 Transformation and creation of competent cells

Electroporation was used to transform bacterial cells with plasmid DNA by applying electric pulses to create transient pores in the cell membrane. For this process, the cells needed to be competent, meaning they were capable of taking up external DNA. To induce competence, 2 mL of bacterial culture in the exponential growth phase (OD_{600} of 0.6 – 0.8) were centrifuged at 16.372 g for 30 seconds. The cells were then washed four times with ice-cold H_2O for *E. coli* or a 3 M sorbitol solution for *S. oneidensis*. After washing, the cells were resuspended in 200 µL of ddH_2O. For the transformation, 100 µL of washed cells were mixed with either 100 ng of plasmid DNA or 10 µL of ligation mix in an electroporation cuvette (1 mm electrode gap, Bio-Rad, Feldkirchen, Germany). Electroporation was carried out using electrical pulses from a MicroPulser (Bio-Rad, Feldkirchen, Germany). For *E. coli*, pulses of 1.8 kV for 3 - 5 ms were applied, while for *S. oneidensis*, pulses of 1.2 kV for 2 – 4 ms were used. Immediately after electroporation, the cells were transferred to 1 mL of LB-medium and incubated to recover: *E. coli* at 37 °C for 1 h and *S. oneidensis* at 30 °C for 2 h.

2.2.8 Conjugation and seamless genetic modification of *S. oneidensis*

To genetically modify *S. oneidensis* seamlessly, the suicide vector pMQ150 was employed. The pMQ150 plasmid was linearized, and 500 bp regions flanking the genomic section targeted for deletion were fused and integrated at the restriction cut sites via ligation (see Section 2.2.6). For gene integration (e.g., *araP_RFP* in this study), the transgene was ligated between the 500 bp homology regions. The resulting circular plasmid was then transformed into *E. coli* WM3064 (JG 98; see Section 2.2.7).

The *pir* gene carried by *E. coli* WM3064 encodes the π-protein, essential for the replication of the pMQ150 plasmid due to its R6K origin of replication. This strain was subsequently used to conjugate *S. oneidensis*. Conjugation was performed by co-streaking the donor and recipient strains on the same agar plate containing kanamycin and diaminopimelic acid (DAP) at 30 °C for 1 – 2 days. Since *S. oneidensis* cannot replicate the pMQ150 plasmid, cell death occurs unless the plasmid integrates into the genome. Due to the presence of homology regions, integration is highly specific to the intended genomic site.

To isolate *S. oneidensis*, the modified strain was transferred to new agar plates containing kanamycin. *E. coli* WM3064, being auxotrophic for DAP, cannot form colonies in the absence of DAP. Therefore, only *S. oneidensis* with integrated pMQ150 plasmid can grow. Single

colonies were selected and incubated overnight in liquid LB-medium. In the next step, recombination was promoted by plating cells on agar plates containing sucrose. The pMQ150 plasmid harbors the *sacB* gene, which encodes levansucrase, an enzyme that converts sucrose into polymers toxic to the cell. This selective pressure encourages recombination and the loss of the pMQ150 plasmid backbone integrated during the initial recombination event.

Due to the homologous regions flanking the target site, recombination can result in two possible outcomes: (1) the cells revert to their original genotype by deleting the plasmid, or (2) the desired deletion or integration occurs. These outcomes occur with roughly equal probability, depending on the impact on fitness. Therefore, colonies must be screened via PCR (see Section 2.2.3) and confirmed by Sanger sequencing (see Section 2.3.1) to validate the genetic modifications.

2.2.9 Stop codon conversion

The plasmid pCYR104, containing dCAS9-AID and the sgRNA expression cassette, was generously provided by Chen *et al*. (2023) from Tianjin University (https://doi.org/10.1016/j.synbio.2022.09.005). The sgRNA target sequence was introduced into the plasmid using 120 bp DNA oligonucleotides (forward and reverse) that included the target sequence and 50 bp overhangs. The plasmid was digested with *BsaI* and purified from an agarose gel using the Promega Wizard™ SV Gel and PCR Cleanup System (Section 2.2.6).

Before Gibson assembly, the oligonucleotides were annealed to form dsDNA in Duplex Buffer (100 mM potassium acetate, 30 mM HEPES, pH 7.5) at a concentration of 1 µM. The solution was heated to 95 °C for 2 min and then gradually cooled to room temperature. Concentration was determined with Qubit™ as described in Section 2.2.4.

The target sequence was integrated into the plasmid via Gibson assembly (Section 2.2.6) using a 10-fold excess of oligonucleotides and introduced into *E. coli* WM3064 by electroporation. (Section 2.2.7) Correct integration was verified by amplification with primers 4399 and 4400 (Table 8) followed by Sanger sequencing.

The plasmid was then introduced into *S. oneidensis* through conjugation with the WM3064 strain on LB-agar plates supplemented with kanamycin (50 µg/mL), DAP (60 µM), and IPTG (0.8 mM) as an inducer. After 48 hours, *S. oneidensis* was transferred to plates without DAP. Single colonies were screened for stop codon conversion using flanking primers 4418 to 4421

for ISSOD2 and ISSOD1 (Table 8). Finally, whole-genome sequencing (WGS) was conducted to confirm conversions across the genome.

2.3 DNA sequencing

2.3.1 Sanger sequencing

The sequencing of PCR products and plasmids was done externally using Mix2Seq Kits (Eurofins Genomics, Ebersberg) for Sanger method (Sanger *et al*., 1977). The analysis of the data was performed via CLC genomic workbench (Qiagen version 20.0.4) or with the online based tool Benchling: Cloud-based platform for biotech R&D.

2.3.2 MinION sequencing for whole genome sequencing

The library preparation was carried out using Oxford Nanopore's Native Barcoding Kits and sequenced on a MinION device equipped with an R10.4.1 flow cell (Oxford Nanopore). All procedures adhered to the manufacturer's instructions. Basecalling was performed using Dorado v0.7.0 in super-accuracy mode, with read filtering based on quality, including adapter and barcode trimming. CLC genomic workbench (Qiagen version 20.0.4) was used for sequencing data analysis and assemblies.

2.4 Data analysis and availability

2.4.1 Analysis of transcriptomic data

Subsets of transcriptomic data from internal laboratory experiments, combined with published data available on the NCBI platform, were collected for analysis. Out of the initial 20 datasets in total only 4 were used for the final data acquisition. Most datasets lacked sufficient information about transposases expression and were dropped from the analysis.

Metadata was filtered based on quality criteria and for reads corresponding to transcription of transposable element loci (90 % identity). The selected subsets were merged to quantify the read counts of individual transposons, which were then normalized and expressed as transcripts per million (TPM).

The mean TPM values were interpreted as representing the proportion of total TE activity, with 100 % representing the cumulative TE activity across all experiments. For the identification of

individual TEs, 400 bp upstream and downstream of the TEs were added in the analysis in order to lower errors arising from homologous sequence analysis within a family.

2.4.2 Identification of IS mobility

All steps were carried out using CLC Genomic Workbench (Qiagen, version 20.0.4), with standard parameters applied, unless otherwise specified.

Given that the transfers in the stress experiment likely resulted in a community of subpopulations with diverse insertion events of insertion sequences, assembly could not be performed without losing information on low-abundance integration events. As a result, raw sequencing data was utilized to create a BLAST dataset for each trial. For IS identification, a *blastn* search was conducted for each IS against the respective dataset (created from individual sequencing). This allowed the extraction of sequences associated with the targeted IS. Filters were applied to exclude sequences where reads were shorter than 90 % of the total IS length or had less than 90 % identity to the reference.

All reads were then mapped to the *S. oneidensis* pangenome. New insertions were manually identified by the presence of reads causing gaps in the reference genome. A single read was considered sufficient to count as an integration event. The identity of the TEs was confirmed using BLAST analysis against the IS Finder database (https://isfinder.biotoul.fr/).

For deletions, regions 500 bp upstream and downstream of each IS were merged *in silico*. Subsequently, all reads were mapped to these fused sequences. If mapping revealed reads covering the merged region, it was classified as a deletion at that position.

For comparison the pipeline sniffles version 2.0.7 was used. Reads were mapped against re-sequenced MR-1 WT genome (biosample SAMN46377450) via minimap in the map-ont configuration. Mappings were analyzed with the non-germline parameter and the single snfs were condensed to a VCF. The results were then analyzed in excel.

2.4.3 Variant calling

For variant detection CLC genomic workbench was used. Here fixed ploidy variant detection was used according to standard parameters and compared with variants corresponding to variant probability of 100 % and minimum count filter of 10.

Variant detection using Minimap2 (Li, 2018) and combined with variant calling BBtools (Bushnell *et al*., 2017) variant calling pipelines on the Galaxy platform (Afgan *et al*., 2018) were all used with standard parameters.

2.4.4 Phylogenetic analysis of ISSOD2 integrations

For the ISSOD2 phylogeny all sequences of ISSOD2 copies from the precursor strain combined with all found insertions of that family were gathered and compared. To compare the sequences all reads were cropped exactly at the inverted repeats. A sequence alignment was performed and rendered into a phylogeny tree using CLC genomic workbench with standard parameters. The root was set to be the ISfinder ISSOD2 consensus sequence. As closest relative ISAca1 from *Acinetobacter calcoaceticus* was chosen with an amino acid similarity of 89 %.

2.4.5 Data availability and genome assembly

All sequencing datasets produced in here were deposited on NCBI database under a bioproject with the accession number PRJNA1214554. Of note assembly of MR1.1 (JG1980) followed through metadata analysis of all sequencing data of the stress experiment (biosample SAMN46377464). Likewise, MR1.1 with stop codon induced ISSOD2 copies (JG1981) was derived from all data found in the second stress experiment (biosample SAMN46377465). Data for the ISSOD1 silencing are found under biosample SAMN46377466 (JG2034). Assembly is based on silencing experiment 1. Megaplasmid reduction data is contained in the biosample SAMN46377467 (JG2045). A resequencing of the *S. oneidensis* MR-1 wild type can be found as an assembly (SAMN46377450) and raw sequencing data (SAMN46377449)

2.5 Stress experiments

For the stress experiments, *S. oneidensis* MR-1 was precultured in minimal medium containing iron citrate. This step was taken to adopt MR-1 to iron citrate respiring conditions. The resulting culture was used as a starting point for the experiment (MR1.1) and divided to be subjected to three types of stressors (I-III): (I) UV exposure for 2 min at 14 W/m², resulting in a total dose of 1680 J/m² (per manufacturer specifications) (II) heat shock at 42 °C for 20 min (III) low concentrations of kanamycin (2.5 µg/mL).

Once the iron citrate reduction was approaching completion, indicated by a color change in the medium, samples were taken (~72 h). Optical density was measured at 655 nm, and the cell suspension was diluted to OD1 before being exposed again to the respective stressor.

Subsequently, 300 µL of the treated suspension was used to re-inoculate the iron citrate containing medium. This process was repeated over 15 cycles. One control strain was cultured and transferred additionally without stressing factors.

In a second stress experiment (*ISSOD2_stop_codon JG1981*), cells were grown in LB-medium instead of minimal medium with iron citrate as electron acceptor. They were exposed to the same UV conditions as in the first experiment. OD was measured at 600 nm and adjusted to OD1 before UV exposure. Following this, 50 µL of the treated cell suspension was used to inoculate 5 mL of LB-medium in reaction tubes. This procedure was also repeated for 15 cycles. Here MR1.1 without stop codons in the ISSOD2 copies was used as a control strain.

2.6 Adaptation experiment

To evaluate whether the resistance of the strains to their respective stress conditions increased after completing all cycles, triplicates of each strain from the stress experiments were compared to the *Shewanella oneidensis* MR-1 wild type (WT). The cells were suspended in 96-well plates and grown in LB-medium. They were then subjected to one of three conditions: increasing UV exposure durations (2 - 20 min), rising kanamycin concentrations (2.5 - 7.5 µg/mL), or incubation at 37 °C. Growth was monitored using a TECAN Infinite 200 PRO plate reader, measuring OD_{600} every 20 min for up to 16 h.

2.7 Megaplasmid reduction

A plasmid based on the pBAD backbone was designed to include all antitoxins (ATs) identified on the megaplasmid of *S. oneidensis*. The ATs were organized into a single expression cassette under the control of the arabinose promoter (P_{ara}). Identification of the ATs was carried out using NCBI annotations and verified with the TADB3.0 TA-Finder tool (Guan *et al*., 2024) under standard parameters.

To construct the AT cassette, individual ATs were amplified with overhang primers 4325 - 4334, 4339 - 4343 and 4356 - 4359 (see Table 8) and subsequently fused together using PCR. The individual and fused PCR products were purified using the Promega Wizard™ SV Gel and PCR Cleanup System. The full-length insert was then ligated into a linearized pBAD plasmid (digested with *NcoI* and *PmeI*) using Gibson assembly (Section 2.2.6 - Gibson *et al*., 2009). Correct integration was validated through PCR amplification of the AT cassette region

from the pBAD backbone, followed by Sanger sequencing using primers specific to the AT transition positions (primers 0051 and 0052 see Table 8).

The assembled plasmid, pBAD_AT1-10, was introduced into *S. oneidensis* by electroporation (see Section 2.2.7). Colonies were grown on LB-agar containing kanamycin (50 µg/mL) and arabinose (5 mM). Colonies lacking an RFP signal after 3 days of incubation were selected and transferred to fresh LB-plates containing the antibiotic and inducer. Additional selection was performed using test PCRs targeting various positions on the megaplasmid. After 20 transfers, candidates with the fewest positive PCR results were selected for WGS.

3. Results

3.1 Identification of transposases

For the analysis of transposase activity, first the elements needed to be identified and categorized. To identify transposases, information on transposon annotations for the *S. oneidensis* pangenome was initially gathered from NCBI data. This list was further extended by incorporating predicted transposable elements identified using the bioinformatic tools ISEScan (Xie & Tang, 2017) and ISMapper (Hawkey *et al*., 2015). The comprehensive list of TEs was then compared to the identified and predicted elements reported in the study by Romine *et al*. (2008). The findings confirmed that the identified TEs were consistent with the 219 TEs published in that study, and the list was deemed exhaustive.

Miniature inverted-repeat transposable elements were excluded from the analysis, as they are likely dependent on trans-acting TE activity and do not represent autonomous elements (Siguier, *et al*., 2006). The locations of the TEs on the chromosome and megaplasmid are shown in Figure 7 (indicated in red). Based on sequence homology, TEs were grouped into families, with the resulting cladogram presented in Figure 6. Closely related TEs are clustered in the tree, although the homology within families appears slightly distorted due to the inclusion of upstream and downstream regions required for unambiguous transcript identification (see Section 4.1.2).

The TE families (insertion sequence *Shewanella oneidensis*) ISSOD1 and ISSOD2 are highlighted as examples. A total of 41 TE families are proposed for *S. oneidensis* (Fredrickson *et al*., 2008; Romine *et al*., 2008), of which 25 are officially described, categorized, and incorporated into the ISFinder database - a widely recognized platform for insertion sequence family classification. The number of family members for each described TE family is provided in Table 14, while hypothetical TEs not officially categorized were grouped under "others".

3.2 Transcriptomic analysis of transposase activity

An effort to identify the most active transposases was conducted at the transcript level. Cumulative data from multiple experiments were compiled into a meta-dataset of transcripts, serving as a proxy for TE activity (see Section 2.4.1). The transcript count for each individual TE was normalized as transcripts per million (TPM), representing the percentage of total TE

activity. This information is visualized in Figure 6 as a bar diagram (on the right). Truncated or disrupted TE sequences were excluded from the analysis.

Table 14: ISSOD families of *S. oneidensis* with their copy number and ascertained percentages from total TE activity. Under the category of "others" are 24 hypothetical TEs from 16 postulated IS families.

Family	Activity [%]	Num. Of TEs	Family	Activity [%]	Num. Of TEs	Family	Activity [%]	Num. Of TEs
ISSOD1	5.5	45	ISSOD10	3.0	4	ISSOD19	0.4	1
ISSOD2	2.3	4	ISSOD11	2.5	13	ISSOD20	0.2	1
ISSOD3	2.6	19	ISSOD12	1.6	4	ISSOD21	0.3	1
ISSOD4	28	49	ISSOD13	2.9	4	ISSOD22	0.3	1
ISSOD5	3.4	6	ISSOD14	0.7	2	ISSOD23	0.8	2
ISSOD6	7.1	9	ISSOD15	0.5	1	ISSOD24	1.1	1
ISSOD7	9.9	4	ISSOD16	1.4	3	ISSOD25	0.8	5
ISSOD8	5.6	3	ISSOD17	3.5	1	Others	12.1	24
ISSOD9	2.9	2	ISSOD18	0.6	1	Total	100	210

The activity of individual TEs varied over four orders of magnitude, ranging from 0.009 % to 15.4 %. Interestingly, both extremes were represented by members of the ISSOD4 family, indicating significant variability in the mobility dynamics not only between TEs but also across copies of the same TE family. When considering total activity across TE families, ISSOD4 emerged as the most predominant. The overall distribution of TE activity across all families is provided in Table 14. Although the ISSOD1 family has a high number of 45 copies in the pangenome it is predicted to only account for 5.5 % of overall TE activity. According to the transcriptome analysis all TEs are potentially active with some showing near background level expression considering TEs make up the amount of 0.9 % of total transcripts.

3.3 Stress experiment and TE activity on the genomic level

To validate the *in silico* predictions, a stress experiment was designed to identify transposable element activity at the level of genetic manifestation. This WGS approach involved triplicates under varying stress conditions (UV, temperature, and heat shock; see Section 2.5). These stressors were selected based on their potential to enhance TE transposition, as supported by previous studies (Eichenbaum & Livneh, 1998; Lartigue *et al*., 2006; Tanaka *et al*., 2012). The experimental design spanned 15 cycles, aiming to induce transposition events and evaluate the impact of individual stressors on IS family activation. Additionally, 4 replicates from UV-stressed cells were transferred and subjected to 15 additional cycles of exposure and recovery. Consequently, the results based on WGS data presented here encompass 14 experimental trails, containing one control strain.

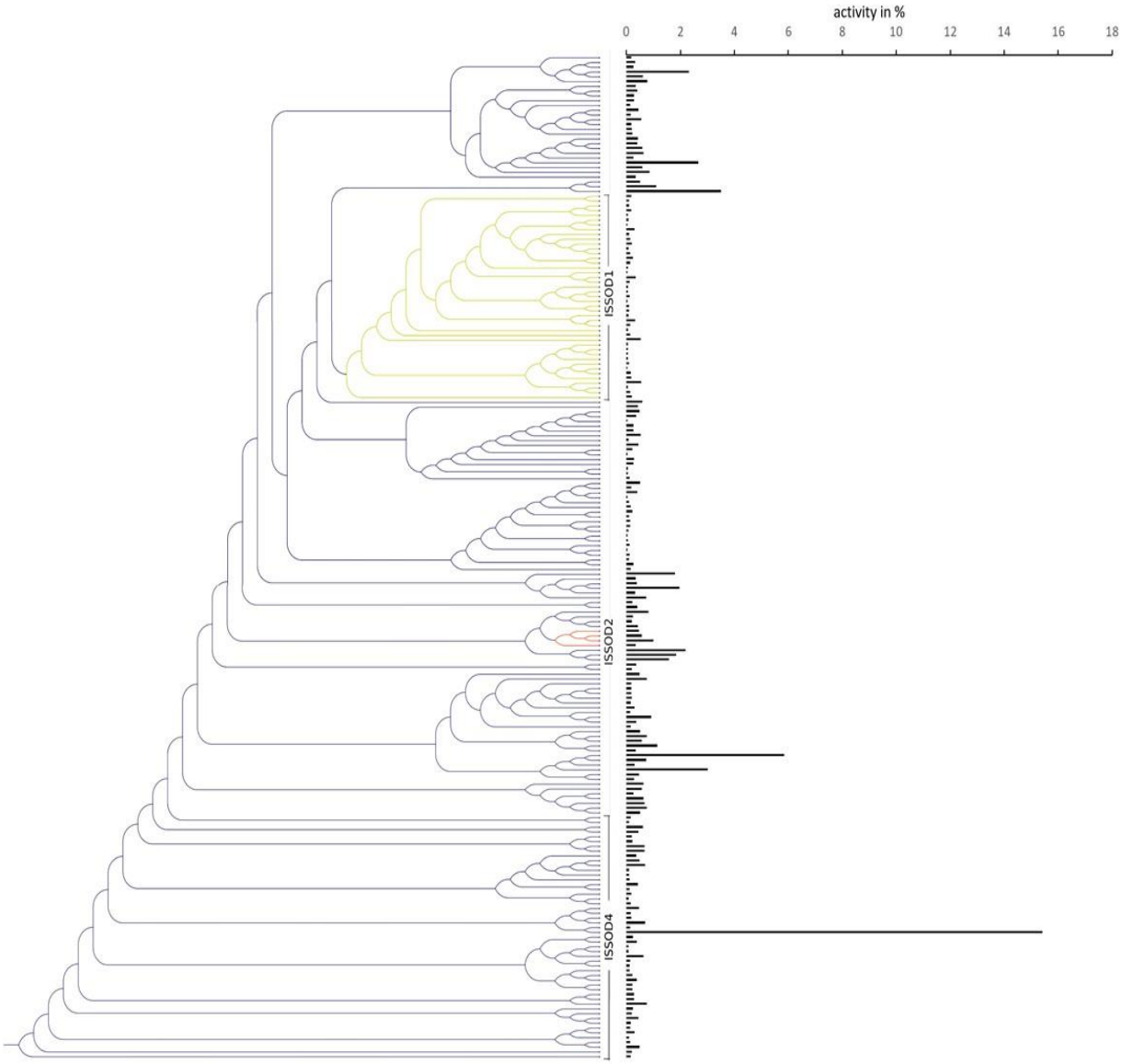

Figure 6: Cladogram of all identified TEs in *S. oneidensis* together with their respective activities. The individual TE families cluster together as a result of their sequence homologies. Bars represent the activity of individual TE from the calculated normalized total (in %). ISSOD1 and ISSOD2 insertion sequence families are highlighted in yellow and red, respectively. Additionally, the ISSOD4 family is indicated.

Prior to initiating the experiment, the *S. oneidensis* MR-1 strain was cultured in minimal medium containing ferric citrate as the electron acceptor to establish a preculture. Interestingly, even in this precursor strain, changes in the copy numbers of several ISSOD families were detected compared to the annotated genome sequence (NCBI RefSeq assembly ASM14616v2), suggesting spontaneous transposition activity prior to stress induction (Table 15). This early activity underscores the dynamic nature of TE integration in *S. oneidensis*, even under non-stress conditions. Hence, the precursor strain will be referred to as MR1.1 (submitted to the NCBI databank SAMN46377464). Notably, one of the newly identified insertions corresponds

to an integration observed by Cheng *et al*. (2020), with the distinction that the integration in this study originated from the ISSOD4 family (Supplementary Figure S1).

Table 15: The differences in TE number of the *S. oneidensis* MR-1 and the adapted precursor strain MR1.1.

	Strain	
ISSOD family	**MR-1**	**MR1.1_precursor**
ISSOD1	45	47
ISSOD2	4	7
ISSOD4	49	50
ISSOD9	2	3

In addition to all identified transposable elements, all positions where insertions occurred on the chromosome and megaplasmid are mapped in Figure 7 (indicated in blue). A total of 204 insertions were observed, scattered across the entire pangenome, with certain regions exhibiting higher insertion rates, forming hotspots.

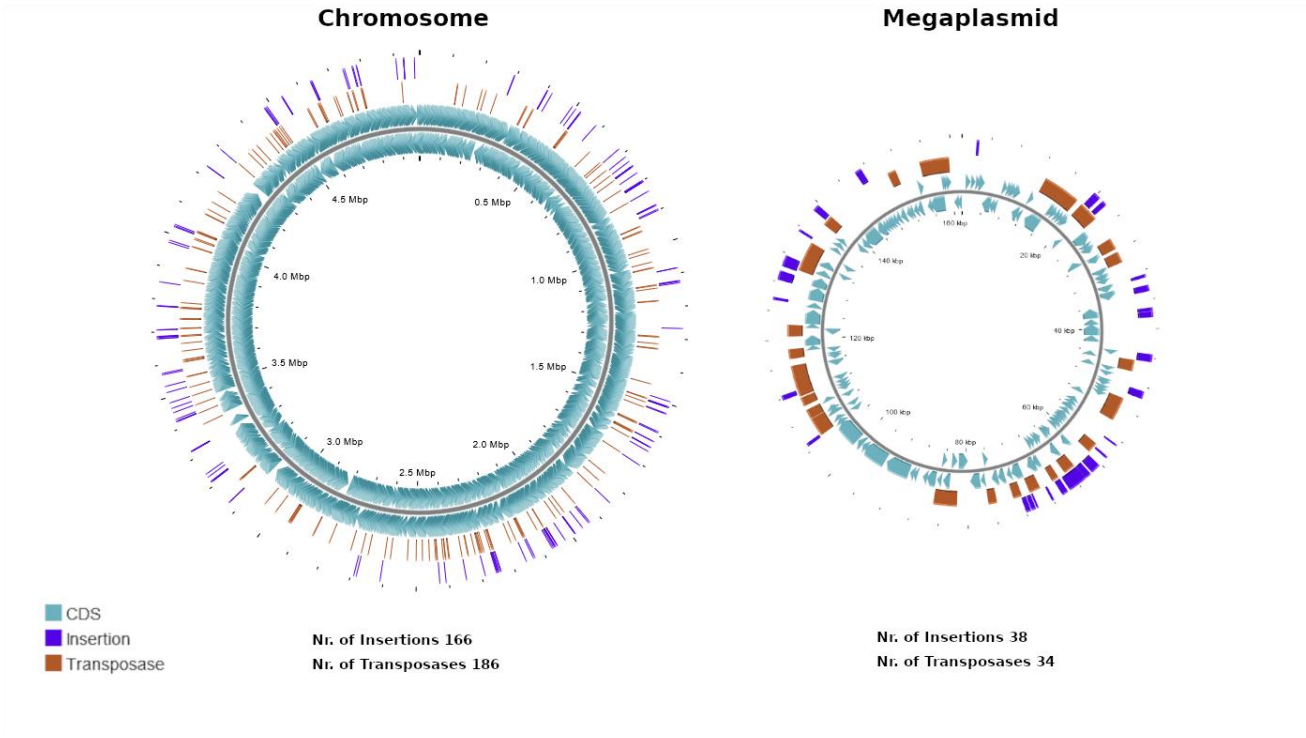

Figure 7: Representation of the chromosome and megaplasmid of *S. oneidensis* with all transposases and positions of integrations resulting from stress exposure. The number of identified transposase copies in the precursor is given below and the positions are marked. Insertions were found to occur across the whole genome. Some areas appear to be affected with higher frequency.

In line with prior expectations, the number of integrations was higher on the megaplasmid compared to the chromosome. The highest activation followed UV irradiation causing over 55 % of overall observed integrations (not including UV2; see Table 16). UV2 represents the results from an analysis based on cells exposed to 15 additional cycles of radiation as a continuation of two trails from experiment UV1 in duplicate, amounting to 30 cycles of stress exposure and are not considered for comparison. Sequencing data from 6 trails were used to identify possible activity of other TE and MITEs. Not a single read indicated any motility of these elements.

Table 16: All integration events with the originating ISSOD family identified in the stress experiment are listed. Additionally, the percentage of activity from the total of all insertions is given. The number of events on the megaplasmid and the chromosome is given and compared to the fraction of the total DNA amount they occupy. C is control, T is temperature, AB is antibiotics and UV corresponds ultraviolet exposure. UV2 represents results from the analysis of trails with 15 additional cycles of UV exposure after completion of the first UV1 trail.

integration	total	%total	In AB	In T	in UV 1	in UV 2	in C (n=1)
ISSOD1	28	13.7	3	2	13	9	1
ISSOD2	171	83.8	31	22	67	44	7
ISSOD3	1	0.5	0	0	1	0	0
ISSOD4	3	1	0	0	0	2	0
ISSOD6	1	0.5	0	0	0	1	0
ISSOD9	1	0.5	0	0	0	1	0
total	204		34	24	81	57	8
	from total	**from total %**	**% of bp from genome**				
MP	38	18.6	3.2				
Chromosome	166	81.4	96.8				

When comparing the findings from this experiment with predictions based on transcriptomic analyses, significant differences emerge. For instance, while a high level of activity was predicted for the ISSOD4 family, the genetic analysis shows that the ISSOD2 family dominates, accounting for 83.8 % of activity. Conversely, ISSOD4 contributes merely 1 % of activity, despite having 50 copies, underscoring that copy number is not directly related to TE activity. Additionally, ISSOD1 exhibited an activity level of 13.7 %, which contrasts sharply with predictions derived from transcriptomic data. A similar activity pattern was observed in the megaplasmid deletion experiment (see Section 3.7), where analysis across four trials revealed the counts found in Table 17.

Table 17: Number of integrations found in the megaplasmid reduction assay. The number is derived from metadata of 4 trails after 20 transfers (see Section 2.7).

MP deletion	ISSOD1	ISSOD2	ISSOD3	ISSOD4
Number of total insertions	15	39	1	1

For the ISSOD7 family, where four TEs were predicted to account for approximately 10 % of activity, no reads indicating ISSOD7 motility were detected in the stress experiments. This highlights a significant disparity between TE activity at the RNA transcript level and actual DNA-level integration. Based on these findings, ISSOD1 and ISSOD2 are identified as the key families driving the majority of TE activity in *S. oneidensis*. Throughout the entire experiment only two deletions could be identified for one copy of ISSOD6 and one copy of ISSOD22.

Table 18 lists genes or regions predominantly affected by integration. Because there were no follow up experiments on the phenotype except for stress adaptation and analyses were conducted in mixed cultures, there is no feedback on gene function by disruption. It is apparent, that intergenic or redundant loci were predominantly affected. Most integration observed, where coding sequences (CDS) were disrupted, represent either TEs itself, hypothetical proteins or protein with domains of unknown function (DUF domain), likely not essential for cell survival. This shows how hotspot areas might evolve. Genetic loci with redundant function are more likely to be subject to integrations, almost exclusively being redundant themselves. An example can be found in the region around 60 kbp on the MP in Figure 11.

Table 18: List of targets predominantly affected by TE integration.

Gene or locus	transposase	Toxin (type 2 toxin-antitoxin)	Intergenic	Hypothetical protein	DUF domain protein	Sigma factor - σ^{54}
Number of integrations	53	2	47	41	12	9

3.4 ISSOD2 phylogeny

Given that ISSOD2 constitutes the majority of transposable element activity, a focused analysis was conducted to identify its most active members in the precursor strain. New integration events could originate from one of the four base copies in the MR1 wild-type strain or from the four additional copies that emerged before the experiment began in the precursor MR1.1 (ISSOD2base 1 – 4 in MR1 and ISSOD2_all_new1 - 4 in MR1.1 in Figure 9). To track these

events, all 185 integration sequences of ISSOD2 that were transposed and copied in the stress experiments were aligned to identify polymorphisms among the copies.

IS copies accumulate polymorphisms over time, which are passed on during transposition (Figure 8). This allows for tracing certain base pair mutations to specific ISSOD2 lineages, identifying the base copy from which transposition originated.

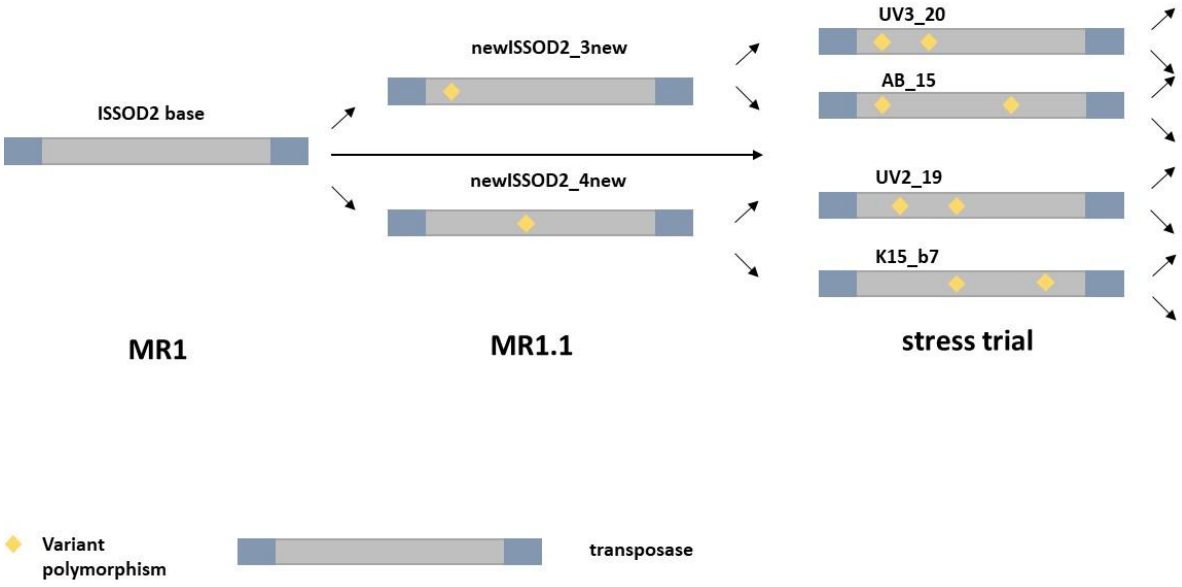

Figure 8 : Schematic illustration of the propagation pattern of the ISSOD2 family. Shared patterns in the SNVs can be linked to common ancestry and be used as a proxy for activity of individual base copies. The yellow squares represent a base exchange that can be used to infer the origin of a newly integrated ISSOD2 copy.

Some SNVs unambiguously identified that particular transposition events stemmed from a specific ISSOD2 base copy. Notably, SNVs consistently found in all "newISSOD_all_new" elements and "base 1" suggest their ongoing activity (see Supplementary Figures 4 - 7). These findings indicate that the elements remained active post-transposition and gradually diverged.

A comparison of all copies from the UV 3_20 experiment revealed SNVs that appeared multiple times but were absent in the precursor base copies (Supplementary Figures 8–9). This suggests that several copies originated from a common ancestral copy, not represented by a base copy, supporting the hypothesis that successive waves of expansion produced additional active copies. Conversely, some copies exhibited signs of deterioration over time, indicating a slowdown in expansion (Supplementary Figure 10).

To visualize an activity profile based on the progressive mutation, a phylogenic tree was created that represents the degree to which the identified new integrations are related in the sequence alignment. Copies derived from the same precursor should cluster closely in the resulting phylogenetic tree (Figure 9).

The root for the phylogenetic tree was chosen as the consensus sequence available on the ISFinder platform. For contextual placement, ISAca1, the closest related IS element from *Acinetobacter calcoaceticus*, was included as an outgroup. The analysis revealed multiple branching clusters, possibly representing distinct waves of expansion.

Notably, all four ISSOD2 copies found in the MR-1 wild type strain clustered closely with the consensus sequence, reflecting their high or identical sequence identity to the archetype. These copies represent the original source of all subsequent ISSOD2 copies, making it difficult to trace individual insertion events to specific precursor IS copies. However, one exception, designated as “base_1,” appeared on a separate, smaller branch which can be explained by the specific SNV found for this copy (Supplementary Figure 4; see Figure 9).

Sequences clustered around the base elements are inferred to have been inserted early in the experiment. The four additional ISSOD2 copies found in the precursor strains (stress experiment one and two) and therefore present across all experimental trails, were observed to branch off further from the base cluster. Notably, in the case of “newISSOD2_all_3new” and “newISSOD2_all_4new,” as well as “newISSOD2_all_1new” and “newISSOD2_all_2new” combined, substantial numbers of additional copies were identified within their respective branches. This clustering pattern, along with unique SNVs linking new copies to their predecessors, suggests that newly transposed ISSOD2 copies continued to serve as active sources for subsequent transposition events.

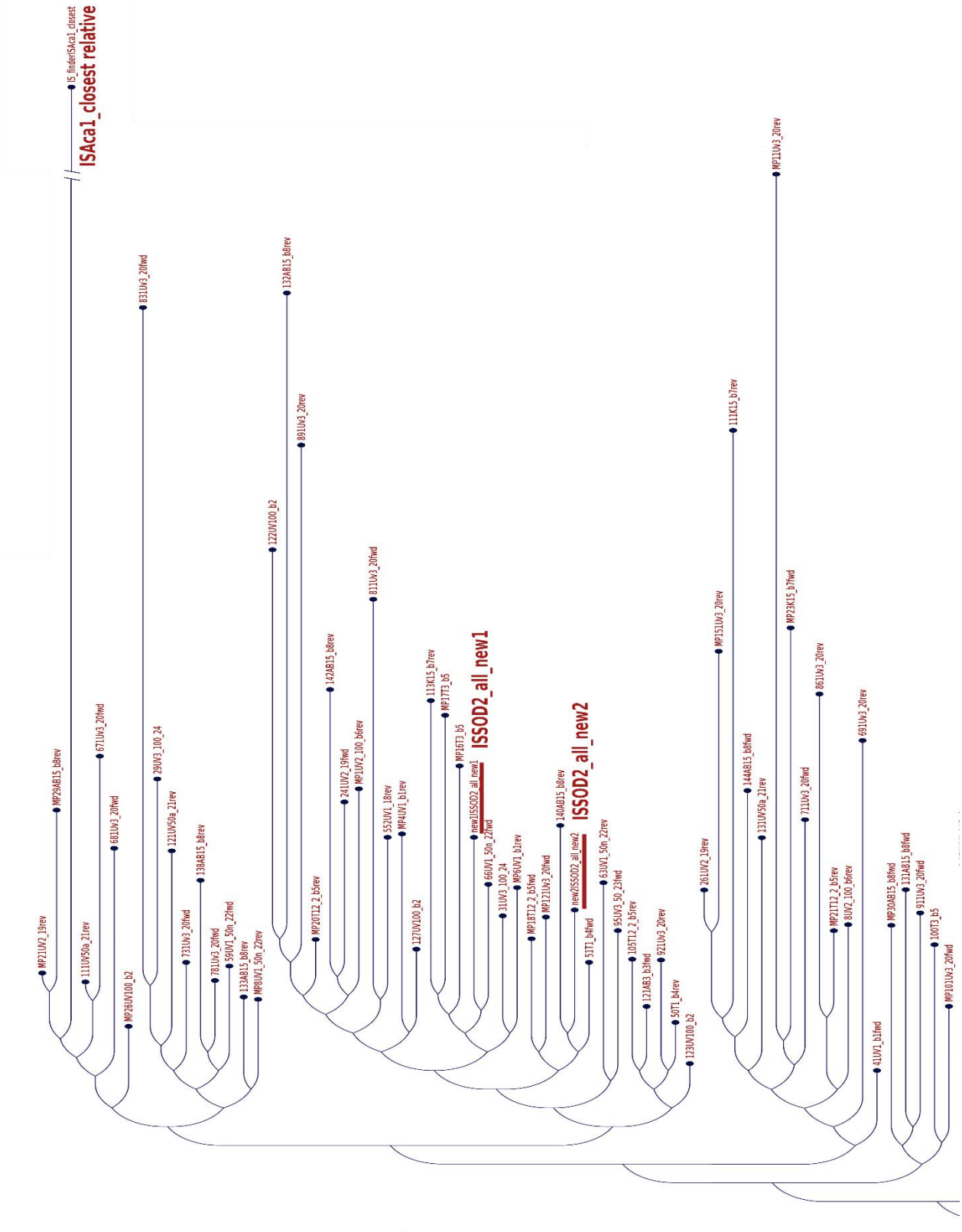
IS_finderISAca1_closest
ISAca1_closest relative
ISSOD2_all_new1
ISSOD2_all_new2

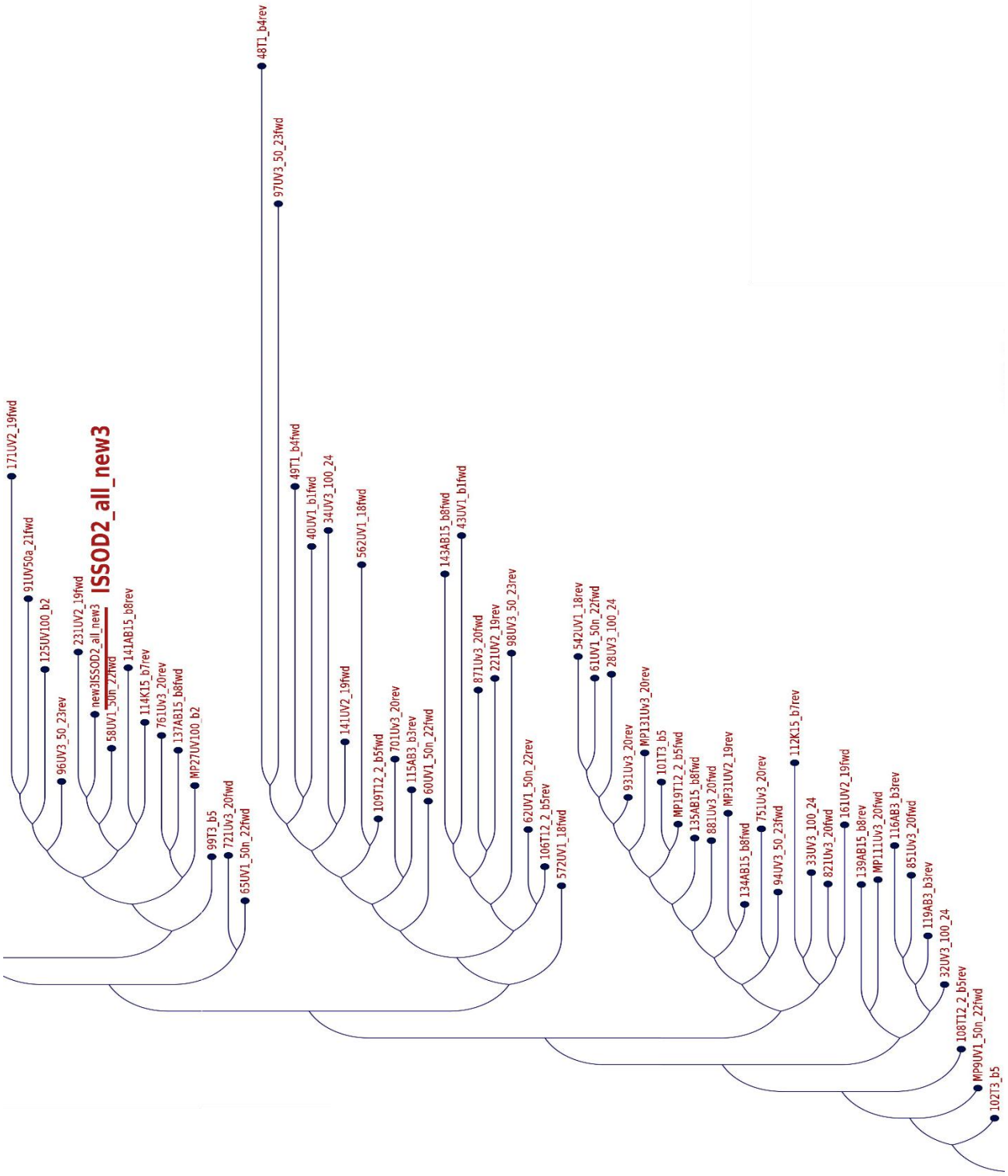
ISSOD2_all_new3
171UV2_19fwd
91UV50a_21fwd
125UV100_b2
96UV3_50_23rev
231UV2_19fwd
new3ISSOD2_all_new3
58UV1_50n_22fwd
141AB15_b8rev
114K15_b7rev
761Uv3_20rev
137AB15_b8fwd
MP27UV100_b2
99T3_b5
721Uv3_20fwd
65UV1_50n_22fwd
48T1_b4rev
97UV3_50_23fwd
49T1_b4fwd
40UV1_b1fwd
34UV3_100_24
562UV1_18fwd
141UV2_19fwd
109T12_2_b5fwd
701Uv3_20rev
115AB3_b3rev
60UV1_50n_22fwd
143AB15_b8fwd
43UV1_b1fwd
871Uv3_20fwd
221UV2_19rev
98UV3_50_23rev
62UV1_50n_22rev
106T12_2_b5rev
572UV1_18fwd
542UV1_18rev
61UV1_50n_22fwd
28UV3_100_24
931Uv3_20rev
MP131Uv3_20rev
101T3_b5
MP19T12_2_b5fwd
135AB15_b8fwd
881Uv3_20fwd
MP31UV2_19rev
134AB15_b8fwd
751Uv3_20rev
94UV3_50_23fwd
112K15_b7rev
33UV3_100_24
821Uv3_20fwd
161UV2_19fwd
139AB15_b8rev
MP111Uv3_20fwd
116AB3_b3rev
851Uv3_20fwd
119AB3_b3rev
32UV3_100_24
108T12_2_b5rev
MP9UV1_50n_22fwd
102T3_b5

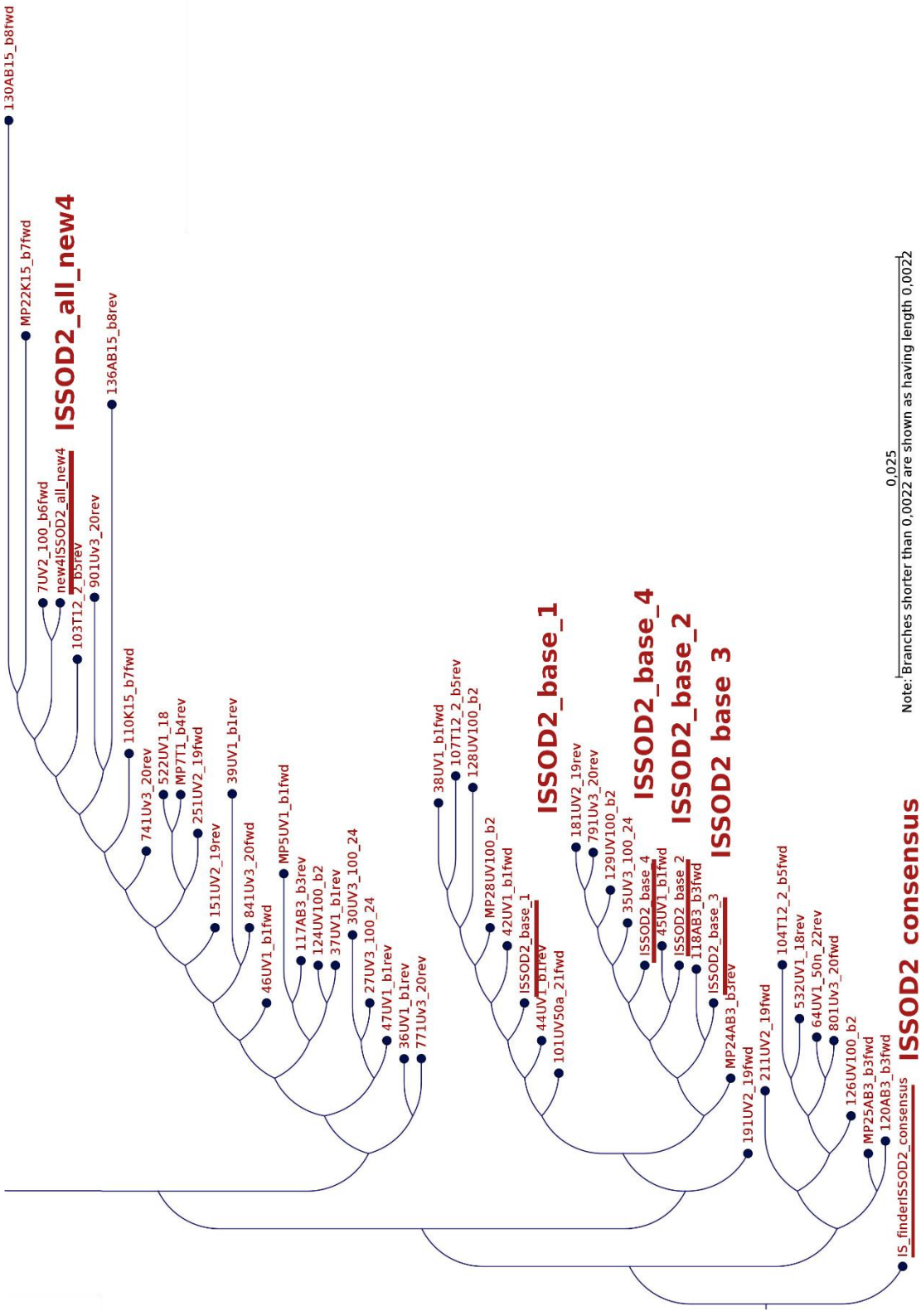

Figure 9: Phylogenetic tree of all ISSOD2 copies from integrations analyzed in this study. The root positions and consensus sequence are highlighted with a red underscore. ISAca1 was chosen as a closest relative and appears closer here as represented by actual sequence relation to fit the figure.

3.5 Adaptation experiment

To evaluate whether adaptation occurred in response to repeated stress exposure, the endpoint strains after the stress cycles to the *S. oneidensis* MR-1 were compared. For each trial and stressor, triplicate cultures were inoculated into a 96-well plate, exposed to gradually increasing stress levels (see Section 2.6), and compared to WT viability under these conditions. The experiment aimed at identifying any fitness advantages gained through transposition-mediated adaptation. The corresponding growth curves are presented in Figure 10.

Under non-selective growth conditions, the viability of the evolved strains was comparable to wild type performance, suggesting minimal or no detrimental mutations. However, as stress levels increased, overall viability generally decreased. In the case of antibiotic exposure, two out of three evolved strains outperformed the wild type, while one strain appeared more susceptible to stress caused by the antibiotic. Under temperature stress, one strain exhibited similar viability to the wild type, another was less viable, and one outperformed the wild-type at 37 °C. UV exposure was the only stressor where all evolved strains consistently outperformed the wild type. Notably, all triplicates, including the wild type, remained viable after 20 minutes of UV exposure. In summary, adaptation was observed in 5 out of the 9 cases.

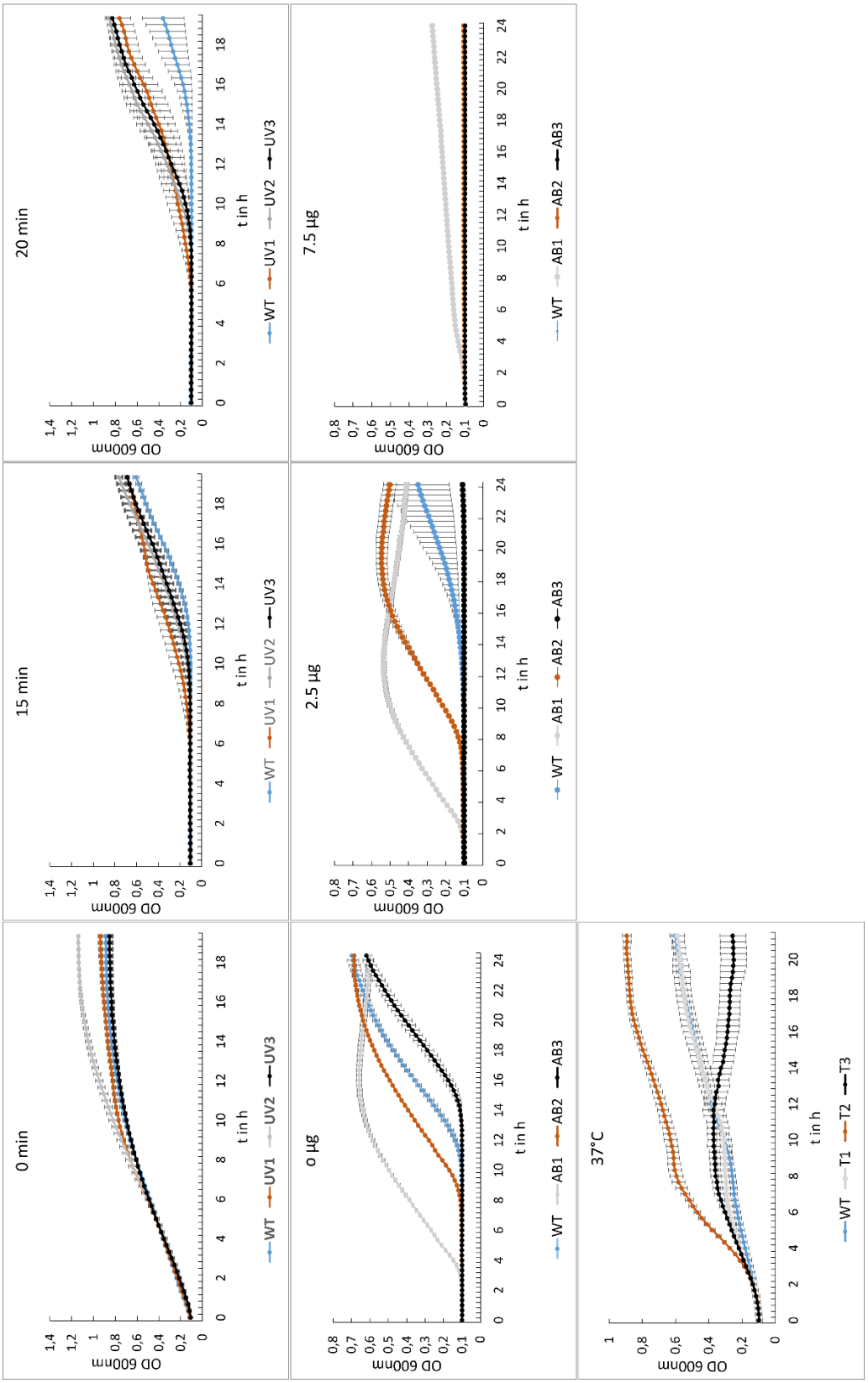

Figure 10: Growth curves of the adaptation experiments. The potential adaptation of strains from the stress experiment was assessed. Strains that previously underwent 15 cycles of stress induction were exposed to increasing intensities of kanamycin, UV radiation, or elevated temperatures (37°C) and compared to *S. oneidensis* MR-1 under the same conditions. Overall, fitness declined as stress intensity increased. However, 5 out of 9 adapted strains outperformed the wild-type strain.

3.6 Stop codon conversion and inactivation of ISSOD1 and ISSOD2

After identifying the most active IS families, targets for introducing stop codons into the transposases of both ISSOD1 and ISSOD2 using the CRISPR-dCas9 cysteine deaminase system were designed. Notably, the high sequence similarity within transposase families allowed the use of a single sgRNA to target all transposase copies of a given family. The MR1.1_precursor strain was chosen for these experiments to ensure comparability with the insertion frequencies observed in previous experiments. All seven ISSOD2 copies in the precursor strain were successfully modified with stop codons.

To evaluate whether this conversion effectively halted transposable element motility, the stress induction experiment limited to UV exposure (see Section 2.5) was repeated. The observed integrations are listed in Table 19. The modification successfully halted transposition, as evidenced by the absence of ISSOD2 insertions, compared to the 14 insertions observed in the WT control under identical conditions. These findings confirm that stop codon conversion effectively inactivates ISSOD2 activity. Furthermore, again a distinct preference for integration into the MP was observed, with 41 % of the insertions occurring in this region.

For ISSOD1, the same approach was applied in four independent experiments. Between 6 and 19 out of 45 transposase gene targets were successfully mutated in each experiment, resulting in the conversion of a total of 75 % of all ISSOD1 copies across the attempts. However, in all four cases, it was later discovered that ISSOD9 integration into the dCas9 deaminase disrupted further stop codon conversion.

Table 19: Comparison of numbers of integrations of all insertion sequence families for inactivated ISSOD2 strains with the control strain. Stop codon silenced strains are indicated with ΔISSOD2. The experiment was repeated three times. The number of hits with corresponding percentage on the megaplasmid are given.

	WT	ΔISSOD2-UV1	ΔISSOD2-UV2	ΔISSOD2-UV3
ISSOD1	0	5	1	1
ISSOD2	14	0	0	0
ISSOD6	1	0	0	0
Total	22			
Hits on MP	9	≙ 41 % of all hits		

3.7 Megaplasmid reduction

The possibility to delete the megaplasmid was tested, to potentially further stabilize *S. oneidensis* genetically. To achieve this, a pBAD-based plasmid containing all ten antitoxin genes from the toxin-antitoxin (TA) pairs located on the MP, driven by an inducible promoter was designed. For the purpose of simplified readouts an RFP reporter strain was developed. Here, the fluorescent protein was introduced in one copy of the ISSOD9/tn3 transposase found on the MP (see Section 2.2.8). In this strain the pBAD_AT1-10 plasmid was introduced and transferred serially. Throughout the experiment, the AT-cassette was continuously expressed. The hypothesis was that the presence of the antitoxin genes on the plasmid would, over time, lead to the loss of the MP. Once the RFP signal was lost, subsequent transfers were coupled with PCR tests targeting the MP backbone. Selected colonies were then subjected to whole-genome sequencing.

While complete MP loss was not achieved, a reduction of its size by approximately 56 kbp, equivalent to 35 % of the total length, was feasible. The DNA segments deleted during this process are illustrated in Figure 11, with their respective sizes detailed in Table 20. The areas are annotated according to their most noticeable feature.

Notably, six AT-gene pairs were removed from the megaplasmid. Interestingly, the *ori/repA* region was entirely lost. The loss of the *ori/repA* region was unexpected but aligns with observations from independent sequencing datasets, which frequently showed this region located separately from the rest of the MP backbone. This suggests the presence of an alternative, undefined origin of replication (*ori*) on the MP (seq data on NCBI SAMN46377467).

All WGS assemblies of *S. oneidensis* conducted in this study yielded three distinct contigs. One for the chromosome and two for the MP. Both resulting MP fragments contained copies of ISSOD9, leading to the hypothesis that the *ori/repA* flanking ISSOD9/Tn3 transposases might represent a stabilized cointegrate intermediate formed via the Tn3 transposition mechanism (see discussion Section 4.5).

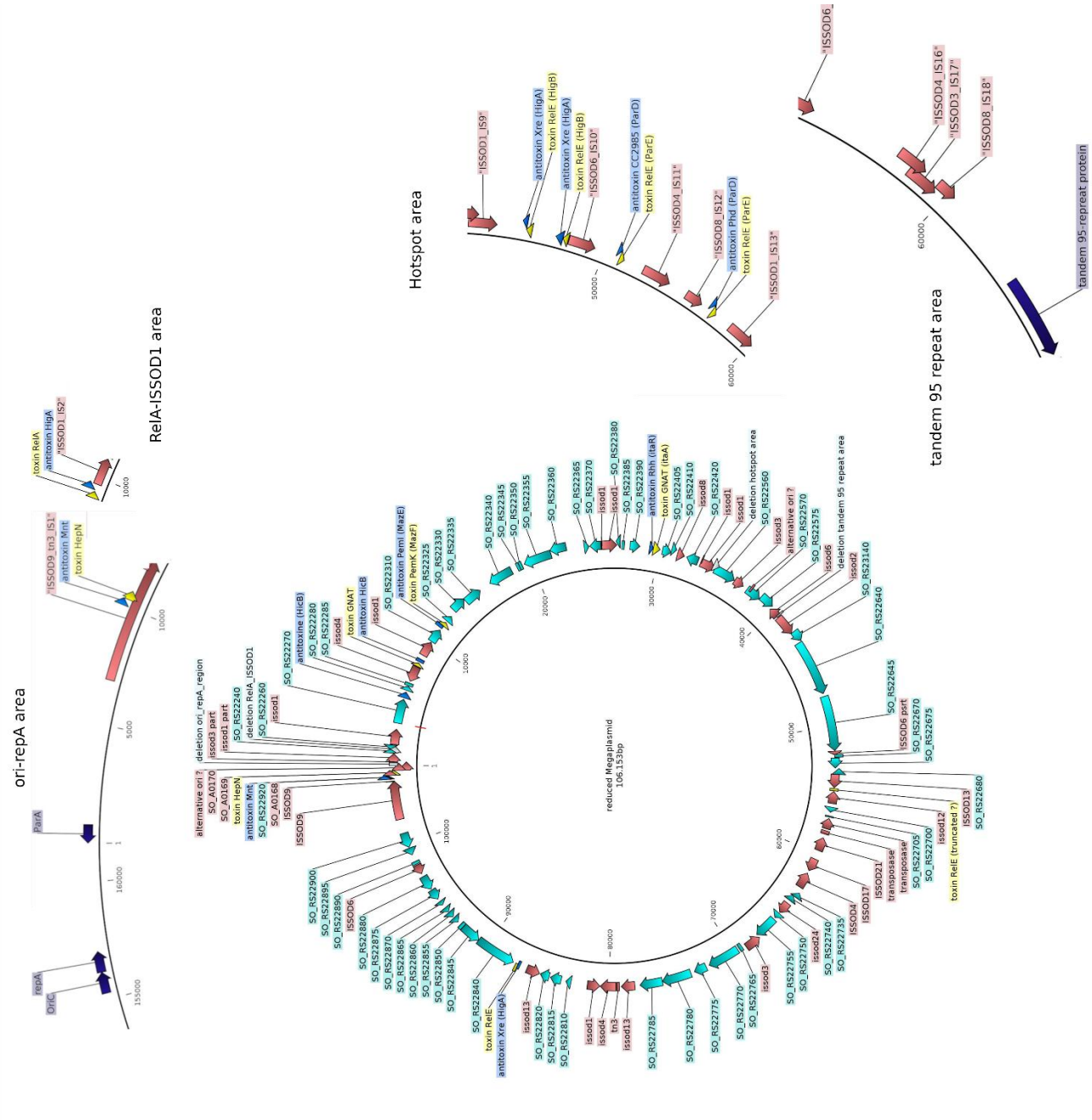

Figure 11: An annotated version of the reduced megaplasmid and the deleted areas. The areas are placed relative to the positions they previously occupied in the original MP and are named according to their most noticeable feature. Indicated in red are TEs. Antitoxins and corresponding toxins are colored in blue and yellow, respectively.

To test the cointegrate hypothesis, replicons, each containing a single ISSOD9/Tn3 copy derived from a hypothetical cointegrate resolution, were generated *in silico*, (as shown in Figure 12). Analysis of sequencing reads spanning the ISSOD9/Tn3 flanking regions revealed uninterrupted reads crossing these boundaries. These reads did not align with a megaplasmid configuration where *ori/repA* remains flanked by two ISSOD9/Tn3 copies (assembly NCBI SAMN46377450). This observation suggests that some MPs underwent recombination or

cointegrate resolution, pointing to a metastable state of the MP. This instability appears to be centered at the interface between ISSOD9 copies and the MP backbone, where both parts typically coexist.

Table 20: Regions that were deleted from the megaplasmid of *S. oneidensis*. The sections were named after a representative feature and their sizes are given and compared to the total of the original megaplasmid.

Area	*Ori/repA*	hotspot	RelA/ISSOD1	Tandem-95-repeat	**Total**	Megaplasmid SO MR-1
Size (bp)	19252	16509	1933	18022	**55716**	161613

Multiple insertions of ISSOD2 and ISSOD9, into the pBAD_AT1-10 plasmid, were found after 20 transfers. The assessment if complete MP loss failed due to essential genes, incomplete expression of all ATs or disruption of AT expression caused by integration of ISSOD2 or ISSOD9 is therefore inconclusive.

3.8 Analysis of the acetoin production strain

In a different study concerned with the acetoin production strain (as described in Section 1.3) the problems with production were reevaluated. The production plasmid carrying the acetoin genes was sequenced and found to contain an incomplete *alsS-alsD* expression cassette. The expression cassette was replaced with a functional version; however, anaerobic acetoin production still could not be achieved despite glucose consumption. In this study, disruption of the Cas-deaminase plasmid and the AT-expression cassette plasmid by ISSOD9 was identified in 8 independent trials. This suggested that acetoin production was disrupted due to transposable element integration, likely arising from ISSOD9 transposition. Based on this whole-genome sequencing of an adapted strain created by Miriam Edel, named 1732_SO_10A (*S. oneidensis* MR-1 Δλ Δ*ackA pta* Δ*ldhA*::P_{stc}*glk_galP* +pBADP_{stc}*alsSD* _10A) was conducted, confirming that the production cassette was disrupted at the *alsD* locus. Based on this finding, another strain from the same adaptation, 1730_SO_B4 (*S. oneidensis* MR-1 ΔλΔ*ackA pta* Δ*ldhA*::P_{stc}*glk_galP* +pBADP_{stc}*alsSD*_4B), was analyzed. Due to the limitations arising from previous Illumina sequencing data of this strain, identifying multicopy element integrations, such as TEs, posed challenges. To address this, all reads associated with ISSOD9 were first filtered separately and then mapped to the pBAD_*alsS-alsD* plasmid. Indeed, mapping reads were identified that associated both with the *alsS* region of the plasmid and the ISSOD9 TE. This integration could only be detected based on predictions from experiments conducted in this study, linking

ISSOD9 activity to plasmid disruption. These findings demonstrate that in both cases, acetoin production was rendered infeasible due to TE integration dynamics.

4. Discussion

4.1 Transposase activity

4.1.1 A general consideration

Though transposable elements are often dismissed as genomic parasites - a viewpoint still prevalent today - the situational evaluation often should be considered more complex. Although likely related to viruses, TEs seem to be divided by one evolutionary nuance comparing the invading selfish nature. In this study, all UV-adapted strains exhibited higher fitness than the wild type *S. oneidensis* strain after repeated irradiation exposure. While many transposition events are detrimental, numerous reports indicate that TEs can help shape the genome by forming operons (Kanai *et al*., 2022), facilitating beneficial rearrangements or cause advantageous integrations (Siguier *et al*., 2006; Wagner, 2006). For example, in *S. oneidensis*, an ISSOD1 insertion rescued an electron transport - deficient phenotype, increasing host fitness under ferric citrate - reducing conditions (Schicklberger *et al*., 2013). TE activity is not merely programmed to proliferate uncontrollably but rather reaches an equilibrium with the host over time. Hence the relationship between host and elements, after an initial transposition burst, is conceptually more reminiscent of co-existence (Good *et al*., 2017; Iranzo *et al*., 2014). Although the benefits conferred by TEs may be indirect, the co-evolution of hosts and transposons places these elements at a crossroads between expansion and the host's need to adapt for survival (Kleckner, 1990). Unchecked accumulation of TE copies would inevitably decrease host fitness, as described by Muller's ratchet (Siguier *et al*., 2014), whereas deletional bias could lead to complete TE loss over time (Mira *et al*., 2001). Yet, neither scenario appears to dominate in nature. Results here further indicate that TE activity cannot be inferred solely from copy number. In the *S. oneidensis* strain, stress-induced activation of TEs increases the likelihood of host adaptation to environmental changes. The environmental context is crucial when assessing the role of genetic elements: traits like CO_2 fixation, degradation abilities, or antibiotic resistance might impose a metabolic burden if unnecessary, but under changing conditions, they may offer a significant fitness advantage (Schneider & Lenski, 2004).

In this light, the role of TEs in nature might be sought. After acquisition via e.g. horizontal gene transfer and an initial burst of expansion, as in the case of ISSOD2, a baseline TE activity is maintained, balancing deletion bias against the metabolic costs of high TE numbers (as seen with ISSOD4). This balance preserves the potential for adaptation, enabling TEs to expand the

genetic toolkit necessary for responding to new challenges, such as UV irradiation or growth facilitated by iron citrate respiration. Over time, these elements may even adopt regulatory roles or be domesticated by the host (possibly as with IS73_ISSOD4; Consuegra *et al*., 2021; Siguier, Perochon, *et al*., 2006; Tempel *et al*., 2022; Zhang *et al*., 2019)

4.1.2 Transcriptomic analysis

In the transcriptomic analysis, only about 1 % of overall transcripts could be ascribed to transposable elements, despite 5.6 % of all coding sequences being TE-related. This low transcript number suggests that overall TE mobility is restrained. Generally, insertion sequences are among the lowest expressed genes due to the potentially detrimental consequences of their activity (Kleckner, 1990; Nagy & Chandler, 2004). The highest predicted activity was attributed to the 49-member ISSOD4 family, which is estimated to account for over one quarter of all TE activity. However, when compared to the genetic evidence from the stress experiment, two key differences emerge: first, the overall TE activity inferred from transcriptomic data appears to be highly underestimated, and second, the major contributors to observed insertions are the ISSOD1 and ISSOD2 families. Additionally, ISSOD9, with a predicted activity of 2.9 %, was found to predominantly integrate into plasmids in 10 independent experiments.

Sequencing the actual genetic manifestations of transposition is likely more accurate than transcriptomic analysis, which provides only a snapshot of gene expression (Bourque *et al*., 2018). While mixed culture transcript levels can yield predictive mean values, multiple factors contribute to discrepancies between transcript abundance and actual transposition events.

As described in the introduction (Section 1.5.2), IS1 and IS3 elements (e.g. ISSOD1 and ISSOD2) possess intricate regulatory mechanisms built into their structure (Sekine *et al*., 1999). These transposases comprise two overlapping open reading frames, and the expression of a fusion product from both ORFs is necessary for transposition (Siguier *et al*., 2015). This process requires programmed translational frameshifting - ribosomal slippage - to produce the full-length protein (Chandler & Fayet, 1993). A common byproduct is a small ORF-A protein that contains an inverted-repeat-binding leucine zipper motif (Haren *et al*., 1998), which further regulates TE expression. Transcriptomic analyses are typically unable to differentiate among the various products derived from such compact elements. An integral step in the transposition mechanism is the formation of a circular intermediate with a highly active P_{junc} promoter (Lewis

et al., 2004), which leads to a brief surge in transcripts at the time of mobilization - posing challenges for the time resolution of transcriptomics.

TE activity can also be modulated by their genomic localization. Background transcript levels may partly reflect transcriptional readthrough (Turnbough, 2019), while other factors - including chromatin density, secondary structures at the residing loci, host DNA-binding regulators, chaperones, and epigenetic modifications such as methylation - can affect transcription (Nagy & Chandler, 2004). Furthermore, some TEs produce antisense RNA (Ross *et al*., 2010) that mediates self-silencing, and translation initiation sites may be sequestered by secondary structure formation (Rezsöhazy *et al*., 1993). These factors vary over time, influencing transcript counts. The mutation of IS can render them catalytically inactive while still being transcribed. In addition, TEs may be expressed from upstream promoters (Escoubas *et al*., 1991). Rarely, transactivation from other TE copies within the same family may occur.

Analyzing multicopy elements is inherently challenging. TEs often carry their own, typically weak, promoters (as seen in IS3 elements with identical promoter sequences across family members – Nagy & Chandler, 2004), which adds another level of regulation (Siguier *et al*., 2014). In this study, it was attempted to identify individual TEs by matching 400 base pairs of upstream and downstream regions of the elements to the resulting transcripts. If elements are transactivated or produce readthrough transcripts, active TEs can be individually distinguished. Conversely, reads that originate from external promoter components (for IS3 elements such as ISSOD1 and ISSOD2, or IS256 elements such as ISSOD4) may be attributed to upstream regions and do not necessarily encode TE sequences (Prentki *et al*., 1986). In these cases, the expression of downstream genes is maintained without conferring transposition potential (Schmitz-Esser *et al*., 2011). The IS73_ISSOD4 copy - representing 15 % of all TE transcripts (see Supplementary Figure S2) - likely falls into these categories.

In summary, the presence of TE transcripts does not directly equate to active transposition; rather, it reflects the complex regulatory network associated with transposons. The ISSOD4 family possibly represents an IS element that underwent expansion and has since been integrated into the host regulatory network, maintaining activity primarily for regulation (Chuong *et al*., 2017). In contrast, ISSOD2 might represent a recently acquired element that is still undergoing expansion harboring adaptation potential.

An alternative approach to assessing TE activity would be to quantify transposon proteins within the proteome (Maringer *et al*., 2017). Although such proteomic analyses still suffer from low time resolution and cannot differentiate among individual IS copies, they do measure proteins that are actually translated. Romine *et al*. have provided evidence, via proteomics, for the activation of ISSOD1, ISSOD4, and ISSOD9 under the conditions tested. However, the question remains as to why ISSOD2 appears inconspicuous in proteomic data while ISSOD4 was found to be actively translated.

4.1.3 Stress experiments

This part of the study aimed to identify key factors influencing transposable element motility in *S. oneidensis* on the level of genetic integration. Nanopore sequencing was combined with manually analyzing long reads. While labor-intensive, this approach minimizes biases associated with additional steps such as amplification and adaptor usage (such as ISseq; Wright *et al*., 2017). Most pipelines designed for detecting insertion polymorphisms are optimized for eukaryotic hosts. To compare the results of identified variants in the stress experiment, the Sniffles2 pipeline (Smolka *et al*., 2024) was applied, which detected only 52 out of 204 variants, suggesting incomplete variant identification. Highly repetitive sequences of relatively small size, such as the insertion sequences analyzed in this study, may have been misidentified as false variants and disregarded. To improve accuracy, it would be necessary to adjust pipeline parameters or modify analysis steps. Thus, the results suggest that the manual workflow captured nearly four times as many integration events without creating bias.

By applying stress, a burst of TE integrations was aimed to be induced within a short timeframe, allowing for more effective observation of transposition dynamics. The stress experiment revealed that ISSOD2 and ISSOD1 were the most active IS under the applied conditions. The pattern of TE motility remained consistent across different stress factors and was also observed in the control for the second stress experiment. Transposition activity was investigated by culturing cells with ferric citrate as an electron acceptor to simulate conditions found in bioelectrochemical systems more closely, compared to LB-medium incubation. In the precursor strain (MR1.1), several insertions predated the stress stimulus. The additional IS copies observed after stress exposure were consistent with the activity detected prior to the experiment. This, along with previous reports on ISSOD2 and ISSOD1 integrations (Bordi *et al*., 2003; Cheng *et al*., 2020; Schicklberger *et al*., 2013), suggests that the observed TE activity is an inherent feature of *S. oneidensis* rather than a direct consequence of the applied stress

conditions. Additionally, this pattern appears independent of transposition events in the precursor strain, as it was also observed in the MP reduction experiment using MR-1 wild type (see Table 17).

Stress influences TE activity through multiple mechanisms, often as an indirect effect. Differential activation of genetic loci containing IS elements may occur in response to transcriptional regulators involved in cellular stress responses (Capy *et al*., 2000). For example, RpoS, a sigma factor that regulates stress-induced transcription, plays a crucial role in this process (Ferenci, 2008; Hengge, 2008). Another Sigma factor - σ^{54} was found to be affected by integration in many of the stress exposed trials in this study (see Table 18). Disrupting its function might rewire the regulatory network and allow the cell to bypass regulatory constraints, adjusting its metabolic processes and stress responses (Ma *et al*., 2021; Shingler, 1996). This on the other hand might restrain downstream adaptation when conditions change and lead to lower fitness over time. Furthermore, stress-induced cellular damage may facilitate IS integration through strand breaks or increased accessibility via DNA repair pathways. The SOS response, mediated in part by RecA signaling, can promote DNA mismatches and recombination via error-prone polymerases, thereby increasing insertion potential (Baharoglu & Mazel, 2014).

The observed insertions following growth facilitated by ferric citrate reduction may have resulted from stress associated with transitioning from LB-medium in an oxygen-rich environment to anoxic conditions, requiring significant gene expression changes. This transactivation could have led to increased IS activity (Kleckner, 1990; Vandecraen *et al*., 2017). Conversely, higher stress intensity may have arisen from oxygen exposure in the UV trials during transfers, as the cells were radiated outside of the flasks to prevent UV absorption by glassware. Unquantified factors such as pH fluctuations and nutrient availability during incubation could also have contributed to cellular stress.

This study aimed to detect insertions with high sensitivity, focusing on identifying low-frequency alleles in the population via metagenomic analysis. Estimating a precise mutation rate due to transposition remains challenging. The whole-genome sequencing data represent a consortium of transpositional subtypes of the precursor strain, each carrying different insertions. Since only endpoint analysis was conducted, distinguishing insertions at the level of individual lineages was not possible.

Assuming a generation time of ~3 hours on ferric citrate (estimated from data of this study and literature; Schuetz *et al*., 2009), the experiment spanned approximately 360 generations. Across 14 trials with 204 insertions, this equates to ~15 insertion events per trial or 0.04 (4×10^{-2}) insertions per generation. As this number would corresponds to a single lineage in each trail it is highly overestimated. If each insertion event is assumed to create a distinct lineage, the maximum number of sub lineages would be 40 (according to 40 insertions in trail UV3_20) leading to a mutation rate based on TE motility of $\sim 3 \times 10^{-3}$ per generation. This estimation of the maximum mutation rate is vague as sub lineages can contain multiple insertions or no insertions at all but likely corresponds to the order of magnitude in which transposition arose per generation. That means that TE in *S. oneidensis* showed a roughly 10- to 100-fold higher activity compared to *E. coli*, which exhibits insertion rates of $\sim 10^{-4}$ to 10^{-5} per generation (Papadopoulos *et al*., 1999). While this increased activity aligns with stress-induced TE mobilization, the control sample still exhibited a relatively high insertion frequency (8 events; ~6 x 10^{-4} per generation). It is important to note that the observed insertions likely underestimate the actual number of sub lineages. Furthermore, these estimates do not account for detrimental insertions. Mutation rates can vary significantly across conditions and populations, but based on the number of observed insertions, *S. oneidensis* appears to have a relatively high transposition frequency (Schneider & Lenski, 2004).

To compare IS activity across trials, an analysis for single nucleotide variant identification was performed (Supplementary Table S1). The rationale behind this approach was that SNV counts could provide additional insights into the number of distinct subgroups in the population, independent of insertions, potentially offering an estimate of bottlenecks following stress stimulation. However, this approach proved unreliable due to the significantly higher error rate of nanopore sequencing compared to Illumina sequencing (Bejaoui *et al*., 2025) when using CLC workbench. This introduced a strong bias linked to sequencing depth: when normalized to read count, lower sequencing depth resulted in a higher relative error, leading to an overestimation of variant numbers. Consequently, these findings were excluded from the result section.

A partial mitigation strategy involved applying a 100 % cutoff or a minimum count of 10, considering only SNVs present in all reads or at least with a higher minimum coverage. This minimized some error-driven detections, but it also limited the analysis to fixed mutations, disregarding much of the actual genetic diversity. Nonetheless, even with this stringent

criterion, the control group exhibited a higher number of SNVs than the UV-treated samples (when compared to a 20 % cutoff). However, the issue of sequencing depth bias and genome coverage variability persisted.

Due to the limitations of variant detection in CLC Workbench pipelines, a second approach was used, combining read mapping with Minimap2 (Li, 2018) and variant calling with the BBTools pipeline (Bushnell *et al*., 2017) on the Galaxy platform (Afgan *et al*., 2018) to compare the control with UV3_20. This analysis revealed a significantly higher number of SNVs on the MP than on the chromosome, suggesting potential artifacts from repetitive sequences, particularly insertion sequences and perhaps hinting at a faster rate of deterioration compared to the chromosome. As a result, the MP was excluded from further analysis. After normalizing for read count, the number of SNVs on the chromosome was 146 for the control and 61 for UV3, maintaining a consistent ratio with the CLC Workbench analysis (see Supplementary Table S2).

Despite these biases, UV radiation was expected to induce significantly more SNVs than the control. However, in the control, temperature, and antibiotic trials, the number of detected SNVs suggested the presence of more subgroups than the observed insertion events. This discrepancy may be explained by differences in selection pressures: the control group likely experienced weaker selection than the UV-treated samples, where diversity - despite an increased mutation rate - was reduced due to lethal effects of radiation and the accumulation of deleterious insertions. This pattern, (illustrated in Supplementary Figure S3) suggests that SNV detection, could in part have been higher in populations with fewer IS subgroups, meaning that the actual IS activity in UV-treated samples might be underestimated.

In the second UV experiment, which included 30 transfers, the number of insertions and SNVs did not increase, likely due to similar restrictive bottlenecks. Notably, insertions detected in the first UV experiment did not represent fixed mutations and should not be expected to recur in subsequent trials. The initial burst of ISSOD2 transposition may have declined due to the accumulation of insertions and the competitive advantage of higher-fitness sub-lineages. Some ISSOD2 elements also showed signs of inactivation due to deterioration (Supplementary Figure S10). This observation is consistent with the strict rules influencing IS expansion described above.

The elevated number of insertions in the UV3_20 trial compared to all others could indicate the emergence of a hypermutator sub-lineage. These strains often carry defects in DNA processing

and repair genes, such as mutations in mismatch repair (*mutS*, *mutL*) (Pursell *et al*., 2024), DNA polymerases, base excision repair (*mutM*, *mutY*, *mutT*) (Oliver *et al*., 2010), or regulatory elements like *recA* and *lexA*, which enhance the SOS response (Bridges, 2001; Jolivet-Gougeon *et al*., 2011). Such mutations increase overall mutation rates and can confer short-term adaptive advantages by generating beneficial mutations more frequently. However, continuous high mutation rates also accumulate deleterious mutations, potentially reducing long-term fitness. Combined with tight population bottlenecks, this may explain why insertion counts were lower in trials with 30 transfers.

IS-mediated mutations are found to occur at a 3- to 4-fold lower frequency than SNVs, but their impact at the gene level is more pronounced (Consuegra *et al*., 2021). While SNVs may be silent - resulting in synonymous codon changes or non-disruptive mutations - IS integrations are far more likely to cause immediate phenotypic changes. These changes occur through direct gene disruption, alterations in gene expression upon insertion or excision, gene duplication, or genome rearrangement. Consequently, IS motility is expected to have a greater impact on genetic integrity than SNVs alone (Good *et al*., 2017). Here a much higher insertion-rate is found, reinforcing the idea that TE activity plays a dominant role in genomic variability in *S. oneidensis*.

To fully elucidate TE dynamics and transposition rates, single-cell analysis would be beneficial. Nonetheless, *S. oneidensis*, as a widely used model organism, presents significant implications for experimental design and data interpretation. These findings suggest that TE activity could influence laboratory studies, particularly in tightly controlled environments where metabolic pathways are streamlined, forcing the organism into a narrow niche. Under these conditions, many host genes may *a priori* be placed in a neutral or non-essential position, making them more susceptible to TE insertions, as selective pressures for maintaining certain genes diminishes and increase overall motility (Barrick *et al*., 2009). The majority of integration was still found in intergenic regions, TEs themselves or hypothetical proteins (see Results 3.3; Table 18), showing that this trend is not pronounced over the period of this experiment.

Only two deletions were identified across the entire experiment, which is consistent with the transposition mechanism ISSOD-family elements. The active TEs in this study (ISSOD1, ISSOD2, ISSOD9) follow a "copy-and-paste" mechanism, meaning that loss of copies occurs only through deletions rather than transposition itself (as observed in the ISSOD1-toxin regions deletion Figure 11). The two deletions identified (ISSOD6 and ISSOD22) are representative of

"cut-and-paste" transposition. The absence of corresponding insertions following excision events can be attributed to the nature of whole-genome sequencing in a heterogeneous consortium. If excision occurs in a single subgroup, sequencing may capture the excision event in some reads, while the majority of reads originate from subgroups where the excision has not taken place, obscuring the detection of subsequent insertions.

4.2 ISSOD2 phylogeny

To evaluate the activity of individual ISSOD2 copies, a sequence comparison of all insertions detected across the stress experiment trials was conducted, focusing on nucleotide polymorphisms. This alignment aimed to identify recurring sequence changes in IS copies that could be traced back to common ancestral elements - i.e., base copies present in the progenitor strain - to uncover expansion patterns. Since transposable elements are redundant and typically non-essential, their sequences diverge progressively due to the lack of positive selection (Lanciano & Cristofari, 2020). In a phylogenetic alignment, these changes can potentially be traced back to the origin of each element.

However, this approach has several limitations. It is unable to distinguish between relayed activity from identical copies, such as ISSOD2 base copies 2 - 4. Additionally, since UV irradiation induces high mutation rates (Shibai *et al*., 2017), early TE copies may acquire mutations that do not reflect later expansions but instead position them closer to unrelated copies in the phylogeny. This challenge is exacerbated by the fact that insertions were identified based on single-read coverage, making sequencing errors particularly impactful especially when applying nanopore sequencing.

Despite these limitations, the analysis revealed major patterns in ISSOD2 expansion. Thus, the observed eight phylogenetic branches could represent distinct waves of transposition. Given that insertion sequences are found to exert activity predominantly in *cis*, certain SNV comparable in multiple copies in the same area (new4ISSOD2_all_new; base1; new3ISSOD2_all_new; see Supplementary Figure S4 - 7) strongly suggest to be related. The close clustering of *new1ISSOD2_all* and *new2ISSOD2_all* within the same branch further supports the hypothesis that they are derived from a common progenitor or each other. This finding indicates that ISSOD2 expansion is accelerated by newly inserted copies relaying transposition activity themselves. The progression of expansion is illustrated in Figure 8.

Interestingly, some UV_3_20 copies share common SNVs that are absent from any identified base copy, suggesting that later-stage insertions continue to propagate transposition events. Conversely, deterioration of certain ISSOD2 elements, rendering them inactive (Supplementary Figure S10) was observed as well. This suggests that expansion follows a similar trajectory across all experimental conditions and stressors, with all ISSOD2 copies contributing equally to overall transposition activity.

It is important to note that the phylogenetic tree does not necessarily place ancestral copies at the beginning of branches, as the base copies - though originating earlier - were sampled from endpoint analyses and have undergone subsequent mutations. Simple juxtaposition does not allow differentiation of the temporal sequence of changes. However, for all new root positions (newISSOD2_all_new) the parallel occurrence of insertions at identical loci in 14 independent experimental trials makes it highly unlikely that these insertions arose independently. Instead, they must be attributed to ISSOD2 activity predating stress stimuli.

Direct repeat (DR) analysis could serve as an additional method to track the progression of ISSOD2 transposition. DR sequences are formed upon TE integration and remain as "scars" if a TE copy is later excised (Wagner *et al*., 2007). However, this method is inherently limited in this analysis because DRs are not part of the IS element itself. To avoid biases introduced by DR sequence variation due to repair mechanisms at the insertion site, sequences were cropped at the inverted repeat boundaries of the transposed element. Furthermore, since ISSOD2 propagates via a “copy-and-paste” mechanism, DR scars do not necessarily reflect transposition activity and can be disregarded in this context.

Although this analysis does not directly measure the activity levels of individual ISSOD2 members, it strongly suggests that newly integrated ISSOD2 copies remain active in both mobilization and mutagenesis. This continuous activity can increase copy numbers rapidly and potentially trigger a transposition burst within the population. Importantly, there is no evidence that any particular root copy is associated with a significantly higher number of subsequent insertions, indicating that ISSOD2 activity is evenly distributed among copies.

4.3 Reduction of TE mobility via early stop codon induction

To investigate whether early stop codon induction could reduce transposable element mobility, a CAS-deaminase system was implemented in this study. Since ISSOD1 and ISSOD2 were identified as the TEs responsible for most transposition events, these families were targeted for

stop codon conversion to silence their activity. Silencing these elements was expected to significantly reduce the genetic instability associated with TE mobilization. Because the family members exhibit high sequence homology, a single guide RNA was designed to target all copies within a family. In the case of ISSOD2, this strategy was effective across all eight copies; note that the MR1.1 precursor strain initially contained seven copies. In the stop codon–induced strains, the presence of an eighth copy (all carrying the stop codon) suggests that the additional copy arose before or during the C→T conversion process. Importantly, none of these trials exhibited even a single additional ISSOD2 integration compared to the 14 transpositions detected in the control strain without stop codon modifications. Based on activity data from the first stress experiment, this single-step alteration could lower total TE activity by approximately 84 %.

Complete silencing of ISSOD1 was not achieved. However, conversion was successful at 75 % of the target positions across all four trials, implying that factors such as chromosomal localization, accessibility, and methylation had a minor effect on conversion efficiency. Notably, all trials displayed integration of ISSOD9 into the CAS locus, which prevented further protein expression and ultimately led to the breakdown of the system. The incomplete conversion of ISSOD1 is therefore attributed to interference from ISSOD9 activity. It is anticipated that complete silencing of the ISSOD1 family can be achieved after inactivating ISSOD9. When combined with ISSOD2 deletion, these measures could potentially abolish over 97 % of total TE activity in *S. oneidensis* in just two steps.

The stop codon approach offers the advantage of simultaneously targeting multiple copies. Although conventional Cas9-mediated editing could also target multiple sites, generating several double-strand breaks is highly lethal to bacteria (Mehta & Haber, 2014) and the conversion rate is often limited (Ben-Tov *et al*., 2024). In contrast, stop codon conversion, while still imposing some stress on the cells, has a much higher success rate (Billon *et al*, 2017). One drawback of this method is that TEs continue to be transcribed and partially translated, thereby adding to the metabolic burden. A homologous recombination approach might alleviate this issue; however, it suffers from low efficiency due to DSB toxicity with Cas9 or requires time-consuming targeting of individual deletions via recombineering (e.g., using pMQ150). Moreover, there remains a low probability that a random mutation could revert the early stop codon back to a coding triplet, potentially reinitiating transposition and even reactivating other

copies via homologous recombination. Despite these minor drawbacks the stop codon conversion method is considered most suitable for multicopy deactivation.

Chen *et al*. have demonstrated an approach in which multiple sgRNAs are expressed from a single expression cassette, with self-splicing elements or host processing releasing individual guides. This strategy could be adapted to target multiple IS families simultaneously. Based on the integration dynamics observed in this study, it is critical to silence the ISSOD9 family early when engineering a robust genetic chassis, as engineering tools - such as plasmids - are at risk of disruption by active TEs.

4.4 Megaplasmid reduction as a strategy to increase genetic stability

The hypothesis that removing the megaplasmid could stabilize *S. oneidensis* genetically is supported by the findings of this study. Although the MP constitutes only 3.2 % of the total genomic content, it accounts for a disproportionately high percentage of TE integrations - 18.6 % in the first stress experiment and up to 41 % in the second. In general, plasmids tend to acquire insertion sequences more frequently than chromosomes. Megaplasmids are frequently acquired or expanded through horizontal gene transfer and typically lack essential genes, making them prone to high rates of insertion. Thus, eliminating the MP, containing 34 TEs, could remove a significant reservoir from which transposable elements may spread and greatly lower the overall transposition potential in the organism (Deutschbauer *et al*., 2011; Hall *et al*., 2022; He *et al*., 2015).

There is evidence suggesting that the MP harbors only non-essential genes (Deutschbauer *et al*., 2011), although its stability is maintained by toxin-antitoxin (TA) systems (Jurėnas *et al*., 2022). To disrupt the retention mechanism mediated by these TA modules, a plasmid containing all the identified antitoxin genes was engineered.

Additionally, an RFP reporter system was implemented to simultaneously track regional losses and recombination events at the ISSOD9 interface. The metabolic burden imposed by RFP expression was intended to promote recombination or resolution of a hypothesized cointegrate at the ISSOD9 junctions (see below 4.5). This may prompt deletions of the MP backbone as post-segregational killing (Van Melderen & De Bast, 2009) is bypassed via antitoxin expression. Instead, cointegrate resolution or recombination events resulted in the complete loss of the *ori/repA* region. This surprising observation suggests the presence of a secondary origin

of replication on the reduced MP backbone. Using Ori-Finder (Dong *et al*., 2023), two alternative replication origins were predicted near the *parA* gene, at positions [30,067–30,252] and [105,1818–325] on the reduced MP (Supplementary Figure S12; S13). The *parAB* locus is typically involved in plasmid partitioning during cell division, and in some plasmids, regions near *parAB* may serve as secondary replication origins, although this is conjectural at the time (Gao, 2015).

In addition to the loss of the *ori/repA* region, other portions of the MP were successfully deleted. A notable 16-kbp segment, referred to as the "hotspot area," exhibited the highest integration activity. This region contains multiple IS elements, toxins, and non-essential genes, and its deletion precisely corresponded to an area flanked by ISSOD1 copies, indicating a homologous recombination event. These areas are found to contribute greatly to variability in host genetics and underscore the dynamic nature of the MP. Thus, a deletion should stabilize the genetic scaffold (Gerton *et al*., 2000; Grodner *et al*., 2024). In one instance, an ISSOD1 copy together with one of the TA pairs was deleted. Further analysis of the pBAD_AT1-10 plasmid revealed additional ISSOD2 and ISSOD9 integrations, rendering the plasmid physiologically inactive. Because regions containing TA pairs were deleted, it is inferred that the TA expression cassette was at least partially functional. However, it remains inconclusive whether the failure to achieve complete MP loss was due to plasmid interruption, incomplete TA cassette expression, or the presence of essential or accessory genes on the MP.

In this study, several sequencing reads were identified that spanned both the MP and the chromosome - events not explained solely by IS homology - possibly indicating that megaplasmid integration into the chromosome can occur. These observations indicate that reducing or eliminating the megaplasmid can benefit the genetic stability of the host chassis. Furthermore, the deletion of nine TEs from the MP and a highly dynamic hotspot region in the reduced MP should contribute to a substantial reduction in overall TE activity.

4.5 ISSOD9's interaction with mobile DNA and hypothesized Cointegration

The predictions based on transcriptomic data as well as the stress experiment place ISSOD9 as an insignificant contributor to the overall mobilome activity in *S. oneidensis*. However, in experiments where plasmids were introduced a drastic increase in activity stimulation was observed. All plasmids in the ISSOD1 deletion, MP reduction and acetoin production experiments were found to be disrupted by ISSOD9 integration (see Supplementary

Figure S11). In the case of ISSOD1 silencing the disruption occurred rapidly after 48 h of incubation, indicating the steep increase in activity in the presence of an external replicon. This surge in activity might be related to Tn3 dependence on host replication machinery, specifically β-slide clamp interaction, for transposition (Tang *et al*., 2024) as ISSOD9 is part of this group. Replication machinery recruitment for plasmid replications with high copy numbers might therefore increase opportunities for transposition. This suggests that ISSOD9 has developed to integrate into mobile DNA facilitating higher frequency of horizontal gene transfer of that element (Kretschmer & Cohen, 1977). This highlights the dynamic nature of IS activity in *S. oneidensis*, reinforcing its potential impact on genomic stability, adaptation, and evolutionary trajectories.

The loss of the *ori/repA* region prompted the investigation of the nature of the ISSOD9 *ori/repA* intersection, as it is flanked by two copies of the transposase. In the result section 3.7 it is explained that the transition of Tn3 elements is achieved via a cointegrate intermediate where a new copy is found in a DNA fusion molecule with the old copy and their respective DNA regions. The MP *ori/repA* region with two flanking ISSOD9 copies is reminiscent of such an intermediate. It was therefore investigated if the MP might represent a stabilized cointegrate (Shapiro, 1979). The cointegrate hypothesis is supported by indications of Tn3 like transposases causing a largely unexplored phenomenon of self-immunity, preventing transposition into replicon already invaded by a copy of that element, possibly regulating its expansion in a host (Wallace *et al*., 1981).

In all sequencing data it was found that, conversely to the original assembly (NCBI RefSeq assembly ASM14616v2), the MP was divided into two separate contigs. These contigs represent assembled entities that are found to be circular, meaning reads confirm that *ori/repA* region together with an ISSOD9 copy was separated from the rest of the MP backbone containing an ISSOD9 copy as well (see Figure 12). The correct assembly was confirmed by analyzing reads manually found to correspond with this constellation, where some cells maintain a cointegrate form, while the great majority separate the *ori/repA* region. In order to preclude internal sequencing or assembly error an additional dataset NCBI's ASM3384304v1 was used for comparison, leading to the same assembly of two separate replicons. This shows that this metastable state of the MP is a consistent feature. The flanking repeated sequence of ISSOD9 in this region complicates any assembly as the two identical regions are only separated by 15kbp and are over 4kbp long. The possibility of an incorrect assembly that initially missed

the meta-state or falsely combined these replicons cannot be excluded as the assembly was possibly based on short reads sequencing (Romine *et al*., 2008).

The difficulties in the mapping at that area also indicates that the insertions in this region in the stress experiment are likely to be overlooked as the identification is based on unmapping regions in the reference genome. The ambiguity of the mapping causes unmatched reads where the information of additional insertion will be missed. The dominance in MP integration might thus in reality be even more pronounced.

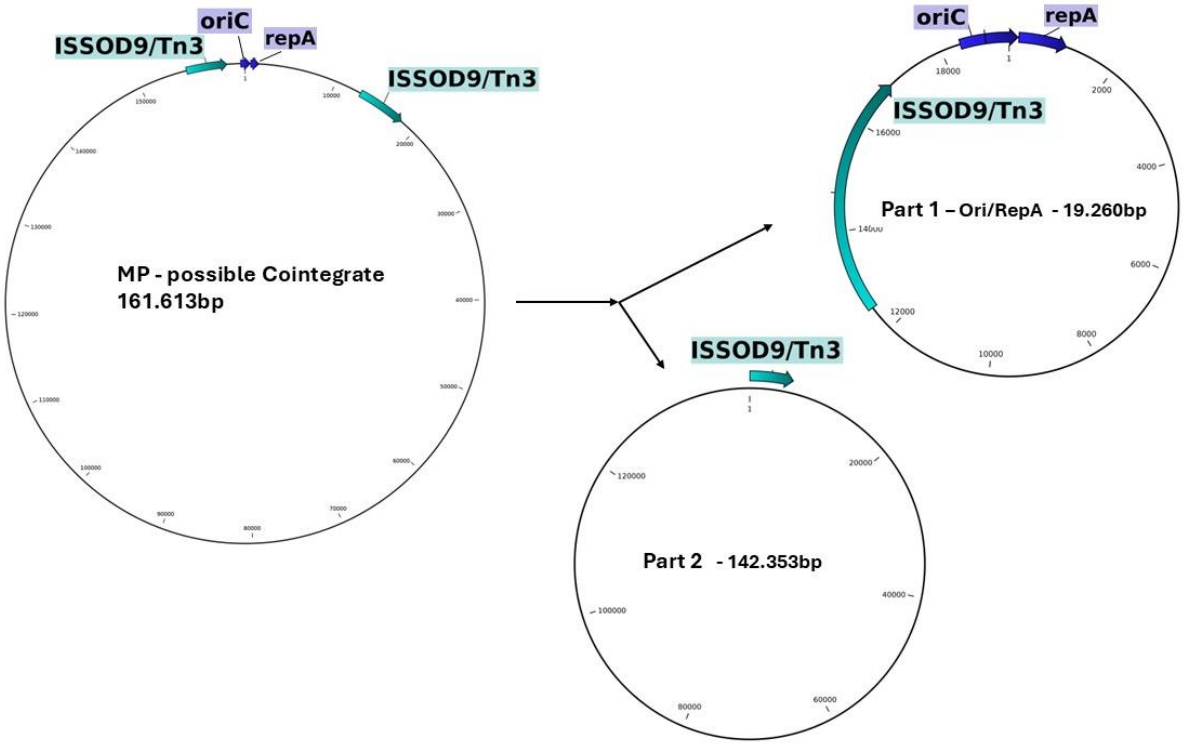

Figure 12: Proposed metastable state of the megaplasmid. The MP as originally assembled contains the *ori/repA* region for the replication initiation flanked by two ISSOD9 elements, reminiscent of a cointegrate intermediate in the transposition mechanism of these elements. The resolution of this construct would cause the emergence of two separate replicons, both containing an ISSOD9 copy.

The question arises why the *ori/repA* replicon, if dispensable, as shown in the MP reduction, would usually be retained by the cells. Although pronounced differently across all sequencings, as for resequencing of the MR-1 wild-type (SAMN46377449) where merely two reads associated with this region are found, it remains present throughout. The only experiment where complete *ori/repA* loss was confirmed is in the MP deletion experiment.

One explanation may involve the toxin-antitoxin balance. The ISSOD9 transposase contains a toxin antitoxin pair, therefore the separated *ori/repA* region contributes to the toxin antitoxin

balance. When lost, the antitoxin of a single copy of ISSOD9 from the MP backbone might not suffice to facilitate survival. The addition of a second copy via AT cassette expression may thus help in the loss of the region (Monti *et al*., 2007; Talavera *et al*., 2019). It is questionable whether the toxin-antitoxin balance has such a significant impact on stabilization, especially considering that the replicon persists in strains where ISSOD9 has integrated into multicopy plasmids - resulting in increasing numbers of the toxin-antitoxin system (up to over a hundred with pUC-*ori* in acetoin production strain). In such cases, losing a single antitoxin copy would have a minimal effect on the overall ratio, suggesting that other factors are likely responsible for stabilizing the *ori/repA* region. Perhaps the metabolic burden elicited by RFP expression on this replicon outweighed the stabilizing effect observed in other cases. The MP does not contain any genes or an *oriT* for conjugation (Heidelberg *et al*., 2002; Romine *et al*., 2008). It is thus impossible for the plasmid to be kept in the population by HGT. The nature of the metastability necessitates further investigation.

As GC content of *ori/repA* is comparable to the rest of the backbone it is difficult to hypothesize about the MP origin. It is likely that cointegration formed via invasion of ISSOD9 containing plasmid. As GC content to chromosome is comparable it could represent a rearranged section from the original genome or a plasmid that was extended gradually with forming a metastable cointegrate at some point.

4.6 *S. oneidensis* Production strain

The findings of this study have significant implications for a potential production strain of *S. oneidensis*. The integration of ISSOD4 into the flagellum operon was found to be identical to a previously reported integration of ISSOD2 at the same location (Supplementary Figure 1). This strain exhibited reduced biofilm formation, despite the fact that flagellar expression is typically repressed in mature biofilms. Motility, however, plays a crucial role in the initial biofilm formation process (Guttenplan & Kearns, 2013; Thormann *et al*., 2004). Biofilms are considered to be potentially favorable for bioproduction (Philipp *et al*., 2024). Since such integrations may go unnoticed in experimental or industrial settings, this underscores the importance of investigating transposable element activity in this strain.

The failure to produce acetoin in previous studies could not be clearly attributed to the disruption of the *alsD* and *alsS* genes. A reevaluation of this issue led to the identification of an incomplete *alsS* cassette. After genetic engineering efforts to repair the *alsS* and *alsD* genes,

repeated attempts to produce acetoin under anaerobic conditions were unsuccessful. In this study, it was found that the failure was initially caused by the integration of ISSOD9 into the expression cassette - an observation that had repeatedly been missed in sequencing analyses. Notably, Illumina sequencing is particularly prone to overlooking transpositions, as shorter reads can be incorrectly aligned to other copies of the element (Yasir *et al*., 2022).

The observed ISSOD9 integration occurred even after just two transfers in an experiment involving ISSOD1 CAS deaminase, demonstrating the highly dynamic nature of transposition. It is therefore reasonable to assume that acetoin production, after reconstruction of the expression cassette, failed due to repeated integration. The absence of a functional acetoin cassette likely led to pyruvate accumulation, which in turn resulted in the formation of lactate and other fermentation byproducts, including trace amounts of acetate and succinate. To conclusively reevaluate acetoin production, inactivation of ISSOD9 is proposed, to determine whether transposon integration is responsible for the failure of this production strain. Furthermore, the increased transposon activity in the presence of plasmids has major implications for working with *S. oneidensis*, as plasmids are essential tools for genetic engineering and transgene expression.

The activity pattern of the ISSOD2 insertion sequence suggests that this element may undergo a transposition burst. The rapid expansion of ISSOD2 across multiple conditions accounted for the majority of TE activity, significantly impacting the genetic stability of the strain. A transposable element with such high expansion potential can disrupt efforts to uncover genetic features of this model organism and may lead to the emergence of non-producing strains, potentially hindering both scientific research and industrial applications.

Tailored, engineered strains are susceptible to maladaptation in ongoing evolutionary processes (Czajka *et al*., 2020), particularly since product yield and complexity often do not confer fitness advantages. This highlights the critical need to monitor TE activity in *S. oneidensis* and other production strains. Any biological production system is subject to mutational pressures, and transposition is particularly detrimental, as it introduces genetic disruptions that can have more severe effects than point mutations. The risk is further amplified in bacterial communities due to potential horizontal gene transfer, raising concerns for production consortia that include *S. oneidensis* (Castle *et al*., 2021; Endy, 2005).

This study presents a potential approach to reducing overall transposon activity. Other strategies to mitigate genetic drift have also been explored, including the deletion of SOS response elements and error-prone repair machinery, as well as improvements in DNA repair mechanisms. Notably, a version of *E. coli* with a reduced genome and lower transposase activity already exists, offering a potential model for stabilizing production strains (Csörgo *et al*., 2012; Pósfai *et al*., 2006).

4.7 Closing remarks

In this study a way to uncover the major contributors to the genetic variability in *S. oneidensis* is presented accurately describing motility pattern of IS in this organism.

The dual role of transposable elements in *S. oneidensis* is highlighted, contributing to both genome instability and adaptation. Stress conditions triggered TE activity, with ISSOD1 and ISSOD2 being the most active, while ISSOD9 showed increased transposition upon plasmid introduction, posing risks to plasmid stability.

Targeted inactivation of ISSOD2 reduced TE mobility by 84 % in a single step, while ISSOD1 silencing was hindered by ISSOD9 interference. Additionally, evidence is provided that the megaplasmid is possibly a metastable cointegrate. Key factors determining genetic dynamics associated with the MP were identified and reduced in part. A complete loss of MP and a total silencing of the ISSOD1 family is deemed feasible if ISSOD9 activity is preventively abolished.

These findings underscore the need to monitor TE activity in engineered *S. oneidensis* strains, particularly when using plasmid-based systems. By silencing key transposases and reducing MP instability, strategies to enhance genome stability in *S. oneidensis* are proposed, offering insights for future bioengineering applications.

5. References

Afgan, E., Baker, D., Batut, B., van den Beek, M., Bouvier, D., Cech, M., Chilton, J., Clements, D., Coraor, N., Grüning, B. A., Guerler, A., Hillman-Jackson, J., Hiltemann, S., Jalili, V., Rasche, H., Soranzo, N., Goecks, J., Taylor, J., Nekrutenko, A., & Blankenberg, D. (2018). The Galaxy platform for accessible, reproducible and collaborative biomedical analyses: 2018 update. *Nucleic Acids Research*, *46*(W1), W537–W544. https://doi.org/10.1093/nar/gky379

Baharoglu, Z., & Mazel, D. (2014). SOS, the formidable strategy of bacteria against aggressions. *FEMS Microbiology Reviews*, *38*(6), 1126–1145. https://doi.org/10.1111/1574-6976.12077

Barrick, J. E., Yu, D. S., Yoon, S. H., Jeong, H., Oh, T. K., Schneider, D., Lenski, R. E., & Kim, J. F. (2009). Genome evolution and adaptation in a long-term experiment with *Escherichia coli*. *Nature*, *461*(7268), 1243–1247. https://doi.org/10.1038/nature08480

Beblawy, S., Bursac, T., Paquete, C., Louro, R., Clarke, T. A., & Gescher, J. (2018). Extracellular reduction of solid electron acceptors by *Shewanella oneidensis*. *Molecular Microbiology*, *109*(5), 571–583. https://doi.org/10.1111/mmi.14067

Bejaoui, S., Nielsen, S. H., Rasmussen, A., Coia, J. E., & Andersen, D. T. (2025). Comparison of Illumina and Oxford Nanopore sequencing data quality for *Clostridioides difficile* genome analysis and their application for epidemiological surveillance. *BMC Genomics* (2025) 26:92 https://doi.org/10.1186/s12864-025-11267-9

Ben-Tov, D., Mafessoni, F., Cucuy, A., Honig, A., Melamed-Bessudo, C., & Levy, A. A. (2024). Uncovering the dynamics of precise repair at CRISPR/Cas9-induced double-strand breaks. *Nature Communications*, *15*(1). https://doi.org/10.1038/s41467-024-49410-x

Bolotin, A., Quinquis, B., Sorokin, A., & Dusko Ehrlich, S. (2005). Clustered regularly interspaced short palindrome repeats (CRISPRs) have spacers of extrachromosomal origin. *Microbiology*, *151*(8), 2551–2561. https://doi.org/10.1099/mic.0.28048-0

Bordi, C., Iobbi-Nivol, C., Méjean, V., & Patte, J. C. (2003). Effects of ISSo2 insertions in structural and regulatory genes of the trimethylamine oxide reductase of *Shewanella oneidensis*. *Journal of Bacteriology*, *185*(6), 2042–2045. https://doi.org/10.1128/JB.185.6.2042-2045.2003

Bourque, G., Burns, K. H., Gehring, M., Gorbunova, V., Seluanov, A., Hammell, M., Imbeault, M., Izsvák, Z., Levin, H. L., Macfarlan, T. S., Mager, D. L., & Feschotte, C. (2018). Ten things you should know about transposable elements 06 Biological Sciences 0604 Genetics. *Genome Biology*, *19*(1), 1–12. https://doi.org/10.1186/s13059-018-1577-z

Bridges, B. A. (2001). Hypermutation in bacteria and other cellular systems. *Philosophical Transactions of the Royal Society B: Biological Sciences*, *355*(1405), 29–39. https://doi.org/10.1098/rstb.2000.0745

Bursac, T., Gralnick, J. A., & Gescher, J. (2017). Acetoin production via unbalanced fermentation in *Shewanella oneidensis. Biotechnology and Bioengineering*, *114*(6), 1283–1289. https://doi.org/10.1002/bit.26243

Bushnell, B., Rood, J., & Singer, E. (2017). BBMerge – Accurate paired shotgun read merging via overlap. *PLoS ONE*, *12*(10), 1–15. https://doi.org/10.1371/journal.pone.0185056

Cain, A. K., Barquist, L., Goodman, A. L., Paulsen, I. T., Parkhill, J., & van Opijnen, T. (2020). A decade of advances in transposon-insertion sequencing. *Nature Reviews Genetics*, *21*(9), 526–540. https://doi.org/10.1038/s41576-020-0244-x

Capy, P., Gasperi, G., Biémont, C., & Bazin, C. (2000). Stress and transposable elements: Co-evolution or useful parasites? *Heredity*, *85*(2), 101–106. https://doi.org/10.1046/j.1365-2540.2000.00751.x

Castle, S. D., Grierson, C. S., & Gorochowski, T. E. (2021). Towards an engineering theory of evolution. *Nature Communications*, *12*(1). https://doi.org/10.1038/s41467-021-23573-3

Chandler, M., & Fayet, O. (1993). Translational frameshifting in the control of transposition in bacteria. *Molecular Microbiology*, *7*(4), 497–503. https://doi.org/10.1111/j.1365-2958.1993.tb01140.x

Che, Y., Yang, Y., Xu, X., Brinda, K., Polz, M. F., Hanage, W. P., & Zhang, T. (2021). Conjugative plasmids interact with insertion sequences to shape the horizontal transfer of antimicrobial resistance genes. *Proceedings of the National Academy of Sciences of the United States of America*, *118*(6). https://doi.org/10.1073/pnas.2008731118

Cheng, L., Min, D., Liu, D. F., Zhu, T. T., Wang, K. L., & Yu, H. Q. (2020). Deteriorated biofilm-forming capacity and electroactivity of *Shewanella oneidnsis* MR-1 induced by insertion sequence (IS) elements. *Biosensors and Bioelectronics*, *156*(March), 112136. https://doi.org/10.1016/j.bios.2020.112136

Chuong, E. B., Elde, N. C., & Feschotte, C. (2017). Regulatory activities of transposable elements: from conflicts to benefits. *Nature Reviews. Genetics*, *18*(2), 71–86. https://doi.org/10.1038/nrg.2016.139

Consuegra, J., Gaffé, J., Lenski, R. E., Hindré, T., Barrick, J. E., Tenaillon, O., & Schneider, D. (2021). Insertion-sequence-mediated mutations both promote and constrain evolvability during a long-term experiment with bacteria. *Nature Communications*, *12*(1). https://doi.org/10.1038/s41467-021-21210-7

Cook, J., Oreskes, N., Doran, P. T., Anderegg, W. R. L., Verheggen, B., Maibach, E. W., Carlton, J. S., Lewandowsky, S., Skuce, A. G., Green, S. A., Nuccitelli, D., Jacobs, P., Richardson, M., Winkler, B., Painting, R., & Rice, K. (2016). Consensus on consensus: A synthesis of consensus estimates on human-caused global warming. *Environmental Research Letters*, *11*(4). https://doi.org/10.1088/1748-9326/11/4/048002

Cowan, A. E., Klass, S. H., Winegar, P. H., & Keasling, J. D. (2023). Microbial production of fuels, commodity chemicals, and materials from sustainable sources of carbon and energy. *Current Opinion in Systems Biology*, *36*, 100482. https://doi.org/10.1016/j.coisb.2023.100482

Csörgo, B., Fehér, T., Tímár, E., Blattner, F. R., & Pósfai, G. (2012). Low-mutation-rate, reduced-genome *Escherichia coli*: An improved host for faithful maintenance of engineered genetic constructs. *Microbial Cell Factories*, *11*, 1–13. https://doi.org/10.1186/1475-2859-11-11

Czajka, J. J., Okumuş, B., Koffas, M. A., Blenner, M., & Tang, Y. J. (2020). Mitigation of host cell mutations and regime shift during microbial fermentation: a perspective from flux memory. *Current Opinion in Biotechnology*, *66*, 227–235. https://doi.org/10.1016/j.copbio.2020.08.003

Dehio, C., & Meyer, M. (1997). Maintenance of broad-host-range incompatibility group P and group Q plasmids and transposition of Tn5 in *Bartonella henselae* following conjugal plasmid transfer from *Escherichia coli*. *Journal of Bacteriology*, *179*(2), 538–540. https://doi.org/10.1128/jb.179.2.538-540.1997

Dennis, J. J. (2005). The evolution of IncP catabolic plasmids. *Current Opinion in Biotechnology*, *16*(3 SPEC. ISS.), 291–298. https://doi.org/10.1016/j.copbio.2005.04.002

Deutschbauer, A., Price, M. N., Wetmore, K. M., Shao, W., Baumohl, J. K., Xu, Z., Nguyen, M., Tamse,

R., Davis, R. W., & Arkin, A. P. (2011). Evidence-based annotation of gene function in *Shewanella oneidensis* MR-1 using genome-wide fitness profiling across 121 conditions. *PLoS Genetics*, *7*(11). https://doi.org/10.1371/journal.pgen.1002385

DiCenzo, G. C., & Finan, T. M. (2017). The Divided Bacterial Genome. *Microbiology and Molecular Biology Reviews*, *81*(3), 1–37. https://doi.org/10.1128/MMBR.00019-17

Dong, M. J., Luo, H., & Gao, F. (2023). DoriC 12.0: an updated database of replication origins in both complete and draft prokaryotic genomes. *Nucleic Acids Research*, *51*(1), D117–D120. https://doi.org/10.1093/nar/gkac964

Doolittle, W. F., & Sapienza, C. (1980). Selfish genes, the phenotype paradigm and genome evolution. *Nature*, *284*(5757), 601–603. https://doi.org/10.1038/284601a0

Drewnowski, J., Remiszewska-Skwarek, A., Duda, S., & Łagód, G. (2019). Aeration process in bioreactors as the main energy consumer in a wastewater treatment plant. Review of solutions and methods of process optimization. *Processes*, *7*(5). https://doi.org/10.3390/pr7050311

Edwards, M. J., White, G. F., Butt, J. N., Richardson, D. J., & Clarke, T. A. (2020). The Crystal Structure of a Biological Insulated Transmembrane Molecular Wire. *Cell*, *181*(3), 665-673.e10. https://doi.org/10.1016/j.cell.2020.03.032

Eichenbaum, Z., & Livneh, Z. (1998). UV light induces IS10 transposition in *Escherichia coli. Genetics*, *149*(3), 1173–1181. https://doi.org/10.1093/genetics/149.3.1173

Endy, D. (2005). Foundations for engineering biology. *Nature*, *438*(7067), 449–453. https://doi.org/10.1038/nature04342

Escoubas, J. M., Prère, M. F., Fayet, O., Salvignol, I., Galas, D., Zerbib, D., & Chandler, M. (1991). Translational control of transposition activity of the bacterial insertion sequence IS1. *The EMBO Journal*, *10*(3), 705–712. https://doi.org/10.1002/j.1460-2075.1991.tb08000.x

Fan, C., Wu, Y. H., Decker, C. M., Rohani, R., Gesell Salazar, M., Ye, H., Cui, Z., Schmidt, F., & Huang, W. E. (2019). Defensive Function of Transposable Elements in Bacteria. *ACS Synthetic Biology*, *8*(9), 2141–2151. https://doi.org/10.1021/acssynbio.9b00218

Ferenci, T. (2008). The spread of a beneficial mutation in experimental bacterial populations: The influence of the environment and genotype on the fixation of *rpoS* mutations. *Heredity*, *100*(5), 446–452. https://doi.org/10.1038/sj.hdy.6801077

Flynn, J. M., Ross, D. E., Hunt, K. A., Bond, D. R., & Gralnick, J. A. (2010). Enabling unbalanced fermentations by using engineered electrode- interfaced bacteria. *MBio*, *1*(5), 1–8. https://doi.org/10.1128/mBio.00190-10

Fonfara, I., Richter, H., Bratovič, M., Le Rhun, A., & Charpentier, E. (2016). The CRISPR-associated DNA-cleaving enzyme Cpf1 also processes precursor CRISPR RNA. *Nature*, *532*(7600), 517–521. https://doi.org/10.1038/nature17945

Foster, P. L. (2007). Stress-induced mutagenesis in bacteria. *Critical Reviews in Biochemistry and Molecular Biology*, *42*(5), 373–397. https://doi.org/10.1080/10409230701648494

Fredrickson, J. K., Romine, M. F., Beliaev, A. S., Auchtung, J. M., Driscoll, M. E., Gardner, T. S., Nealson, K. H., Osterman, A. L., Pinchuk, G., Reed, J. L., Rodionov, D. A., Rodrigues, J. L. M., Saffarini, D. A., Serres, M. H., Spormann, A. M., Zhulin, I. B., & Tiedje, J. M. (2008). Towards environmental systems biology of *Shewanella*. *Nature Reviews Microbiology*, *6*(8), 592–603. https://doi.org/10.1038/nrmicro1947

Gao, F. (2015). Bacteria may have multiple replication origins. *Frontiers in Microbiology*, *6*(MAR), 1–4.

https://doi.org/10.3389/fmicb.2015.00324

Gerton, J. L., DeRisi, J., Shroff, R., Lichten, M., Brown, P. O., & Petes, T. D. (2000). Global mapping of meiotic recombination hotspots and coldspots in the yeast *Saccharomyces cerevisiae*. *Proceedings of the National Academy of Sciences of the United States of America*, *97*(21), 11383–11390. https://doi.org/10.1073/pnas.97.21.11383

Gibson, D. G., Young, L., Chuang, R. Y., Venter, J. C., Hutchison, C. A., & Smith, H. O. (2009). Enzymatic assembly of DNA molecules up to several hundred kilobases. *Nature Methods*, *6*(5), 343–345. https://doi.org/10.1038/nmeth.1318

Good, B. H., McDonald, M. J., Barrick, J. E., Lenski, R. E., & Desai, M. M. (2017). The dynamics of molecular evolution over 60,000 generations. *Nature*, *551*(7678), 45–50. https://doi.org/10.1038/nature24287

Gralnick, J. A., & Newman, D. K. (2007). Extracellular respiration. *Molecular Microbiology*, *65*(1), 1–11. https://doi.org/10.1111/j.1365-2958.2007.05778.x

Grodner, B., Shi, H., Farchione, O., Vill, A. C., Ntekas, I., Diebold, P. J., Wu, D. T., Chen, C. Y., Kim, D. M., Zipfel, W. R., Brito, I. L., & De Vlaminck, I. (2024). Spatial mapping of mobile genetic elements and their bacterial hosts in complex microbiomes. *Nature Microbiology*, *9*(9), 2262–2277. https://doi.org/10.1038/s41564-024-01735-5

Guan, J., Chen, Y., Goh, Y.-X., Wang, M., Tai, C., Deng, Z., Song, J., & Ou, H.-Y. (2024). TADB 3.0: an updated database of bacterial toxin-anti toxin loci and associated mobile genetic elements. *Nucleic Acids Research*, *52*, 784–790. https://doi.org/10.1093/nar/gkad962

Guttenplan, S. B., & Kearns, D. B. (2013). Regulation of flagellar motility during biofilm formation. *FEMS Microbiology Reviews*, *37*(6), 849–871. https://doi.org/10.1111/1574-6976.12018

Hackmann, T. J. (2024). The vast landscape of carbohydrate fermentation in prokaryotes. *FEMS Microbiology Reviews*, *48*(4). https://doi.org/10.1093/femsre/fuae016

Hall, B. G. (1999). Transposable elements as activators of cryptic genes in *E. coli*. *Genetica*, *107*(1–3), 181–187. https://doi.org/10.1023/a:1003936706129

Hall, J. P. J., Botelho, J., Cazares, A., & Baltrus, D. A. (2022). What makes a megaplasmid? *Philosophical Transactions of the Royal Society B: Biological Sciences*, *377*(1842). https://doi.org/10.1098/rstb.2020.0472

Haren, L., Polard, P., Ton-Hoang, B., & Chandler, M. (1998). Multiple oligomerisation domains in the IS911 transposase: A leucine zipper motif is essential for activity. *Journal of Molecular Biology*, *283*(1), 29–41. https://doi.org/10.1006/jmbi.1998.2053

Harrison, P. W., Lower, R. P. J., Kim, N. K. D., & Young, J. P. W. (2010). Introducing the bacterial "chromid": Not a chromosome, not a plasmid. *Trends in Microbiology*, *18*(4), 141–148. https://doi.org/10.1016/j.tim.2009.12.010

Hartshorne, R. S., Reardon, C. L., Ross, D., Nuester, J., Clarke, T. A., Gates, A. J., Mills, P. C., Fredrickson, J. K., Zachara, J. M., Shi, L., Beliaev, A. S., Marshall, M. J., Tien, M., Brantley, S., Butt, J. N., & Richardson, D. J. (2009). Characterization of an electron conduit between bacteria and the extracellular environment. *Proceedings of the National Academy of Sciences of the United States of America*, *106*(52), 22169–22174. https://doi.org/10.1073/pnas.0900086106

Hawkey, J., Hamidian, M., Wick, R. R., Edwards, D. J., Billman-Jacobe, H., Hall, R. M., & Holt, K. E. (2015). ISMapper: Identifying transposase insertion sites in bacterial genomes from short read sequence data. *BMC Genomics*, *16*(1), 1–11. https://doi.org/10.1186/s12864-015-1860-2

He, S., Hickman, A. B., Varani, A. M., Siguier, P., Chandler, M., Dekker, J. P., & Dyda, F. (2015). Insertion sequence IS26 reorganizes plasmids in clinically isolated multidrug-resistant bacteria by replicative transposition. *MBio*, *6*(3). https://doi.org/10.1128/mBio.00762-15

Hedges, R. W., & Jacob, A. E. (1974). Transposition of ampicillin resistance from RP4 to other replicons. *MGG Molecular & General Genetics*, *132*(1), 31–40. https://doi.org/10.1007/BF00268228

Heidelberg, J. F., Paulsen, I. T., Nelson, K. E., Gaidos, E. J., Nelson, W. C., Read, T. D., Eisen, J. A., Seshadri, R., Ward, N., Methe, B., Clayton, R. A., Meyer, T., Tsapin, A., Scott, J., Beanan, M., Brinkac, L., Daugherty, S., DeBoy, R. T., Dodson, R. J., … Fraser, C. M. (2002). Genome sequence of the dissimilatory metal ion-reducing bacterium *Shewanella oneidensis. Nature Biotechnology*, *20*(11), 1118–1123. https://doi.org/10.1038/nbt749

Hengge, R. (2008). The two-component network and the general stress sigma factor RpoS (σS) in *Escherichia coli*. *Advances in Experimental Medicine and Biology*, *631*, 40–53. https://doi.org/10.1007/978-0-387-78885-2_4

Hornsey, M. J., & Fielding, K. S. (2020). Understanding (and Reducing) Inaction on Climate Change. *Social Issues and Policy Review*, *14*(1), 3–35. https://doi.org/10.1111/sipr.12058

Hou, H., Lu, W., Liu, B., Hassanein, Z., Mahmood, H., & Khalid, S. (2023). Exploring the Role of Fossil Fuels and Renewable Energy in Determining Environmental Sustainability: Evidence from OECD Countries. *Sustainability (Switzerland)*, *15*(3). https://doi.org/10.3390/su15032048

Iranzo, J., Gómez, M. J., López de Saro, F. J., & Manrubia, S. (2014). Large-Scale Genomic Analysis Suggests a Neutral Punctuated Dynamics of Transposable Elements in Bacterial Genomes. *PLoS Computational Biology*, *10*(6). https://doi.org/10.1371/journal.pcbi.1003680

Jansen, R., Van Embden, J. D. A., Gaastra, W., & Schouls, L. M. (2002). Identification of genes that are associated with DNA repeats in prokaryotes. *Molecular Microbiology*, *43*(6), 1565–1575. https://doi.org/10.1046/j.1365-2958.2002.02839.x

Jinek, M., Chylinski, K., Fonfara, I., Hauer, M., Doudna, J. A., & Charpentier, E. (2012). A programmable dual-RNA-guided DNA endonuclease in adaptive bacterial immunity. *Science*, *337*(6096), 816–821. https://doi.org/10.1126/science.1225829

Jolivet-Gougeon, A., Kovacs, B., Le Gall-David, S. L., Le Bars, H., Bousarghin, L., Bonnaure-Mallet, M., Lobe, B., Guillé, F., Soussy, C. J., & Tenke, P. (2011). Bacterial hypermutation: Clinical implications. *Journal of Medical Microbiology*, *60*(5), 563–573. https://doi.org/10.1099/jmm.0.024083-0

Jurėnas, D., Fraikin, N., Goormaghtigh, F., & Van Melderen, L. (2022). Biology and evolution of bacterial toxin–antitoxin systems. *Nature Reviews Microbiology*, *20*(6), 335–350. https://doi.org/10.1038/s41579-021-00661-1

Kanai, Y., Tsuru, S., & Furusawa, C. (2022). Experimental demonstration of operon formation catalyzed by insertion sequence. *Nucleic Acids Research*, *50*(3), 1673–1686. https://doi.org/10.1093/nar/gkac004

Kasai, T., Suzuki, Y., Kouzuma, A., & Watanabe, K. (2019). Roles of D-lactate dehydrogenases in the anaerobic growth of *Shewanella oneidensis* MR-1 on sugars. *Applied and Environmental Microbiology*, *85*(3), 1–11. https://doi.org/10.1128/AEM.02668-18

Kerisit S.N., K.M. Rosso, M. Dupuis, and M. V. (2007). Molecular Computational Investigation of Electron Transfer Kinetics across Cytochrome-Iron Oxide Interfaces. *Journal of Physical Chemistry C 111, No. 30:11363-11375.*, *PNNL-SA-54356.*

Kipf, E., Zengerle, R., Gescher, J., & Kerzenmacher, S. (2014). How Does the Choice of Anode Material Influence Electrical Performance? A Comparison of Two Microbial Fuel Cell Model Organisms. *ChemElectroChem*, *1*(11), 1849–1853. https://doi.org/https://doi.org/10.1002/celc.201402036

Kleckner, N. (1990). Regulation of transposition in bacteria. *Annual Review of Cell Biology*, *6*, 297–327. https://doi.org/10.1146/annurev.cb.06.110190.001501

Komor, A. C., Kim, Y. B., Packer, M. S., Zuris, J. A., & Liu, D. R. (2016). Programmable editing of a target base in genomic DNA without double-stranded DNA cleavage. *Nature*, *533*(7603), 420–424. https://doi.org/10.1038/nature17946

Koonin, E. V., Makarova, K. S., & Zhang, F. (2017). Diversity, classification and evolution of CRISPR-Cas systems. *Current Opinion in Microbiology*, *37*, 67–78. https://doi.org/10.1016/j.mib.2017.05.008

Kretschmer, P. J., & Cohen, S. N. (1977). Selected translocation of plasmid genes: frequency and regional specificity of translocation of the Tn3 element. *Journal of Bacteriology*, *130*(2), 888–899. https://doi.org/10.1128/jb.130.2.888-899.1977

Kumar, P., Chandrasekhar, K., Kumari, A., Sathiyamoorthi, E., & Kim, B. S. (2018). Electro-fermentation in aid of bioenergy and biopolymers. *Energies*, *11*(2). https://doi.org/10.3390/en11020343

Lanciano, S., & Cristofari, G. (2020). Measuring and interpreting transposable element expression. *Nature Reviews Genetics*, *21*(12), 721–736. https://doi.org/10.1038/s41576-020-0251-y

Lartigue, M. F., Poirel, L., Aubert, D., & Nordmann, P. (2006). In vitro analysis of ISEcp1B-mediated mobilization of naturally occurring β-lactamase gene blaCTX-M of *Kluyvem ascorbata*. *Antimicrobial Agents and Chemotherapy*, *50*(4), 1282–1286. https://doi.org/10.1128/AAC.50.4.1282-1286.2006

Lewis, L. A., Cylin, E., Lee, H. K., Saby, R., Wong, W., & Grindley, N. D. F. (2004). The Left End of IS2: A Compromise between Transpositional Activity and An Essential Promoter Function That Regulates the Transposition Pathway. *Journal of Bacteriology*, *186*(3), 858–865. https://doi.org/10.1128/JB.186.3.858-865.2004

Li, H. (2018). Minimap2: pairwise alignment for nucleotide sequences. *Bioinformatics*, *34*(18), 3094–3100. https://doi.org/10.1093/bioinformatics/bty191

Lon M. Chubiz, C. J. M. (2017). Growth Trade-Offs Accompany the Emergence of Glycolytic Metabolism. *Jornal of Bacteriology*, *199*(11), 1–15. https://doi.org/10.1128/JB.00827-16

Lovley, D. R., & Walker, D. J. F. (2019). *Geobacter* Protein Nanowires. *Frontiers in Microbiology*, *10*(September). https://doi.org/10.3389/fmicb.2019.02078

Lu, C., Chen, J., Zhang, Y., Hu, Q., Su, W., & Kuang, H. (2012). Miniature Inverted–Repeat Transposable Elements (MITEs) Have Been Accumulated through Amplification Bursts and Play Important Roles in Gene Expression and Species Diversity in *Oryza sativa*. *Molecular Biology and Evolution*, *29*(3), 1005–1017. https://doi.org/10.1093/molbev/msr282

Lutz, R., & Bujard, H. (1997). Independent and tight regulation of transcriptional units in *Escherichia coli* via the LacR/O, the TetR/O and AraC/I1-I2 regulatory elements. *Nucleic Acids Research*, *25*(6), 1203–1210. https://doi.org/10.1093/nar/25.6.1203

Ma, M., Welch, R. D., & Garza, A. G. (2021). The σ^{54} system directly regulates bacterial natural product genes. *Scientific Reports*, *11*(1), 1–11. https://doi.org/10.1038/s41598-021-84057-4

MacLean, R. C., Torres-Barceló, C., & Moxon, R. (2013). Evaluating evolutionary models of stress-

induced mutagenesis in bacteria. *Nature Reviews Genetics*, *14*(3), 221–227. https://doi.org/10.1038/nrg3415

Mahdizade Ari, M., Dadgar, L., Elahi, Z., Ghanavati, R., & Taheri, B. (2024). Genetically Engineered Microorganisms and Their Impact on Human Health. *International Journal of Clinical Practice*, *2024*(1), 6638269. https://doi.org/https://doi.org/10.1155/2024/6638269

Maringer, K., Yousuf, A., Heesom, K. J., Fan, J., Lee, D., Fernandez-Sesma, A., Bessant, C., Matthews, D. A., & Davidson, A. D. (2017). Proteomics informed by transcriptomics for characterising active transposable elements and genome annotation in *Aedes aegypti*. *BMC Genomics*, *18*(1), 1–18. https://doi.org/10.1186/s12864-016-3432-5

Marsili, E., Baron, D. B., Shikhare, I. D., Coursolle, D., Gralnick, J. A., & Bond, D. R. (2008). *Shewanella* secretes flavins that mediate extracellular electron transfer. *Proceedings of the National Academy of Sciences of the United States of America*, *105*(10), 3968–3973. https://doi.org/10.1073/pnas.0710525105

McAdam, B., Brennan Fournet, M., McDonald, P., & Mojicevic, M. (2020). Production of Polyhydroxybutyrate (PHB) and Factors Impacting Its Chemical and Mechanical Characteristics. *Polymers*, *12*(12). https://doi.org/10.3390/polym12122908

Mehta, A., & Haber, J. E. (2014). Sources of DNA double-strand breaks and models of recombinational DNA repair. *Cold Spring Harbor Perspectives in Biology*, *6*(9), 1–17. https://doi.org/10.1101/cshperspect.a016428

Mira, A., Ochman, H., & Moran, N. A. (2001). Deletional bias and the evolution of bacterial genomes. *Trends in Genetics*, *17*(10), 589–596. https://doi.org/10.1016/S0168-9525(01)02447-7

Mojica, F. J. M., Díez-Villaseñor, C., García-Martínez, J., & Soria, E. (2005). Intervening sequences of regularly spaced prokaryotic repeats derive from foreign genetic elements. *Journal of Molecular Evolution*, *60*(2), 174–182. https://doi.org/10.1007/s00239-004-0046-3

Monchy, S., Benotmane, M. A., Janssen, P., Vallaeys, T., Taghavi, S., Van Der Lelie, D., & Mergeay, M. (2007). Plasmids pMOL28 and pMOL30 of *Cupriavidus metallidurans* are specialized in the maximal viable response to heavy metals. *Journal of Bacteriology*, *189*(20), 7417–7425. https://doi.org/10.1128/JB.00375-07

Monti, M. C., Hernández-Arriaga, A. M., Kamphuis, M. B., López-Villarejo, J., Heck, A. J. R., Boelens, R., Díaz-Orejas, R., & van den Heuvel, R. H. H. (2007). Interactions of Kid-Kis toxin-antitoxin complexes with the *parD* operator-promoter region of plasmid R1 are piloted by the Kis antitoxin and tuned by the stoichiometry of Kid-Kis oligomers. *Nucleic Acids Research*, *35*(5), 1737–1749. https://doi.org/10.1093/nar/gkm073

Müller, V. (2008). Bacterial Fermentation. In *eLS*. https://doi.org/https://doi.org/10.1002/9780470015902.a0001415.pub2

Mustafin, R. N. (2018). Hypothesis on the Origin of Viruses from Transposons. *Molecular Genetics, Microbiology and Virology*, *33*(4), 223–232. https://doi.org/10.3103/S0891416818040067

Myers, C. R., & Nealson, K. H. (1988). Bacterial manganese reduction and growth with manganese oxide as the sole electron acceptor. *Science*, *240*(4857), 1319–1321. https://doi.org/10.1126/science.240.4857.1319

Nagy, Z., & Chandler, M. (2004). Regulation of transposition in bacteria. *Research in Microbiology*, *155*(5), 387–398. https://doi.org/10.1016/j.resmic.2004.01.008

Nakagawa, G., Kouzuma, A., Hirose, A., Kasai, T., Yoshida, G., & Watanabe, K. (2015). Metabolic

characteristics of a glucose-utilizing *Shewanella oneidensis* strain grown under electrode-respiring conditions. *PLoS ONE*, *10*(9), 1–14. https://doi.org/10.1371/journal.pone.0138813

Okamoto, A., Hashimoto, K., Nealson, K. H., & Nakamura, R. (2013). Rate enhancement of bacterial extracellular electron transport involves bound flavin semiquinones. *Proceedings of the National Academy of Sciences of the United States of America*, *110*(19), 7856–7861. https://doi.org/10.1073/pnas.1220823110

Okamoto, A., Nakamura, R., Nealson, K. H., & Hashimoto, K. (2014). Bound Flavin Model Suggests Similar Electron-Transfer Mechanisms in *Shewanella* and *Geobacter*. *ChemElectroChem*, *1*(11), 1808–1812. https://doi.org/10.1002/celc.201402151

Oliveira, P. H., Touchon, M., Cury, J., & Rocha, E. P. C. (2017). The chromosomal organization of horizontal gene transfer in bacteria. *Nature Communications*, *8*(1), 25–28. https://doi.org/10.1038/s41467-017-00808-w

Oliver, A., & Mena, A. (2010). Bacterial hypermutation in cystic fibrosis, not only for antibiotic resistance. *Clinical Microbiology and Infection*, *16*(7), 798–808. https://doi.org/10.1111/j.1469-0691.2010.03250.x

Panich, J., Fong, B., & Singer, S. W. (2021). Metabolic Engineering of *Cupriavidus necator* H16 for Sustainable Biofuels from CO_2. *Trends in Biotechnology*, *39*(4), 412–424. https://doi.org/10.1016/j.tibtech.2021.01.001

Papadopoulos, D., Schneider, D., Meier-Eiss, J., Arber, W., Lenski, R. E., & Blot, M. (1999). Genomic evolution during a 10,000-generation experiment with bacteria. *Proceedings of the National Academy of Sciences of the United States of America*, *96*(7), 3807–3812. https://doi.org/10.1073/pnas.96.7.3807

Philipp, L. A., Bühler, K., Ulber, R., & Gescher, J. (2024). Beneficial applications of biofilms. *Nature Reviews Microbiology*, *22*(5), 276–290. https://doi.org/10.1038/s41579-023-00985-0

Philipp, L. A., Edel, M., & Gescher, J. (2020). Genetic engineering for enhanced productivity in bioelectrochemical systems. In *Advances in Applied Microbiology* (1st ed., Vol. 111). Elsevier Inc. https://doi.org/10.1016/bs.aambs.2020.01.001

Pinchuk, G. E., Rodionov, D. A., Yang, C., Li, X., Osterman, A. L., Dervyn, E., Geydebrekht, O. V., Reed, S. B., Romine, M. F., Collart, F. R., Scott, J. H., Fredrickson, J. K., & Beliaev, A. S. (2009). Genomic reconstruction of *Shewanella oneidensis* MR-1 metabolism reveals a previously uncharacterized machinery for lactate utilization. *Proceedings of the National Academy of Sciences of the United States of America*, *106*(8), 2874–2879. https://doi.org/10.1073/pnas.0806798106

Pinto, D., Coradin, T., & Laberty-Robert, C. (2018). Effect of anode polarization on biofilm formation and electron transfer in S*hewanella oneidensis*/graphite felt microbial fuel cells. *Bioelectrochemistry*, *120*, 1–9. https://doi.org/10.1016/j.bioelechem.2017.10.008

Pósfai, G., Plunkett, G. 3rd, Fehér, T., Frisch, D., Keil, G. M., Umenhoffer, K., Kolisnychenko, V., Stahl, B., Sharma, S. S., de Arruda, M., Burland, V., Harcum, S. W., & Blattner, F. R. (2006). Emergent properties of reduced-genome *Escherichia coli*. *Science (New York, N.Y.)*, *312*(5776), 1044–1046. https://doi.org/10.1126/science.1126439

Prentki, P., Teter, B., Chandler, M., & Galas, D. J. (1986). Functional promoters created by the insertion of transposable element IS1. *Journal of Molecular Biology*, *191*(3), 383–393. https://doi.org/10.1016/0022-2836(86)90134-8

Pursell, Z., Hall, K., Williams, L., Smith, R., Kuang, E., Ernst, R., Bojanowski, C., Wimley, W., & Morici, L. (2024). Mutational signature analysis predicts bacterial hypermutation and multidrug

resistance. *Nature Communications*, 1–16. https://doi.org/10.1038/s41467-024-55206-w

Qumsani, A. T. (2024). The contribution of microorganisms to sustainable development: towards a green future through synthetic biology and systems biology. *Journal of Umm Al-Qura University for Applied Sciences*, *0123456789*. https://doi.org/10.1007/s43994-024-00180-8

Rabaey, K., & Rozendal, R. A. (2010). Microbial electrosynthesis - Revisiting the electrical route for microbial production. *Nature Reviews Microbiology*, *8*(10), 706–716. https://doi.org/10.1038/nrmicro2422

Rezsöhazy, R., Hallet, B., Delcour, J., & Mahillon, J. (1993). The IS4 family of insertion sequences: evidence for a conserved transposase motif. *Molecular Microbiology*, *9*(6), 1283–1295. https://doi.org/10.1111/j.1365-2958.1993.tb01258.x

Rodionov, D. A., Yang, C., Li, X., Rodionova, I. A., Wang, Y., Obraztsova, A. Y., Zagnitko, O. P., Overbeek, R., Romine, M. F., Reed, S., Fredrickson, J. K., Nealson, K. H., & Osterman, A. L. (2010). Genomic encyclopedia of sugar utilization pathways in the *Shewanella* genus. *BMC Genomics*, *11*(1). https://doi.org/10.1186/1471-2164-11-494

Romine, M. F., Carlson, T. S., Norbeck, A. D., McCue, L. A., & Lipton, M. S. (2008). Identification of mobile elements and pseudogenes in the *Shewanella oneidensis* MR-1 genome. *Applied and Environmental Microbiology*, *74*(10), 3257–3265. https://doi.org/10.1128/AEM.02720-07

Rosado, H. R. and P. (2017). Fossil fuels were key to industrialization and rising prosperity, but their impact on health and the climate means that we should transition away from them. *"Fossil Fuels" Published Online at OurWorldinData.Org. Retrieved from:* "https://Ourworldindata.Org/Fossil-Fuels" [Online Resource].

Ross, J. A., Wardle, S. J., & Haniford, D. B. (2010). Tn10/IS10 transposition is downregulated at the level of transposase expression by the RNA-binding protein Hfq. *Molecular Microbiology*, *78*(3), 607–621. https://doi.org/10.1111/j.1365-2958.2010.07359.x

Rugbjerg, P., Myling-Petersen, N., Porse, A., Sarup-Lytzen, K., & Sommer, M. O. A. (2018). Diverse genetic error modes constrain large-scale bio-based production. *Nature Communications*, *9*(1). https://doi.org/10.1038/s41467-018-03232-w

Rugbjerg, P., & Sommer, M. O. A. (2019). Overcoming genetic heterogeneity in industrial fermentations. *Nature Biotechnology*, *37*(8), 869–876. https://doi.org/10.1038/s41587-019-0171-6

Sanger, F., Nicklen, S., & Coulson, A. R. (1977). DNA sequencing with chain-terminating inhibitors. *Proceedings of the National Academy of Sciences of the United States of America*, *74*(12), 5463–5467. https://doi.org/10.1073/pnas.74.12.5463

Schicklberger, M., Sturm, G., & Gescher, J. (2013). Genomic Plasticity Enables a secondary electron transport pathway in *Shewanella oneidensis*. *Applied and Environmental Microbiology*, *79*(4), 1150–1159. https://doi.org/10.1128/AEM.03556-12

Schmid, M., Frei, D., Patrignani, A., Schlapbach, R., Frey, J. E., Remus-Emsermann, M. N. P., & Ahrens, C. H. (2018). Pushing the limits of *de novo* genome assembly for complex prokaryotic genomes harboring very long, near identical repeats. *Nucleic Acids Research*, *46*(17), 8953–8965. https://doi.org/10.1093/nar/gky726

Schmitz-Esser, S., Penz, T., Spang, A., & Horn, M. (2011). A bacterial genome in transition - An exceptional enrichment of IS elements but lack of evidence for recent transposition in the symbiont *Amoebophilus asiaticus*. *BMC Evolutionary Biology*, *11*(1). https://doi.org/10.1186/1471-2148-11-270

Schneider, D., & Lenski, R. E. (2004). Dynamics of insertion sequence elements during experimental evolution of bacteria. *Research in Microbiology*, *155*(5), 319–327. https://doi.org/10.1016/j.resmic.2003.12.008

Schuetz, B., Schicklberger, M., Kuermann, J., Spormann, A. M., & Gescher, J. (2009). Periplasmic electron transfer via the *c*-type cytochromes MtrA and FccA of *Shewanella oneidensis* Mr-1. *Applied and Environmental Microbiology*, *75*(24), 7789–7796. https://doi.org/10.1128/AEM.01834-09

Schwartz, E., Henne, A., Cramm, R., Eitinger, T., Friedrich, B., & Gottschalk, G. (2003). Complete nucleotide sequence of pHG1: A *Ralstonia eutropha* H16 megaplasmid encoding key enzymes of H_2-based lithoautotrophy and anaerobiosis. *Journal of Molecular Biology*, *332*(2), 369–383. https://doi.org/10.1016/S0022-2836(03)00894-5

Sekine, Y., Aihara, K., & Ohtsubo, E. (1999). Linearization and transposition of circular molecules of insertion sequence IS3. *Journal of Molecular Biology*, *294*(1), 21–34. https://doi.org/10.1006/jmbi.1999.3181

Shapiro, J. A. (1979). Molecular model for the transposition and replication of bacteriophage Mu and other transposable elements. *Proceedings of the National Academy of Sciences of the United States of America*, *76*(4), 1933–1937. https://doi.org/10.1073/pnas.76.4.1933

Shibai, A., Takahashi, Y., Ishizawa, Y., Motooka, D., Nakamura, S., Ying, B. W., & Tsuru, S. (2017). Mutation accumulation under UV radiation in *Escherichia coli*. *Scientific Reports*, *7*(1), 1–12. https://doi.org/10.1038/s41598-017-15008-1

Shingler, V. (1996). Signal sensing by σ^{54}-dependent regulators: Derepression as a control mechanism. *Molecular Microbiology*, *19*(3), 409–416. https://doi.org/10.1046/j.1365-2958.1996.388920.x

Shkumatov, A. V., Aryanpour, N., Oger, C. A., Goossens, G., Hallet, B. F., & Efremov, R. G. (2022). Structural insight into Tn3 family transposition mechanism. *Nature Communications*, *13*(1). https://doi.org/10.1038/s41467-022-33871-z

Siguier, P., Filée, J., & Chandler, M. (2006). Insertion sequences in prokaryotic genomes. *Current Opinion in Microbiology*, *9*(5), 526–531. https://doi.org/10.1016/j.mib.2006.08.005

Siguier, P., Gourbeyre, E., & Chandler, M. (2014). Bacterial insertion sequences: Their genomic impact and diversity. *FEMS Microbiology Reviews*, *38*(5), 865–891. https://doi.org/10.1111/1574-6976.12067

Siguier, P., Gourbeyre, E., Varani, A., Ton-Hoang, B., & Chandler, M. (2015). Everyman's Guide to Bacterial Insertion Sequences. *Microbiology Spectrum*, *3*(2). https://doi.org/10.1128/microbiolspec.MDNA3-0030-2014

Siguier, P., Perochon, J., Lestrade, L., Mahillon, J., & Chandler, M. (2006). ISfinder: the reference centre for bacterial insertion sequences. *Nucleic Acids Research*, *34*(Database issue). https://doi.org/10.1093/NAR/GKJ014

Smolka, M., Paulin, L. F., Grochowski, C. M., Horner, D. W., Mahmoud, M., Behera, S., Kalef-Ezra, E., Gandhi, M., Hong, K., Pehlivan, D., Scholz, S. W., Carvalho, C. M. B., Proukakis, C., & Sedlazeck, F. J. (2024). Detection of mosaic and population-level structural variants with Sniffles2. *Nature Biotechnology*, *42*(October). https://doi.org/10.1038/s41587-023-02024-y

Sturm, G., Richter, K., Doetsch, A., Heide, H., Louro, R. O., & Gescher, J. (2015). A dynamic periplasmic electron transfer network enables respiratory flexibility beyond a thermodynamic regulatory regime. *ISME Journal*, *9*(8), 1802–1811. https://doi.org/10.1038/ismej.2014.264

Sun, J. A., Zhang, L. Y., Rao, B., Shen, Y. L., & Wei, D. Z. (2012). Enhanced acetoin production by *Serratia marcescens* H32 with expression of a water-forming NADH oxidase. *Bioresource Technology*, *119*, 94–98. https://doi.org/10.1016/j.biortech.2012.05.108

Sun, W., Lin, Z., Yu, Q., Cheng, S., & Gao, H. (2021). Promoting Extracellular Electron Transfer of *Shewanella oneidensis* MR-1 by Optimizing the Periplasmic Cytochrome *c* Network. *Frontiers in Microbiology*, *12*(October), 1–13. https://doi.org/10.3389/fmicb.2021.727709

Takahashi, K., Sekine, Y., Chibazakura, T., & Yoshikawa, H. (2007). Development of an intermolecular transposition assay system in *Bacillus subtilis* 168 using IS4Bsu1 from *Bacillus subtilis* (natto). *Microbiology*, *153*(8), 2553–2559. https://doi.org/10.1099/mic.0.2007/007104-0

Talavera, A., Tamman, H., Ainelo, A., Konijnenberg, A., Hadži, S., Sobott, F., Garcia-Pino, A., Hõrak, R., & Loris, R. (2019). A dual role in regulation and toxicity for the disordered N-terminus of the toxin GraT. *Nature Communications*, *10*(1), 1–13. https://doi.org/10.1038/s41467-019-08865-z

Tanaka, K. H., Dallaire-Dufresne, S., Daher, R. K., Frenette, M., & Charette, S. J. (2012). An insertion sequence-dependent plasmid rearrangement in *Aeromonas salmonicida* causes the loss of the type three secretion system. *PLoS ONE*, *7*(3), 1–8. https://doi.org/10.1371/journal.pone.0033725

Tang, Y., Zhang, J., Guan, J., Liang, W., Petassi, M. T., Zhang, Y., Jiang, X., Wang, M., Wu, W., Ou, H.-Y., & Peters, J. E. (2024). Transposition with Tn 3 -family elements occurs through interaction with the host β-sliding clamp processivity factor. *Nucleic Acids Research*, *August*, 10416–10430. https://doi.org/10.1093/nar/gkae674

Tempel, S., Bedo, J., & Talla, E. (2022). From a large-scale genomic analysis of insertion sequences to insights into their regulatory roles in prokaryotes. *BMC Genomics*, *23*(1), 1–19. https://doi.org/10.1186/s12864-022-08678-3

Teravest, M. A., Zajdel, T. J., & Ajo-Franklin, C. M. (2014). The Mtr Pathway of *Shewanella oneidensis* MR-1 Couples Substrate Utilization to Current Production in *Escherichia coli*. *ChemElectroChem*, *1*(11), 1874–1879. https://doi.org/10.1002/celc.201402194

Thormann, K. M., Saville, M., Shukla, S., Pelletier, D. A., & Spormann, A. M. (2004). Initial Phases of Biofilm Formation in *Shewanella oneidensis* MR-1. *186*(23), 8096–8104. https://doi.org/10.1128/JB.186.23.8096

Touchon, M., & Rocha, E. P. C. (2007). Causes of insertion sequences abundance in prokaryotic genomes. *Molecular Biology and Evolution*, *24*(4), 969–981. https://doi.org/10.1093/molbev/msm014

Turnbough, C. L. (2019). Regulation of Bacterial Gene Expression by Transcription Attenuation. *Microbiology and Molecular Biology Reviews*, *83*(3), 1–25. https://doi.org/10.1128/mmbr.00019-19

Van Melderen, L., & De Bast, M. S. (2009). Bacterial toxin-Antitoxin systems: More than selfish entities? *PLoS Genetics*, *5*(3). https://doi.org/10.1371/journal.pgen.1000437

Vandecraen, J., Chandler, M., Aertsen, A., & Van Houdt, R. (2017). The impact of insertion sequences on bacterial genome plasticity and adaptability. *Critical Reviews in Microbiology*, *43*(6), 709–730. https://doi.org/10.1080/1040841X.2017.1303661

Velasquez-Orta, S. B., Head, I. M., Curtis, T. P., Scott, K., Lloyd, J. R., & von Canstein, H. (2010). The effect of flavin electron shuttles in microbial fuel cells current production. *Applied Microbiology and Biotechnology*, *85*(5), 1373–1381. https://doi.org/10.1007/s00253-009-2172-8

Venkateswaran, K., Moser, D. P., Dollhopf, M. E., Lies, D. P., Saffarini, D. A., MacGregor, B. J., Ringelberg, D. B., White, D. C., Nishijima, M., Sano, H., Burghardt, J., Stackebrandt, E., & Nealson, K. H. (1999). Polyphasic taxonomy of the genus *Shewanella* and description of *Shewanella oneidensis* sp. nov. *International Journal of Systematic Bacteriology*, *49 Pt 2*, 705–724. https://doi.org/10.1099/00207713-49-2-705

Von Canstein, H., Ogawa, J., Shimizu, S., & Lloyd, J. R. (2008). Secretion of flavins by *Shewanella* species and their role in extracellular electron transfer. *Applied and Environmental Microbiology*, *74*(3), 615–623. https://doi.org/10.1128/AEM.01387-07

Wagner, A. (2006). Cooperation is fleeting in the world of transposable elements. *PLoS Computational Biology*, *2*(12), 1522–1529. https://doi.org/10.1371/journal.pcbi.0020162

Wagner, A., Lewis, C., & Bichsel, M. (2007). A survey of bacterial insertion sequences using IScan. *Nucleic Acids Research*, *35*(16), 5284–5293. https://doi.org/10.1093/nar/gkm597

Wallace, L. J., Ward, J. M., & Richmond, M. H. (1981). The location of sequences of TnA required for the establishment of transposition immunity. *MGG Molecular & General Genetics*, *184*(1), 80–86. https://doi.org/10.1007/BF00271199

Wang, J., & Azam, W. (2024). Natural resource scarcity, fossil fuel energy consumption, and total greenhouse gas emissions in top emitting countries. *Geoscience Frontiers*, *15*(2), 101757. https://doi.org/10.1016/j.gsf.2023.101757

Wang, X., Lv, M., Zhang, L., Li, K., Gao, C., Ma, C., & Xu, P. (2013). Efficient bioconversion of 2,3-butanediol into acetoin using *Gluconobacter oxydans* DSM 2003. *Biotechnology for Biofuels*, *6*(1), 1–9. https://doi.org/10.1186/1754-6834-6-155

Wehrs, M., Tanjore, D., Eng, T., Lievense, J., Pray, T. R., & Mukhopadhyay, A. (2019). Engineering Robust Production Microbes for Large-Scale Cultivation. *Trends in Microbiology*, *27*(6), 524–537. https://doi.org/10.1016/j.tim.2019.01.006

Wright, M. S., Mountain, S., Beeri, K., & Adams, M. D. (2017). Assessment of insertion sequence mobilization as an adaptive response to oxidative stress in *Acinetobacter baumannii* using IS-seq. *Journal of Bacteriology*, *199*(9), 1–9. https://doi.org/10.1128/JB.00833-16

Wu, Y., Aandahl, R. Z., & Tanaka, M. M. (2015). Dynamics of bacterial insertion sequences: Can transposition bursts help the elements persist? Theories and models. *BMC Evolutionary Biology*, *15*(1), 1–12. https://doi.org/10.1186/s12862-015-0560-5

Xie, Z., & Tang, H. (2017). ISEScan: automated identification of insertion sequence elements in prokaryotic genomes. *Bioinformatics (Oxford, England)*, *33*(21), 3340–3347. https://doi.org/10.1093/bioinformatics/btx433

Yasir, M., Turner, A. K., Lott, M., Rudder, S., Baker, D., Bastkowski, S., Page, A. J., Webber, M. A., & Charles, I. G. (2022). Long-read sequencing for identification of insertion sites in large transposon mutant libraries. *Scientific Reports*, *12*(1), 1–9. https://doi.org/10.1038/s41598-022-07557-x

Zhang, Y., Cheng, T. C., Huang, G., Lu, Q., Surleac, M. D., Mandell, J. D., Pontarotti, P., Petrescu, A. J., Xu, A., Xiong, Y., & Schatz, D. G. (2019). Transposon molecular domestication and the evolution of the RAG recombinase. *Nature*, *569*(7754), 79–84. https://doi.org/10.1038/s41586-019-1093-7

6 Appendix

6.1 Supplementary Tables:

Table 21: SNVs detected for the stress experiment. A fixed ploidy variant detection was performed with CLC genomic workbench. Parameters were adjusted to have an identity frequency of 100 % or detection minimum of 10. As the analysis was performed based on long read nanopore sequencing a strong bias towards read counts arises**.**

Transposome Consortium	Nucleotide polymorphisms (20%)	Nr. Of reads	SNV per normalized read count (50k)	Detection minimum frequency 100%	Normalized to read count	Variant detection count min 10
K15	326	36339	**449**	**17**	**23.5**	**70**
UV1	190	69746	**136**	**11**		
UV2	179	104522	**86**	**7**		
UV3	185	85141	**109**	**11**	**6.5**	**55**
AB1	183	51810	**177**	**11**		**62**
AB2	242	36000	**336**			
AB3	279	31911	**437**			
T1	200	49174	**203**	**10**		
T2	231	35996	**321**			
T3	247	42734	**289**	**29**		**60**
UV1_50	178	106536	**178**			**55**
UV1_100	179	35988	**249**	**9**	**12.5**	**66**
UV3_50	246	59336	**207**			
UV3_100	176	74716	**118**	**10**		**84**
ΔISSOD2 control	131	95485	**69**			
ΔISSOD2_1	154	220145	**35**	**10**		
ΔISSOD2_2	182	131355	**69**			
ΔISSOD2_3	175	203131	**43**	**7**		
ΔISSOD1_1	174	195091	**45**		**38**	
ΔISSOD1_2	276	50087	**275**			
ΔISSOD1_3	193	137499	**70**			
ΔISSOD1_4	293	36276	**404**	**45 (because of stop codon)**	**73**	
MP1	166	17713	**469**			
MP2	244	16389	**744**	**30**		
MP3	205	22527	**455**			
MP4	161	18109	**445**			

Table 22: SNVs detected via Minimap2 combined with variant calling BBtools on the Galaxy platform. The analysis was performed to ameliorate biases arising through long read variant detection. Normalized to read count the ratio of the two analyzed trails UV3 and K15 remains comparable to the first SNV analysis for the chromosome. The high number of SNVs for the MP might arise due to multiplicity of IS or strong deterioration.

Strain	Variants	Chromosome (normalized to read count)	MP
K15	589	**146**	483
UV3	740	**61**	636

6.2 Supplementary Figures:

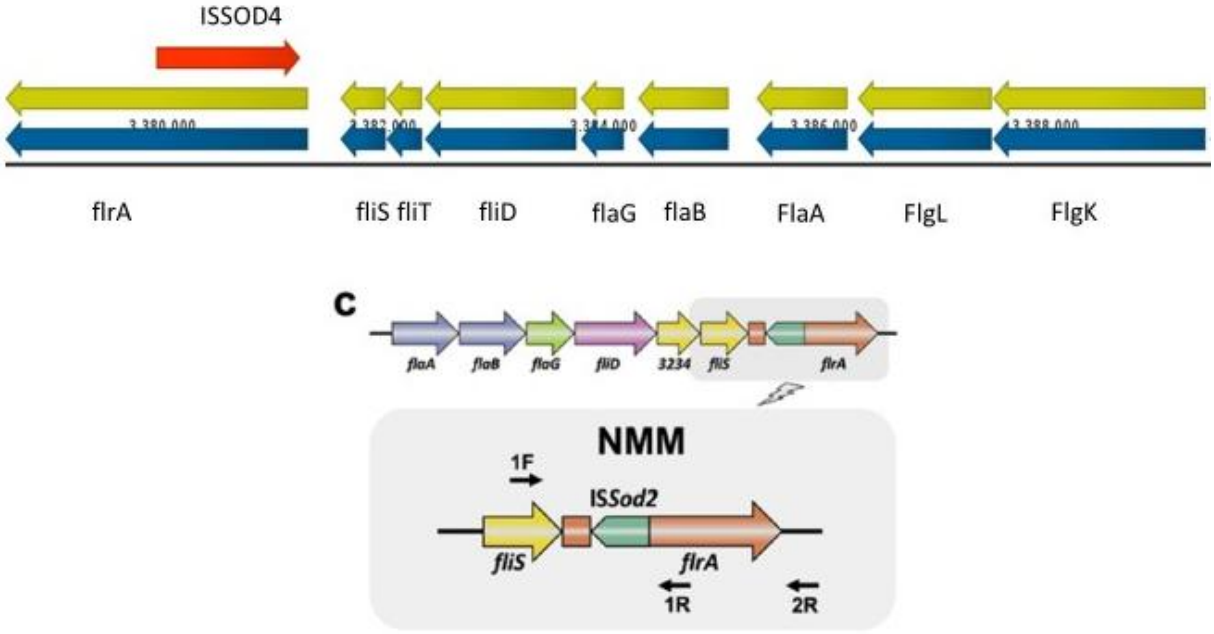

Figure S1: Integration of ISSOD4 into flagellar locus as described by Chen *et al* 2020. Only the reading direction is reversed, otherwise the position corresponds exactly to the proposed position pointing at a common target for integration, influencing biofilm formation. The integration was found to be caused by ISSOD4 instead of ISSOD2.

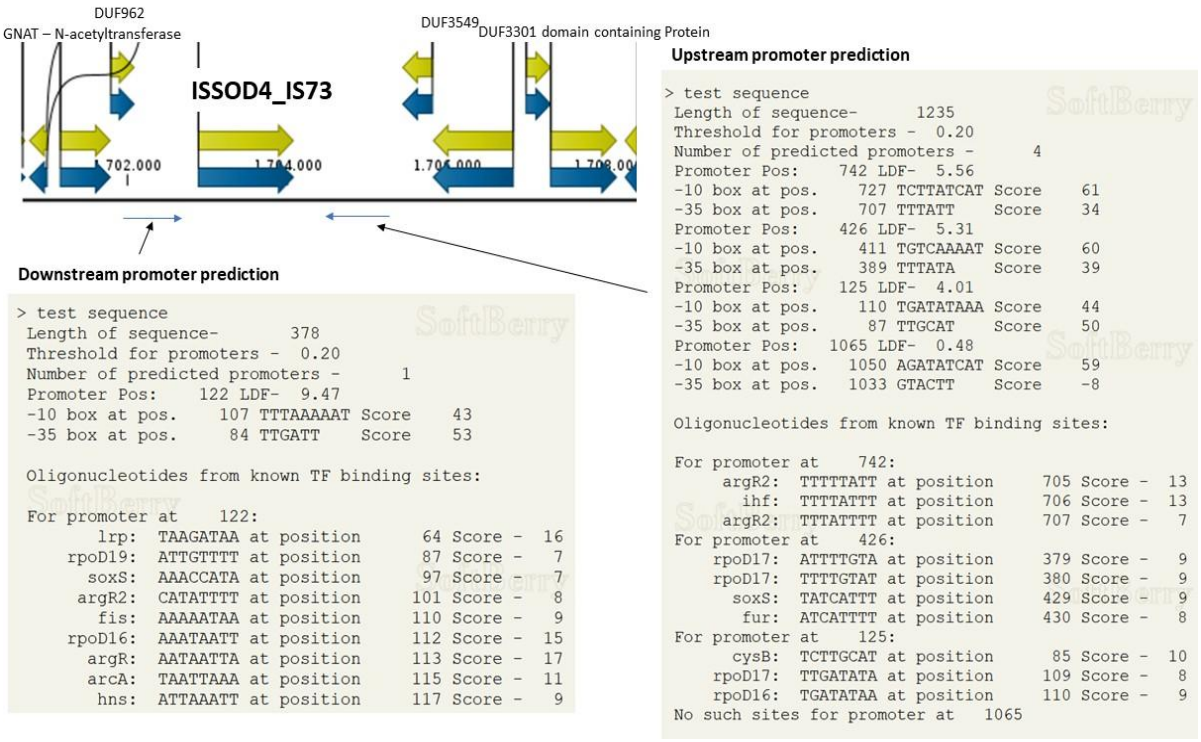

Figure S2: The loci where the most active ISSOD copy of the transcriptome analysis is found. Both upstream and downstream promoter could potentially increase transcript reads. Promotors were predicted by the BPROM - Softberry programs pipeline. Multiple promoter motives can be found in the non-coding regions flanking the ISSOD4_IS73 copy, possibly resulting in high transcription frequency.

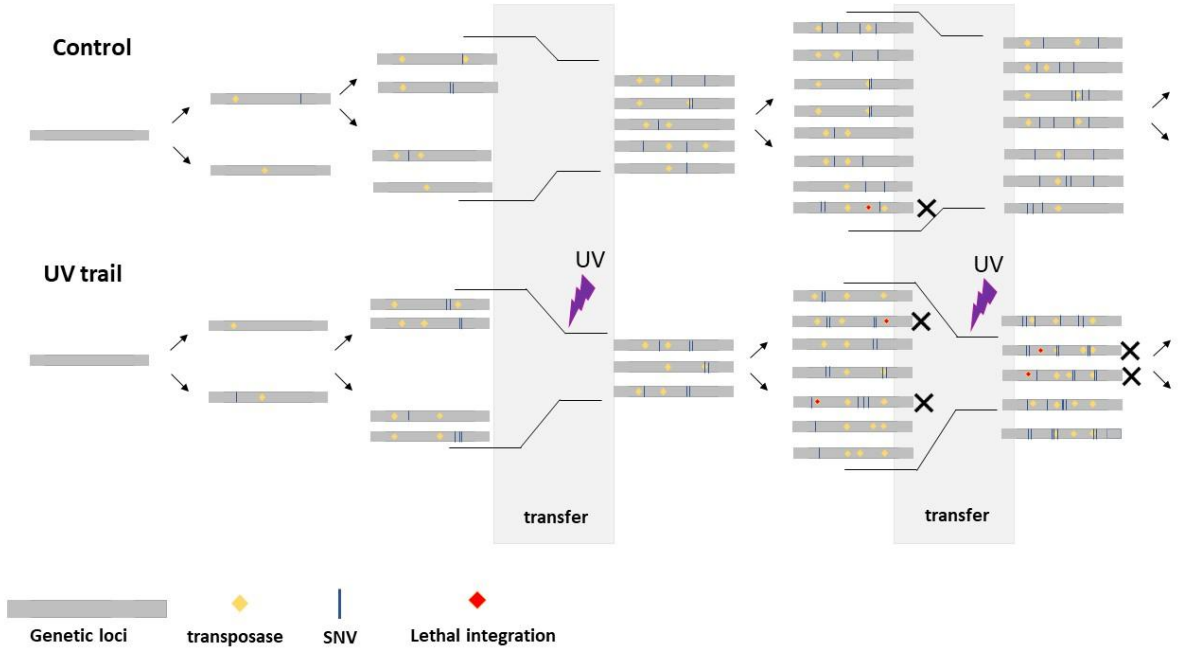

Figure S3: Illustration of proposed bottlenecks in a comparison of UV trails with the control. Though UV trails accumulate more mutations like IS integration and SNVs, diversity is diminished due to lower viability after radiation. As a consequence, fewer sub lineages might appear to have more insertions but less SNV. The transfers signify different bottlenecks for UV trails opposed to the control as DNA damage increases lethality.

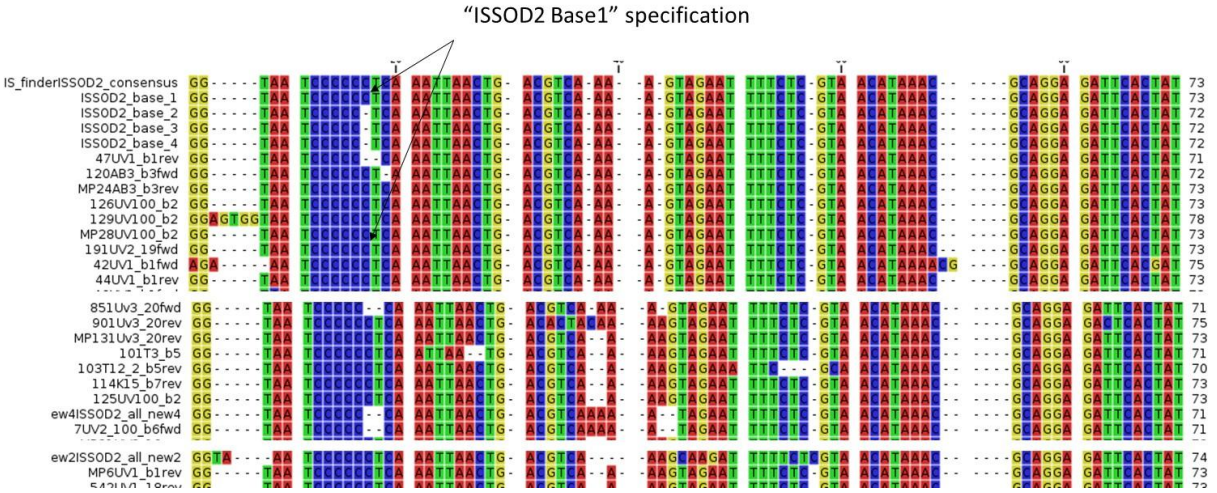

Figure S4: Section from the sequence alignment of all ISSOD2 copies from integrations occurring in the stress experiment identifying ISSOD2_ base1. A cytosine is found at the position indicated by the arrow that only occurs for the ISSOD2_base 1 copy and can't be found in other base copies. The SNV, if present in a newly integrated copy, therefore is likely derived from the ISSOD2_base 1 copy**.**

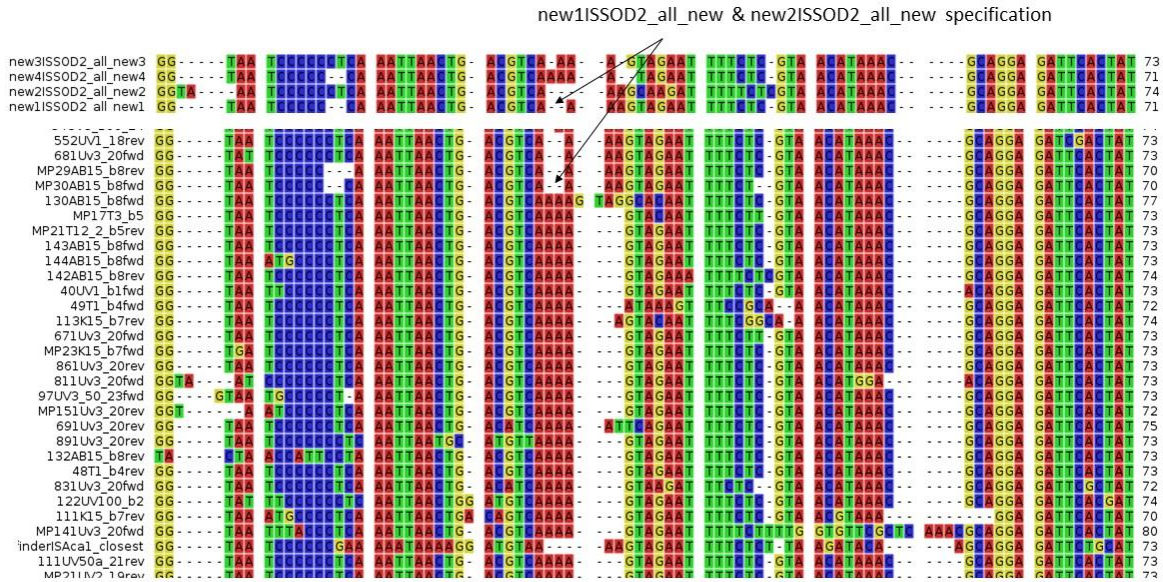

Figure S5: Section from the sequence alignment of all ISSOD2 copies from integrations occurring in the stress experiment identifying new1ISSOD2_all_new & new2ISSOD2_all_new. An adenosine is missing at the position indicated by the arrow that only occurs for these 2 base copies in the precursor strain and can't be found in other base copies. The SNV, if present in a newly integrated copy, therefore is likely derived from new1ISSOD2_all_new or new2ISSOD2_all_new.

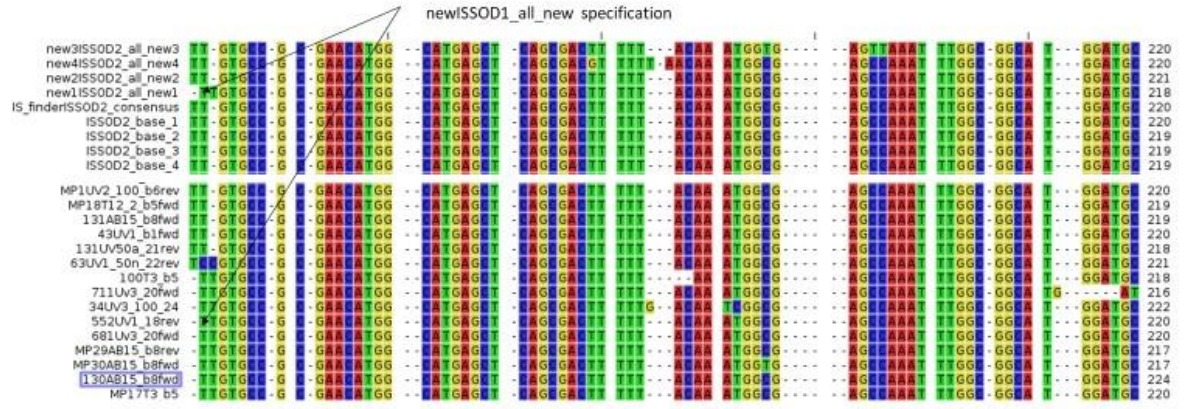

Figure S6: Section from the sequence alignment of all ISSOD2 copies from integrations occurring in the stress experiment identifying a SNV only observed for new1ISSOD2_all_new. A thymine is missing at the position indicated by the arrow that only occurs for the new1ISSOD2_all_new base. The SNV, if present in a newly integrated copy, therefore can be attributed to new1ISSOD2_all_new opposed to new2ISSOD2_all_new.

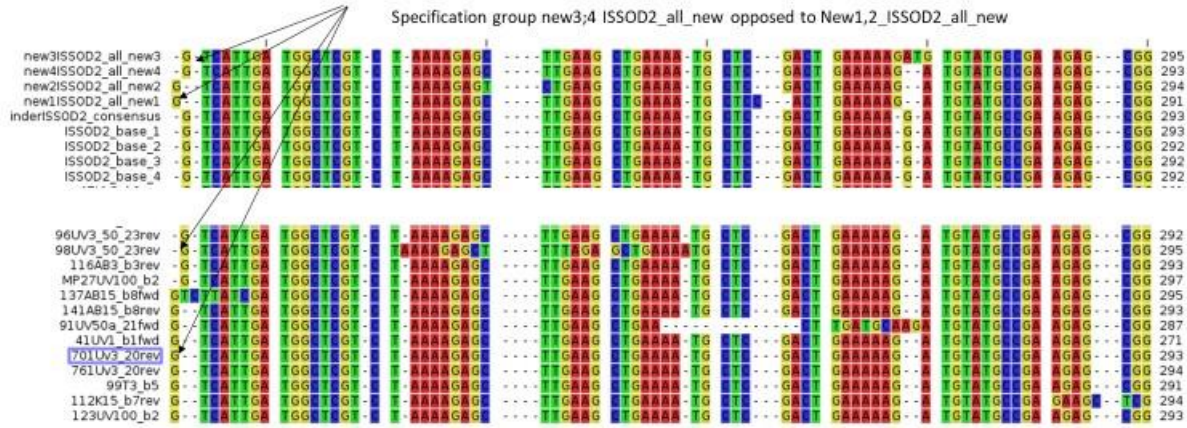

Figure S7: Section from the sequence alignment of all ISSOD2 copies from integrations occurring in the stress experiment identifying SNVs for New1,2_ISSOD2_all_new opposed to New3,4_ISSOD2_all_new. A guanine at the position indicated by the arrow differentiates between the two groups New1,2_ISSOD2_all_new and New3,4_ISSOD2_all_new.

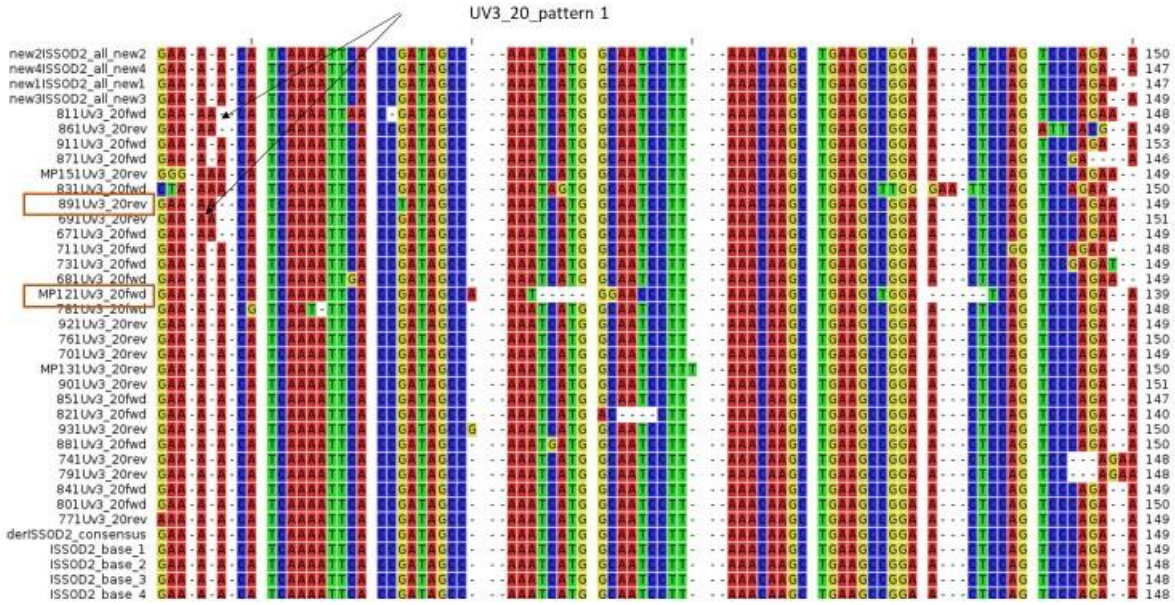

Figure S8: Section from the sequence alignment of all ISSOD2 copies from integrations occurring in the stress experiment identifying SNVs that are only present in a group of ISSOD2 copies from the UV3_20 experiment. The presence of an adenine at the indicated position cannot be found in any base copy and is therefore likely a result of transpositions of another copy in this trail.

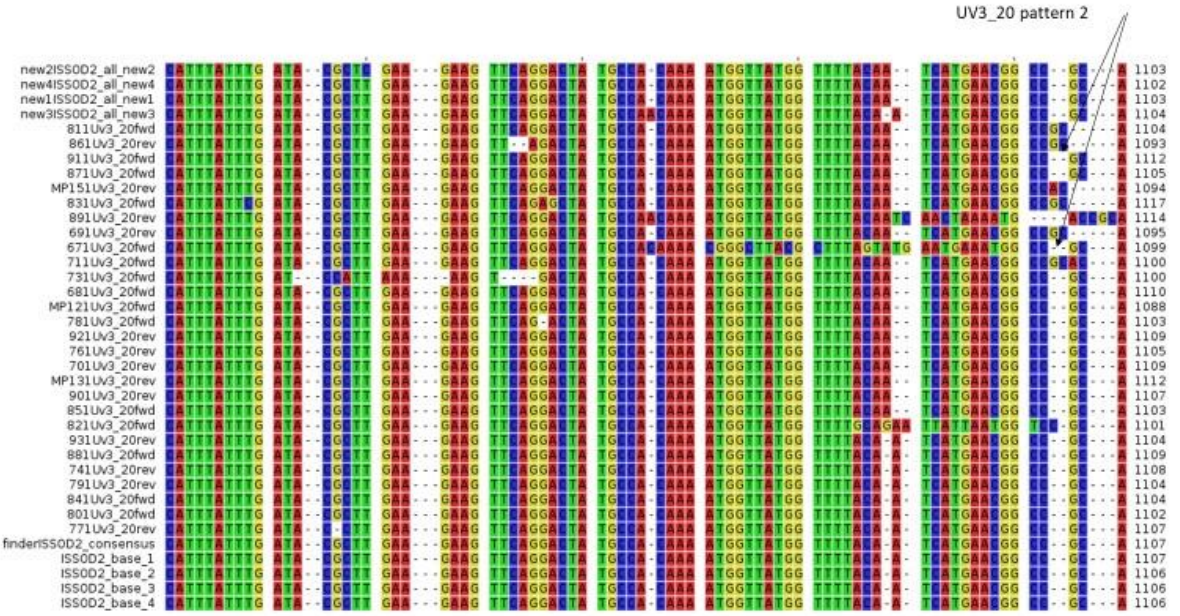

Figure S9: Section from the sequence alignment of all ISSOD2 copies from integrations occurring in the stress experiment identifying a second SNV that is only present in a group of ISSOD2 copies from the UV3_20 experiment. The presence of an adenine at the indicated position cannot be found in any base copy and is therefore likely a result of transpositions of another copy in this trail.

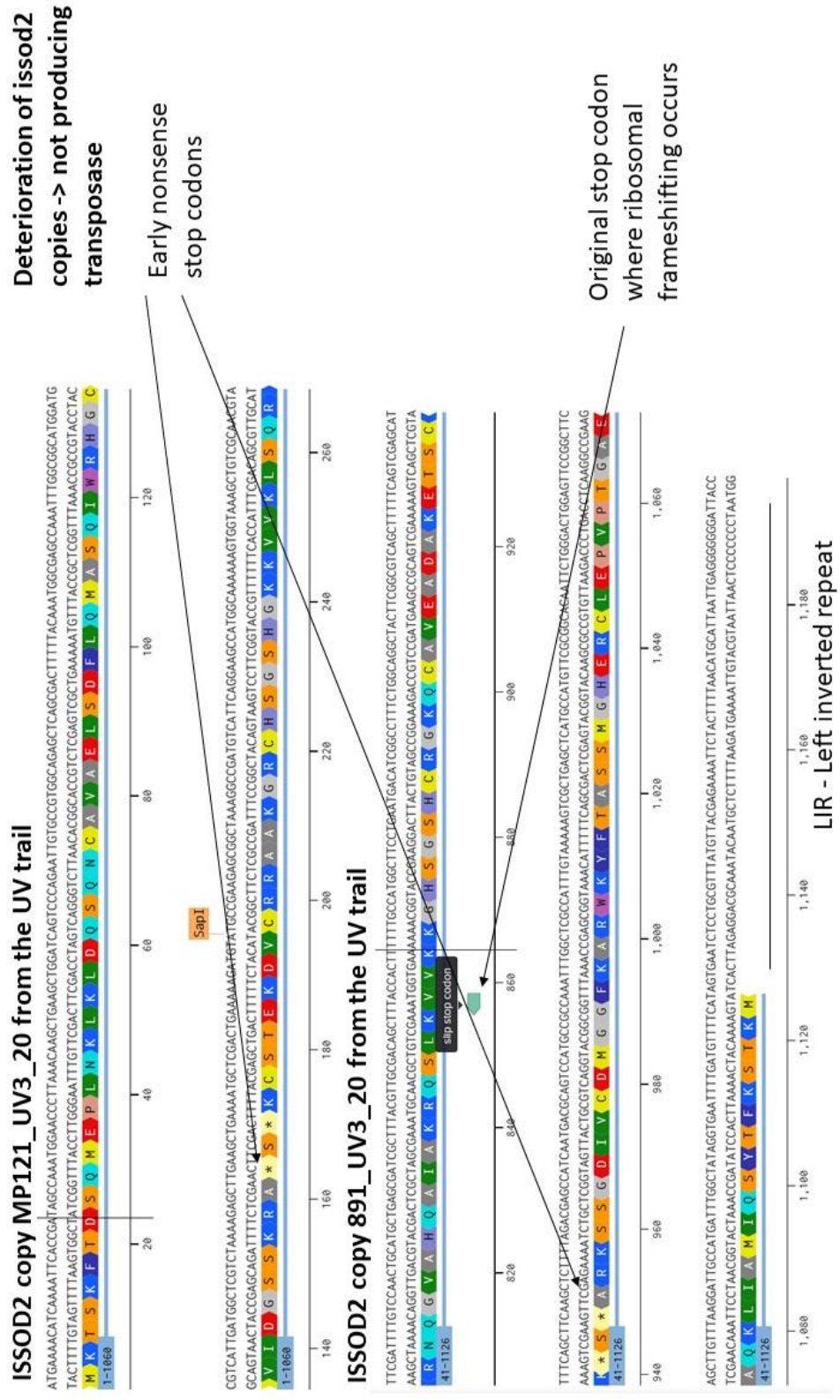

Figure S10: Deteriorated copies of ISSOD2 that show early non-sense stop codons preventing full-length translation and transposition. These two copies are highlighted in the SNV analysis in Supplementary Figure S8 and arose in the same trail UV3_20 but don't share the same SNV identity indicating a different origin. The additional early stop codons should prevent translation into an active transposase.

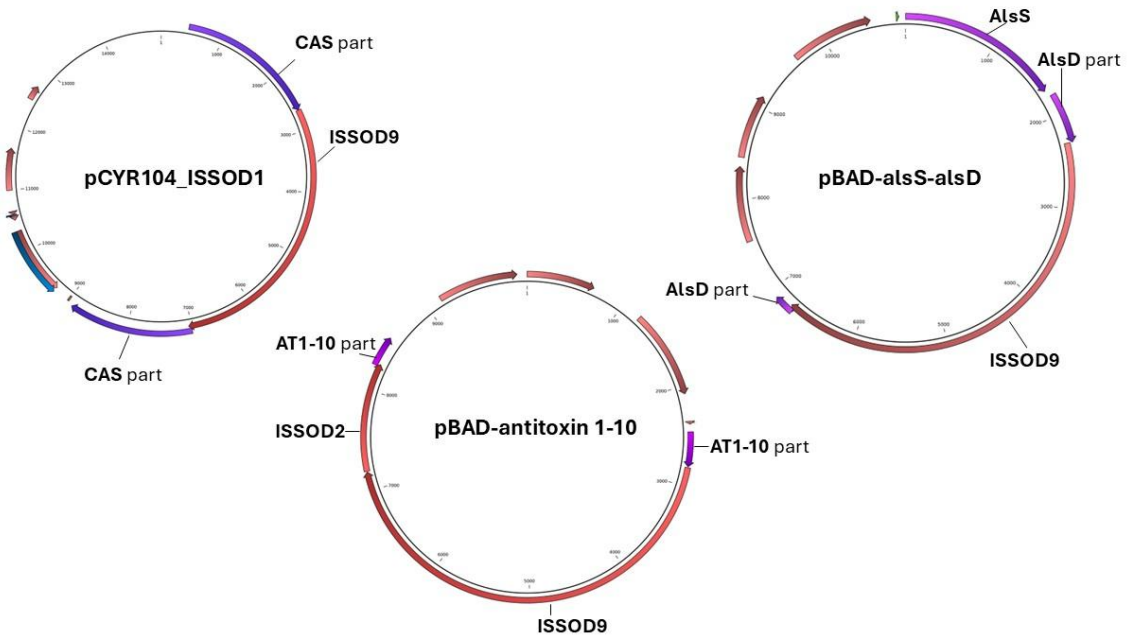

Figure S11: Plasmid charts for plasmids observed to be affected by ISSOD9 integration. In three independent experiments, across 10 trails, the expression cassette integral for plasmid function (shown in blue) was disrupted by ISSOD9 activity. Thus, complete silencing of ISSOD1 family via Cas expression, MP loss via AT expression and acetoin production failed due to TE activity.

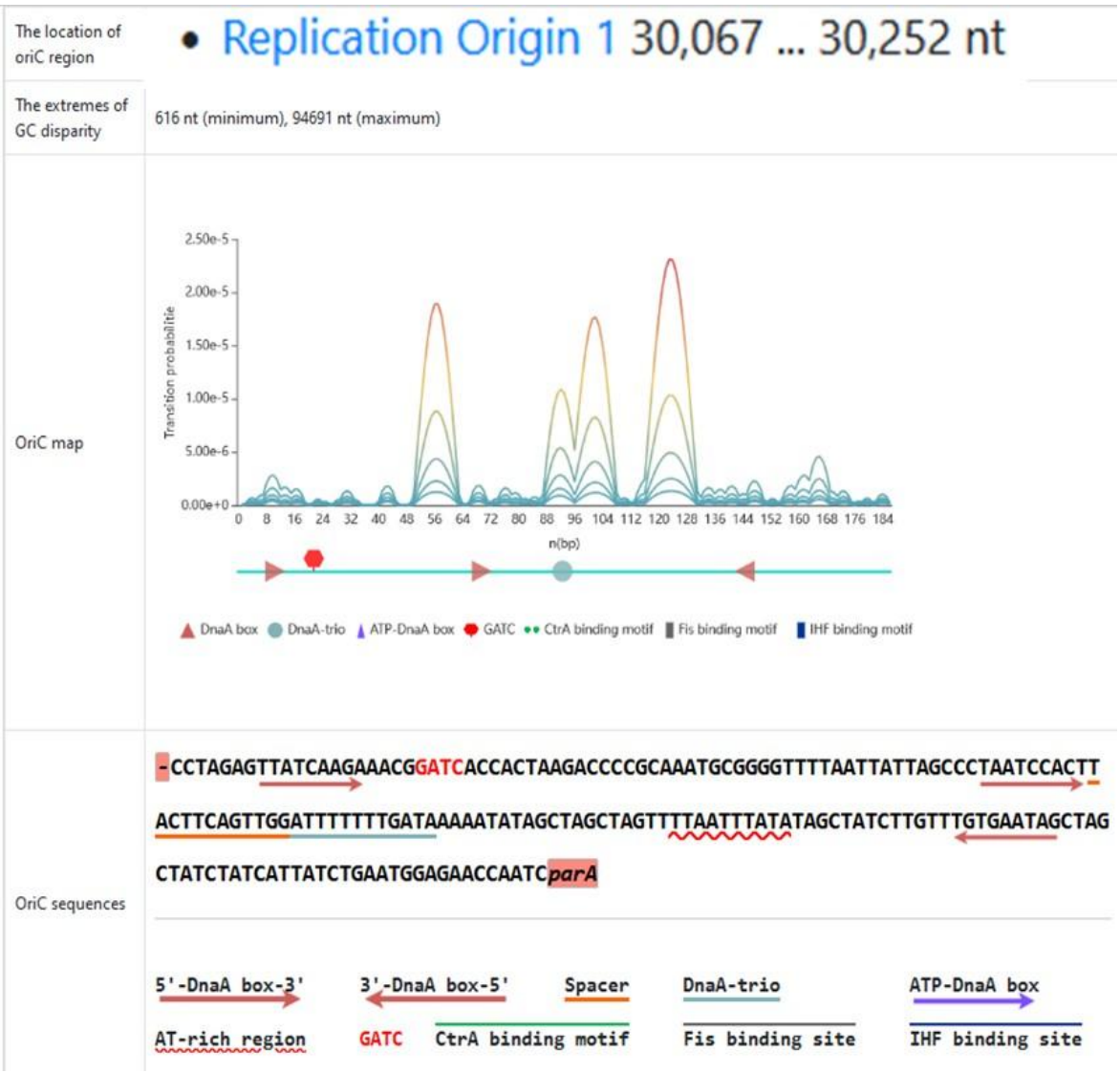

Figure S12: Predicted alternative origin of replication 1 in the reduced megaplasmid according to DoriC 12.0 webtool. The positions with corresponding sequences and patterns for essential structure and binding motives are indicated. Here the *parA* gene functions as an indicator gene for the predicted *ori* as this partitioning gene is often related to origins of replication.

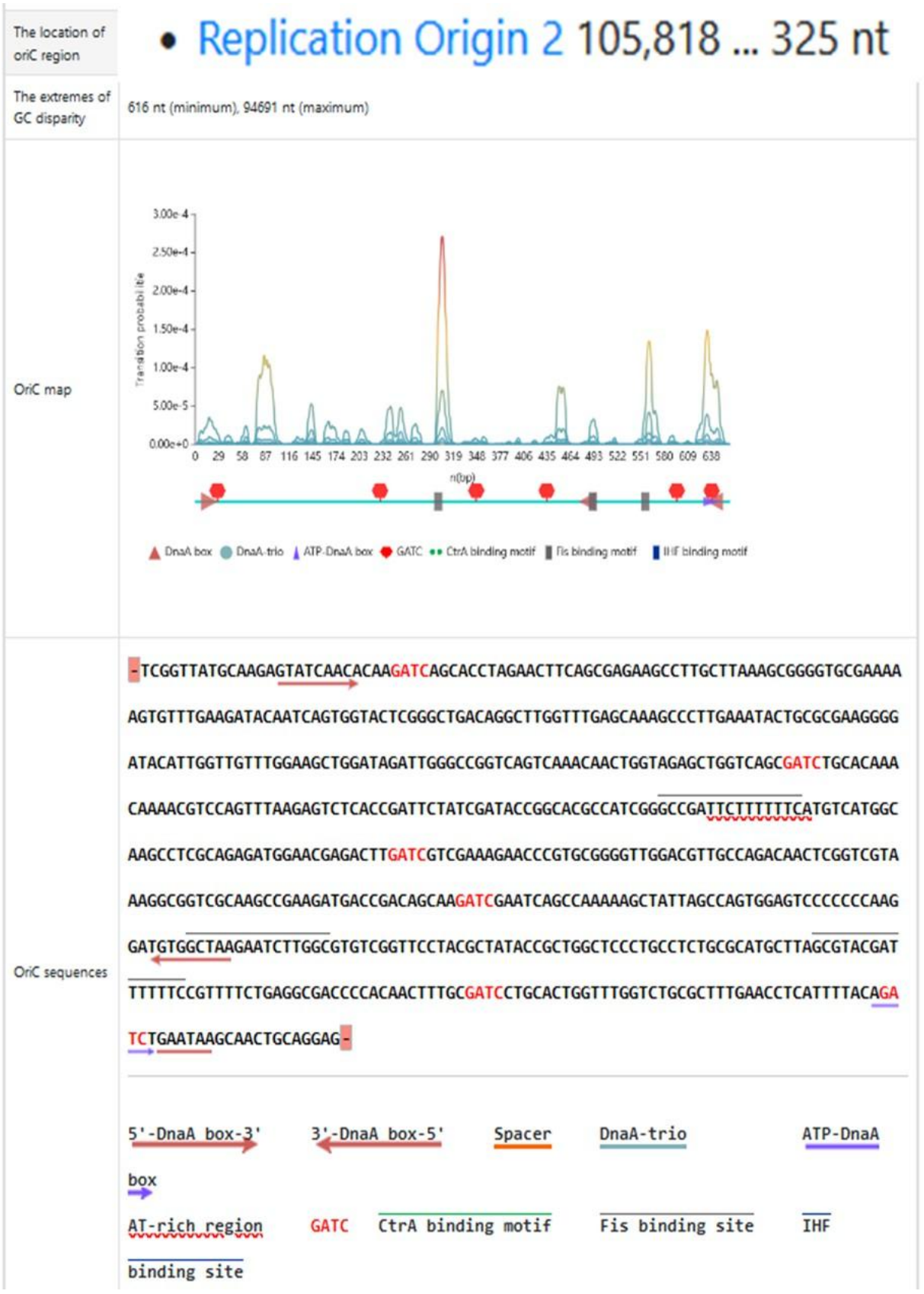

Figure S13: Predicted alternative origin of replication 2 in the reduced megaplasmid according to DoriC 12.0 webtool. The positions with corresponding sequences and patterns for essential structures and binding motives are indicated. Here no indicator gene is present.